



CONTRACT NO. A032-184
FINAL REPORT
AUGUST 1996

Analysis of Data from Lynwood Carbon Monoxide Study

CALIFORNIA ENVIRONMENTAL PROTECTION AGENCY



AIR RESOURCES BOARD
Research Division

ANALYSIS OF DATA FROM LYNWOOD CARBON MONOXIDE STUDY

Final Report A032-184

Prepared for:

**California Air Resources Board
Research Division
2020 L Street
Sacramento, CA 95814**

Prepared By:

**John L. Bowen, Ph.D.
Patricia A. Walsh**

**Energy and Environmental Engineering Center
Desert Research Institute
P.O. Box 60220
Reno, NV 89506**

and

**Ronald C. Henry, Ph.D.
24017 Ingomar Street
West Hills, CA 91304**

August 1996

ABSTRACT

The air quality monitoring site at Lynwood (LYNN), operated by the South Coast Air Quality Management District (SCAQMD), has recorded the highest carbon monoxide (CO) concentrations in the South Coast Air Basin (SoCAB) and in the State of California.

In the winter of 1989-90, the Air Resources Board (ARB), the SCAQMD, and General Motors Research Laboratories (GMRL) sponsored an intensive field study to understand the sources and distribution of CO during stagnation periods in the SoCAB. Supplemental data were collected for 24 hours in December, 1989 (from 1200 PST on Tuesday, 19 December through 1200 PST on Wednesday, 20 December) and 40 hours in January, 1990 (from 1200 PST on Monday, 8 January through 0400 PST on Wednesday, 10 January). Bag samples were collected and analyzed for CO at several sites near Lynwood to characterize concentrations at the middle and neighborhood scales and at other sites in the western SoCAB to measure the extent of the CO cloud. Perfluorocarbon tracers were released at four locations near Lynwood and the collected bag samples analyzed for their presence. Meteorological variables were measured with tether sondes at Lynwood and Vernon to altitudes of 60 m above the ground. Traffic counts were measured at five surface street and six freeway locations. On-road vehicle exhaust emissions were measured with an infrared, remote sensor at several locations in Lynwood and other sites in the SoCAB. CO analyzers were installed in rover vehicles to measure instantaneous CO concentrations on streets in the area.

The overall objectives of this study were to analyze data collected during the winter of 1989-90 and to determine: 1) why CO concentrations are higher at Lynwood than at any other monitoring location; 2) the relative contributions of local and areawide sources; and 3) the relative influence of meteorology, topography, and motor vehicle fleet characteristics on the CO concentrations at Lynwood.

The available data were thoroughly examined. Data collected at a number of bag sampling sites, mostly within 1 to 4 km of Lynwood, had questionable validity. Data from these sites did not exhibit morning and evening maxima in CO concentrations (near 0800 PST and 2300 PST, respectively) that were evident at SCAQMD monitoring stations and other bag sample sites. The presence of these maxima typifies the diurnal variations of CO in urban areas on weekdays. Maxima were either not present or occurred at times that differed appreciably from those at the SCAQMD sites. The diurnal pattern of morning and evening CO maxima should still have been present as in other parts of the SoCAB, even if local sources influenced CO concentrations near these sites. The lack of the usual diurnal variation at some locations may have been caused by malfunctioning samplers that did not collect samples at the intended times. It was not possible to retime the data to obtain maximum CO values at the expected time. These apparent malfunctions also limited the usefulness of many tracer samples as proper timing was critical to ensure valid data. Some problems were also found in data collected by the GM rover vehicles. The samples collected during periods of high traffic volume were biased high when

compared to station measurements, indicating that local traffic affected measurements made by the vehicles.

Bag sample data, including those from malfunctioning samplers, and SCAQMD data were used to investigate the locations of high CO concentrations in the SoCAB. These data confirmed that CO concentrations were higher in the vicinity of the SCAQMD site at Lynwood (LYNN) than at other locations of the SoCAB. While other sites sometimes had CO concentrations as high as at LYNN, CO concentrations were consistently high only at LYNN. The maximum CO concentrations sites showed similarly high values in all directions within 4 km of LYNN. By 7 km from LYNN, the maximum values have decreased to about half the LYNN maximum.

The Diagnostic Wind Model (DWM) was used to generate hourly wind fields in the western part of the SoCAB for the intensive periods. Wind speed and direction from SCAQMD sites and the two tethersonde sites were used to adjust the wind fields to local conditions. Terrain elevations were obtained from topographic maps for input to the DWM.

Terrain elevations were also used to determine the terrain slope throughout the western part of the SoCAB. Terrain in the vicinity of LYNN was found to have the least slope of any SCAQMD CO measurement site. The areal extent of small to moderate slope is greater in the vicinity of LYNN than any other site.

Trajectories of air transported to LYNN and other SCAQMD sites during the intensive periods were computed from the DWM wind fields. During evening hours of days that CO concentrations increased, air arriving at LYNN followed paths from locations to the west and northwest of LYNN until after midnight. The CO concentration was already decreasing when air from the vicinity of downtown Los Angeles (10 km to the north) arrived at LYNN. Evening transport was only a few kilometers an hour. During morning hours, trajectories showed that air was transported to LYNN from the north and northeast. Several hours were required for air to arrive at LYNN from downtown Los Angeles. Transport speeds were higher in the morning than in the evening. On the evening of low CO concentration at LYNN, transport was from the southeast for most of the evening hours.

Upper air soundings obtained at 2 locations during the intensive periods determined the temporal variation of atmospheric stability and winds near the ground for comparison to the change in CO concentrations. The tethersonde site at Lynwood (LTS) showed much stronger thermal stability at night than did the site at Vernon (VTS), 8 km north of LYNN. The lapse rate in potential temperature at LTS was as much as 5 times what it was at VTS. Wind speeds at LTS were about half as large as at VTS. The onset of stability was several hours after the initial increase in CO concentrations but did occur at the time that CO concentrations began increasing faster. CO concentrations decreased when the atmosphere became unstable in the morning.

The on-road remote sensing measurements found that local traffic in the Lynwood area consisted of older, higher emitting vehicles compared to the those at several other sites in the SoCAB. Although Lynwood vehicles were, on average several years older than vehicles in other

cities and in other parts of the SoCAB, the emissions versus age relationship observed for vehicles in Lynwood appeared to be similar to those of other cities.

Fluxes of CO were calculated across GM vehicle paths in an attempt to find local sources. There was some indication of sources but the measurements appear to have been greatly affected by nearby vehicles. Measurements averaged over an entire loop in the vicinity of LYNN were considerably higher than those measured at LYNN at the same time.

Multivariate analysis of the spatial relationship of CO concentrations at various sites was applied to CO and wind data from selected sites. The spatial covariances of CO concentrations were analyzed at these sites using a principle component analysis known as Empirical Orthogonal Function (EOF) analysis with an extension to determine possible sources through the Source Identification Through Empirical Orthogonal Functions (SITEOF) model. Inconsistencies and missing data limited the set of data that could be used in the EOF analysis. Data were selected with the following criteria: 1) site was within 20 km of LYNN, 2) site had less than 7 missing observations (out of 63 for hourly data and out of 32 for 2-hour data), and 3) correlation of site data with those of nearby SCAQMD site was at least 0.4. The last criterion was necessary to remove those unreliable data having temporal variations that did not conform to the normal weekday maxima. A total of 12 sites, of which 6 were SCAQMD sites, met the criteria. Data collected from most of the nearby bag sampling sites were excluded from the analysis because of inconsistencies. To increase available data for analysis, reliable data from both intensive periods, a total of 63 hours, were included in the same analysis. Thus, it is not possible to distinguish possible differences between the two intensive periods.

The EOF analysis yielded three spatial patterns in the data. The first EOF explained 65 to 70% of the variability in the CO data and expressed the fact that CO concentrations at all sites tend to vary together. The second EOF explained 17% to 20% of the variability of the CO data and represented a major feature of the variability in the data. The fact that LYNN was associated with coastal sites while bag sample sites less than 100 meters to the north (HS02 and HS05) were associated with inland sites is consistent with a source of CO existing between LYNN and the bag sample sites. The source appears to have contributed 1 to 3 ppm CO to the maximum concentration at LYNN site during the two intensive periods and less than 1 ppm to the average CO. The source may be due to operations associated with the U.S. Post Office located between the LYNN site and the two bag sample sites. The third EOF explained about 7% of the variability in the CO data and had relatively high values at the Lynwood AQMD site and the two nearby bag sample sites and low values for all the surrounding sites. This pattern is indicative of an additional source area surrounding LYNN of undefined areal extent.

The SITEOF model was applied to the data to estimate, for the combined December and January study periods, the average of the emission rate of CO minus the removal rate of CO, that is, the average net emission rate of CO. The model calculated a net emission rate in a 10 km by 15 km grid around LYNN that was almost 55% higher than the emission inventory estimate. Considering that errors in the SITEOF model have been found in other studies to be about 20%, the model indicates possible inaccuracies in currently available emission inventories.

This analysis focused on the identification of the source regions, transport routes, terrain, meteorological conditions, and different sub-periods of CO concentrations. The findings are summarized in the following:

Source Regions: A good portion of the CO concentrations at LYNN that exceed CO concentrations at other locations appears to originate in the local area. It is likely that the contribution is not a single source but rather a combination of numerous sources in the area.

Transport Routes: Morning transport routes are from the north and northeast with several hours required for air to arrive from the vicinity of downtown Los Angeles. Evening transport routes are from the west and northwest until after midnight when they come from the north. Transport is slower at night than during the morning.

Terrain: The small gradient near LYNN provides less reinforcement to the nocturnal winds which contributes to the low wind speeds at LYNN. This also allows a stronger thermal stability to develop which in turn limits mixing and reduces the dispersion of emitted CO.

Meteorological Conditions: With limited information available concerning atmospheric stability, it appears that the atmosphere in the Lynwood area is more stable at night than at other locations in the SoCAB. Nocturnal wind speeds tend to be low at LYNN but are but are not necessarily the lowest measured in the SoCAB. Measurements show that the lapse rate of potential temperature, and by implication, the stability are as much as 5 times stronger at Lynwood than at Vernon. Nighttime wind speeds are half as much at Lynwood as at Vernon. This leads to less mixing and transport and thus higher CO concentrations.

Sub-periods of CO Concentrations: There are three readily apparent, distinct sub-periods in the diurnal variation of CO concentrations in the SoCAB and in other urban areas. Two sub-periods are associated with the morning and evening maxima that occur because the atmosphere is stable, the wind speeds are low, and emissions are at or near their peak. The third sub-period is associated with the daytime minimum that occurs when the atmosphere is unstable and well-mixed. The decrease in CO concentrations between the evening and morning maxima may indicate a fourth sub-period although its cause may be associated only with the minimum in emissions.

As a general conclusion of the study, significant CO emissions in the Lynwood area are added to an urban air mass with already elevated CO concentrations. A tendency toward more stable meteorological conditions at Lynwood than at other areas exacerbates the CO air quality problem there.

The specific causes for higher concentrations of CO in the Lynwood vicinity than at other locations can be stated as follows:

- 1) Under the appropriate meteorological conditions, a strong, surface-based, thermal inversion sets up soon after sunset and persists until sunrise. This occurs at about the same time throughout the SoCAB but the inversion strength appears to be stronger near Lynwood than at other locations (at least as shown by the limited number of measurement locations of the field study). The stronger inversion would suppress vertical mixing more near Lynwood than at other locations.
- 2) The gradient of terrain is smaller near LYNN than at most other locations in the SoCAB. This relatively flat terrain within 5 km of LYNN results in a smaller slope-induced component for the nocturnal winds.
- 3) The combination of stronger inversions and relatively flatter terrain (and consequently weaker drainage winds) results in less dispersion of pollutants during the nighttime at LYNN than at other locations.
- 4) Low nocturnal wind speeds lead to weak transport of air during evening hours, particularly when wind directions change from westerly to northerly. Air arriving at LYNN during the time of nighttime peak CO concentrations, between 2200 and 0100 PST, had been 10 to 15 km to the west of LYNN several hours earlier at the time of higher emissions associated with the evening rush hour. The air arriving at LYNN at peak CO periods appears to have missed the downtown Los Angeles area and its major freeways by about 5 km.
- 5) Early morning wind speeds are higher than evening wind speeds. Air arriving at LYNN during the time of morning peak CO concentrations, about 0800 PST, is near possible regional sources at the start of the morning rush hour several hours earlier. Emissions generated during rush hour near downtown Los Angeles do not have time to reach LYNN before the morning inversion breaks and vertical mixing begins. Because of the time necessary for transport, emissions within 5 km of LYNN are large contributors to the elevated CO in the morning.
- 6) Vehicles in the vicinity of LYNN are older and have higher emissions than in some other areas of the SoCAB. It is reasonable to assume, however, that a similar vehicle mix extends several kilometers from LYNN although the full extent of the mix was not determined. Compared to other areas in the SoCAB, the local vehicles in the vicinity of LYNN would provide a relatively large source of CO. With the low wind speeds and suppressed mixing, CO generated within 5 km of LYNN would be a major contributor to the total CO concentration at LYNN. Because specific data on vehicle age, vehicle emissions, and traffic counts are not available near other SCAQMD sites, the effect of the vehicle mix and traffic volume near the various sites cannot be quantified.

- 7) The EOF analysis indicated a possible CO source very near LYNN. While this source, possibly associated with operations of the U.S. Post Office just to the north of LYNN, is a contributor to the elevated CO concentrations at LYNN, it should not be singled out as the major influence on the CO concentration at LYNN. High CO concentrations occur in an area surrounding LYNN and the Post Office that cannot be determined from the collected data.

Table of Contents

	<u>Page No.</u>
Abstract	i
List of Tables	ix
List of Figures	xi
1.0 INTRODUCTION	1-1
1.1 Objectives	1-8
2.0 EVALUATION OF DATA	2-1
2.1 CO and Tracer Bag Samples	2-1
2.2 GM Rover Data	2-12
2.3 Terrain Data	2-21
2.4 Meteorological Data	2-23
2.5 Traffic Count Data	2-23
2.6 On-Road Remote Sensing of CO Emissions	2-25
3.0 ANALYSIS OF DATA	3-1
3.1 Maximum CO Concentrations	3-1
3.2 Wind Speeds at SCAQMD Sites	3-1
3.3 Wind Field Generation	3-10
3.4 Trajectory Analysis	3-10
3.4.1 Lynwood Trajectories	3-13
3.4.2 Other SCAQMD Trajectories	3-16
3.4.2 Tracer Trajectories	3-17
3.5 Terrain	3-17
3.6 Tethersonde Data	3-23
3.7 Surface Mixed Layer	3-25
3.8 Comparison of CO concentrations, Traffic Counts, Lapse Rates, and Wind Speed and Direction	3-28
3.9 Empirical Orthogonal Eigenfunction Analysis	3-43
3.9.1 Background for EOF Analysis	3-43
3.9.2 Data Screening and Selection	3-44
3.9.2.1 One-Hour Average Data	3-45
3.9.2.2 Two-Hour Average Data	3-45
3.9.3 Results of EOF Analysis	
3.9.3.1 Spatial Correlations of One- and Two-Hour Average Data	3-45
3.9.3.2 Initial EOF Analysis of One- and Two-Hour CO Data	3-52

	3.9.3.3	SITEOF Model Results	3-56
	3.9.3.4	Discussion of EOF Analysis	3-58
	3.9.3.5	Conclusions from EOF Analysis	3-60
4.0		CONCLUSIONS	4-1
	4.1	Source Regions	4-2
	4.2	Potential Transport Routes	4-3
	4.3	Topographic Features	4-3
	4.4	Meteorological Factors	4-4
	4.5	Sub-periods	4-4
5.0		REFERENCES	5-1
APPENDIX A:		GM Rover Vehicle Data - Comparison Tables	
APPENDIX B:		Hourly Surface Wind Fields Generated from Diagnostic Wind Model	
APPENDIX C:		Trajectories of Air Arriving at: LYNN for December, 1989 LYNN for January, 1990 CELA, HAWT, LGBH for December, 1989 Trajectories of Tracer Releases for December, 1989 Trajectories of Tracer Releases for January, 1990	
APPENDIX D:		One- and Two-Hour Average Data Sets for Empirical Orthogonal Function Analysis	

List of Tables

<u>Table No.</u>	<u>Title</u>	<u>Page No.</u>
1-1	Summary of Carbon Monoxide Data - 1989 South Coast Air Quality Management District	1-2
1-2	Location of Sites for Which Data Are Available	1-3
2-1	Summary of AeroVironment CO Data for December, 1989 Intensive Period - December 19, 1200 to 20, 1100	2-2
2-2	Summary of AeroVironment CO Data for January, 1990 Intensive Period - January 8, 1200 to 10, 0300	2-3
2-3	Summary of South Coast AQMD CO Data for December, 1989 Intensive Period - December 19, 1200 to 20, 1100	2-4
2-4	Summary of South Coast AQMD CO Data for January, 1990 Intensive Period - January 8, 1200 to 10, 0300	2-5
2-5	Evaluation of CO Bag Samples by Similarity to Nearby SCAQMD Sites .	2-13
2-6	Time of Tracer Sample Relative to Release - 1700 through 2300	2-15
2-7	GM Vehicle Paths - Loop and Segment Flags	2-17
2-8	Comparisons of Vehicle Counts - CALTRANS	2-26
2-9	Comparisons of Vehicle Counts - Newport Traffic Studies	2-28
2-10	On-Road CO Measurements	2-29
2-11	On-Road CO Measurements	2-30
3-1	Summary of Maximum CO Concentrations and Scalar Wind Speeds at SCAQMD Sites, December 19, 1200 to 20, 1100	3-2
3-2	Summary of Maximum CO Concentrations and Scalar Wind Speeds at SCAQMD Sites, January 8, 1200 to 10, 0400	3-3
3-3	Arrival of Tracers in Vicinity of Lynwood -Trajectory Analysis	3-18

List of Tables (Continued)

<u>Table No.</u>	<u>Title</u>	<u>Page No.</u>
3-4	Gradient of Topography at Sampling Sites	3-20
3-5	Magnitude of Slope Winds from Diagnostic Wind Model	3-22
3-6	Heights of Mixed Layer During Intensive Periods	3-29
3-7	Available One-Hour Data	3-46
3-8	Basic Statistics of the One-Hour CO Data Set (in ppm)	3-46
3-9	Available Two-Hour Data for EOF Analysis	3-47
3-10	Correlations of All Sites with LYNN Site (Two-Hour Data)	3-48
3-11	Basic Statistics of the Two-Hour CO Data Set (in ppm)	3-49
3-12	Inter-Site Correlations for All Two-Hour Average CO Data	3-51
3-13	Maximum CO Concentrations in the Vicinity of LYNN	3-59
3-14	Comparisons of Average CO Concentrations at HS Sites to LYNN	3-59

List of Figures

<u>Figure No.</u>	<u>Title</u>	<u>Page No.</u>
1-1	Locations of SCAQMD and CC Sample Sites	1-5
1-2	Locations of SCAQMD and AV Sites 1 to 15 km of LYNN	1-6
1-3	Locations of Sample Sites Within 1 km of LYNN	1-7
2-1	CO Concentrations at SCAQMD Sites during December, 1989 Intensive Period..	2-6
2-2	CO Concentrations at SCAQMD Sites during January, 1990 Intensive Period..	2-7
2-3	CO Concentrations at CC Sites during December, 1989 Intensive Period	2-8
2-4	CO Concentrations at CC Sites during January, 1990 Intensive Period	2-9
2-5	CO Concentrations at HS Sites during December, 1989 Intensive Period	2-10
2-6	CO Concentrations at HS Sites during January, 1990 Intensive Period	2-11
2-7	Pontiac CO Measurements Near LYNN and HS Sites	2-14
2-8	Paths of General Motors Vehicles during Collection of Ambient CO Concentration in Vicinity of Lynwood	2-18
2-9	Pontiac CO Concentrations Near LYNN	2-19
2-10	Oldsmobile CO Concentrations Near LYNN	2-20
2-11	CO Concentrations from GM Rover Vehicles on Concurrent Legs	2-22
2-12	Traffic Counts from CALTRANS Sites	2-24
2-13	Traffic Counts from Newport Traffic Sites	2-27

List of Figures (Continued)

<u>Figure No.</u>	<u>Title</u>	<u>Page No.</u>
3-1	Maximum CO Concentrations at SCAQMD and CC Sites for December, 1989 Intensive Period	3-4
3-2	Maximum CO Concentrations at Sites Within 15 km of LYNN for December, 1989 Intensive Period	3-5
3-3	Maximum CO Concentrations at Sites Within 1 km of LYNN for December, 1989 Intensive Period	3-6
3-4	Maximum CO Concentrations at SCAQMD and CC Sites for January, 1990 Intensive Period	3-7
3-5	Maximum CO Concentrations at Sites Within 15 km of LYNN for January, 1990 Intensive Period	3-8
3-6	Maximum CO Concentrations at Sites Within 1 km of LYNN for January, 1990 Intensive Period	3-9
3-7	Example of Wind Field Generated by Diagnostic Wind Model for Morning Hours: 0800 PST, Dec. 20, 1989	3-11
3-8	Example of Wind Field Generated by Diagnostic Wind Model for Evening Hours: 2000 PST, Dec. 19, 1989	3-12
3-9	Example of Trajectory of Air Arriving at LYNN for Morning Hours: 0800 PST, Dec. 20, 1989	3-14
3-10	Example of Trajectory of Air Arriving at LYNN for Evening Hours: 2300 PST, Dec. 19, 1989	3-15
3-11	Gradient of Topography at Locations Where Magnitude is < 10 m/km. . .	3-21
3-12	Magnitude and Depth of Lapse Rate of Potential Temperature for Lowest Significant Level at LTS and VTS	3-24
3-13	Average Wind Speed and Wind Direction at Lynwood and Vernon Tethersonde Sites for December, 1989 Intensive Period	3-26

List of Figures (Continued)

<u>Figure No.</u>	<u>Title</u>	<u>Page No.</u>
3-14	Average Wind Speed and Wind Direction at Lynwood and Vernon Tethersonde Sites for January, 1990 Intensive Period	3-27
3-15	CO at LYNN; Traffic on Long Beach Blvd.; Lapse Rate, Wind Speed, and Wind Direction at LTS - December, 1989	3-30
3-16	CO at LYNN; Traffic on Imperial Highway; Lapse Rate, Wind Speed, and Wind Direction at LTS - December, 1989	3-31
3-17	CO at LYNN; Traffic on Long Beach Blvd.; Lapse Rate, Wind Speed, and Wind Direction at VTS - December, 1989	3-32
3-18	CO at LYNN; Traffic at I-5/I-10; Lapse Rate, Wind Speed, and Wind Direction at LTS - December, 1989	3-33
3-19	CO at LYNN; Traffic on Long Beach Blvd.; Lapse Rate, Wind Speed, and Wind Direction at LTS - January, 1990	3-34
3-20	CO at LYNN; Traffic on Long Beach Blvd.; Lapse Rate, Wind Speed, and Wind Direction at VTS - January, 1990	3-35
3-21	CO at LYNN; Traffic on Imperial Highway; Lapse Rate, Wind Speed, and Wind Direction at LTS - January, 1990	3-36
3-22	CO at LYNN; Traffic at I-5/I-10; Lapse Rate, Wind Speed, and Wind Direction at LTS - January, 1990	3-37
3-23	CO at CELA; Traffic at I-5/I-10; Lapse Rate, Wind Speed, and Wind Direction at LTS - December, 1989	3-39
3-24	CO at HAWT; Traffic at I-405/Compton; Lapse Rate, Wind Speed, and Wind Direction at LTS - December, 1989	3-40
3-25	CO at CELA; Traffic at I-5/I-10; Lapse Rate, Wind Speed, and Wind Direction at LTS - January, 1990	3-41
3-26	CO at HAWT; Traffic at I-405/Compton; Lapse Rate, Wind Speed, and Wind Direction at LTS - January, 1990	3-42

List of Figures (Continued)

<u>Figure No.</u>	<u>Title</u>	<u>Page No.</u>
3-27	Location of Sites Used in EOF Analysis	3-50
3-28	Inter-site Correlations versus Distance of All Sites Used in EOF Analysis Based on Two-Hour Average Data	3-53
3-29	First EOF of CO Data	3-54
3-30	Second EOF of CO Data	3-55
3-31	Third EOF of CO Data	3-57

1.0 INTRODUCTION

The air quality monitoring site at Lynwood, operated by the South Coast Air Quality Management District (SCAQMD), has recorded the highest carbon monoxide (CO) concentrations in the South Coast Air Basin (SoCAB) and the State of California. Table 1-1 summarizes the maximum 1- and 8-hour CO concentrations and the number of days with CO measurements exceeding the State and Federal 1- and 8-hour standards at SCAQMD sites in the SoCAB for 1989. Measurements at Lynwood exceeded standards more than twice as many times as at any other site.

In the winter of 1989-90, the Air Resources Board (ARB), the SCAQMD, and General Motors Research Laboratories (GMRL) sponsored a field study to understand the sources and distribution of CO during stagnation periods in the SoCAB. Additional measurements were made during two intensive periods: 19 December 1200 to 20 December 1200 and 8 January 1200 to 10 January 0400. Thirty-six time-sequential bag samplers were deployed in the SoCAB to collect 1- or 2-hour air samples that were then analyzed for CO concentrations. Several samplers designated as hot spot (HS sites) samplers were installed within 3 km of the SCAQMD air quality monitoring site at Lynwood (LYNN) to characterize the high pollution area. The other samplers were spread throughout the western part of the SoCAB to characterize the extent of the CO cloud (CC sites). Balloon-borne sampling probes were used at one site in Lynwood to obtain CO data in the vertical. Tethersondes were used at Lynwood and Vernon to measure meteorological variables to elevations of 60 m above the ground. Local traffic monitoring stations were established at six locations in Lynwood. CALTRANS traffic counts were obtained from several freeway locations. Tailpipe emissions were measured with a remote sensing instrument and license plate numbers were videotaped at several sites in Lynwood and other locations. Perfluorocarbon tracers were released from four locations near Lynwood. The bag samples analyzed for the presence of these tracers. CO analyzers were installed in rover vehicles to measure instantaneous CO concentrations on streets in the area.

The routine air quality monitoring network of the SCAQMD continued to collect CO and surface meteorological data on its normal schedule. Other surface and upper air meteorological data were collected by the National Weather Service following standard practices.

Locations of monitoring sites in the western part of the SoCAB are listed in Table 1-2. Included in the list are SCAQMD monitoring sites, supplemental monitoring sites operated by AeroVironment, Inc. (AV), tracer release sites, and traffic count locations. Locations are given by street address and by UTM coordinates (all UTM Zone 11). The SCAQMD sites and supplemental CC sites are shown in Figure 1-1. Sites within 15 km of the LYNN site are shown in Figure 1-2. Sites within 1 km of the Lynwood site are shown in Figure 1-3.

Summaries of data collected during the intensive study have been reported (AeroVironment, 1991) which confirmed that the highest CO concentrations in the SoCAB occurred in the Lynwood vicinity. This initial analysis indicated that meteorological conditions and high traffic volumes were dominant factors influencing the CO concentrations but that the

Table 1-1

Summary of Carbon Monoxide Data - 1989
South Coast Air Quality Management District

Site	Max Conc in PPM 1-Hr	Max Conc in PPM 8-Hr	Number of Days Exceeded			
			Federal		State	
			≥ 9.5 PPM 8-Hr	≥ 35 PPM 1-Hr	≥ 9.1 PPM 8-Hr	≥ 20 PPM 1-Hr
Lynwood	31	21.8	55	0	61	16
Hawthorne	23	16.4	25	0	28	2
Burbank	20	13.9	18	0	21	0
Reseda	17	12.5	11	0	15	0
Costa Mesa ^a	16	12.7	5	0	8	0
Anaheim	19	12.1	5	0	5	0
La Habra	24	10.7	6	0	7	7
Pico Rivera	13	10.7	1	0	2	0
Rubidoux	12	10.3	1	0	1	0
Long Beach	13	10.1	2	0	2	0
Los Angeles ^b	14	9.8	2	0	2	0
Whittier	13	8.8	0	0	0	0
Riverside	14	8.5	0	0	0	0
Pasadena	14	8.4	0	0	0	0
San Bernardino	11	8.1	0	0	0	0
W. Los Angeles	12	8.0	0	0	0	0
Pomona	12	7.4	0	0	0	0
Lancaster ^c	13	7.1	0	0	0	0
Azusa	7	5.8	0	0	0	0
Fontana	7	5.8	0	0	0	0
Santa Clarita ^b	12	5.4	0	0	0	0
Upland	8	5.4	0	0	0	0
El Toro	9	5.1	0	0	0	0
Palm Springs ^c	6	2.9	0	0	0	0

^a Station closed 3/12/89. New station opened 11/1/89.

^b Less than 12 full months of data. May not be representative.

^c Operated by the SCAQMD but located in Southeast Desert Air Basin

Table 1-2

Location of Sites for Which Data Are Available

<u>Site</u>	<u>Address</u>	<u>UTM Coordinates</u>	
		<u>East</u>	<u>North</u>
AQMD Sites			
Anaheim (ANAH)	1010 South Harbor Blvd.	415.00	3742.50
Azusa (AZUS)	803 N. Loren Avenue	414.88	3777.62
Burbank (BURK)	228 W. Palm Avenue	379.50	3783.00
Central Los Angeles (CELA)	1630 N. Main Street	386.88	3770.00
Hawthorne (HAWT)	5234 W. 120th Street	373.43	3754.27
La Habra (LAHB)	621 Lambert Road	412.00	3754.00
Long Beach (LGBH)	3648 N. Long Beach Blvd.	390.04	3742.96
Lynwood (LYNN)	11220 Long Beach Blvd.	388.18	3754.75
Pasadena (PASA)	752 Wilson Avenue (Cal Tech)	396.10	3777.30
Pico Rivera (PICO)	3713-B San Gabriel River Pkwy.	402.30	3764.10
Reseda (RESE)	18330 Gault Street	359.00	3785.00
West Los Angeles (WSLA)	VA Hospital Sawtell and Wilshire	365.30	3768.70
Whittier (WHIT)	14427 Leffingwell Road	405.30	3754.00
Costa Mesa (CSTA) (Met Only)	2850 Mesa Verde Dr. East, #116	414.50	3725.90
Compton (COMA) (Met Only)	901 W. Alondra Blvd. (Compton Airport)	385.50	3750.30
Los Alamitos (LSAL) (Met Only)	5660 Orangewood Avenue	404.50	3739.80
Vernon (VER) (Met Only)	2715 E. 50th Street	387.40	3762.50
AeroVironment Sites			
AQ02 (HAWT)	5234 W. 120th Street, Hawthorne	373.43	3754.27
AQ03 (CELA)	1630 N. Main Street, Los Angeles	386.88	3770.00
CC01	1420 Lake Street, Glendale	380.90	3870.40
CC02	1065 Armada Dr., Pasadena	392.80	3781.00
CC03	738 E. Oakdale, Monrovia	408.83	3778.88
CC04	1405 N. Edgemont, Los Angeles	380.50	3773.44
CC05	305 N. Lincoln Avenue, #5, Monterey Park	396.63	3769.72
CC06	12645 Fineview, El Monte	405.86	3767.28
CC07	12070 Beatrice St., Monterey Park	370.13	3761.15
CC08	3678 Fairland Blvd., Los Angeles	376.67	3762.83
CC10	2349 Strong Ave., City of Commerce	392.58	3762.96
CC11	7274 Canyon Dr., Whittier	405.40	3759.65
CC12	700 W. Pine Ave., El Segundo	368.32	3754.24
CC13	13133 S. Hoover St., Los Angeles	381.08	3753.04
CC14	11914 Lyndora, Norwalk	400.30	3753.13
CC15	1703 Ford Ave., Redondo Beach	371.94	3748.35
CC16	17513 Bradwell Ave., Gardena	380.52	3748.52
CC17	203 W. Artesia Bl., Long Beach	391.30	3748.70
CC18	10012 Ramona St., Bellflower	396.40	3748.42
CC19	6940 Walker, Bell	391.70	3759.36
CC20	2300 Dorris Pl., Los Angeles	385.95	3772.80
CC21	2635 Lancaster Ave., E. Los Angeles	389.63	3769.06

Table 1-2 (continued)

Location of Sites for Which Data Are Available

<u>Site</u>	<u>Address</u>	<u>UTM Coordinates</u>	
		<u>East</u>	<u>North</u>
AeroVironment Sites (continued)			
HS01	3351 E. Imperial Hwy., Lynwood	388.16	3754.90
HS02	3301 Beechwood Ave., Lynwood	388.14	3754.82
HS03 (LYNN)	11220 Long Beach Blvd., Lynwood	388.18	3754.75
HS04 (LYNN)	11220 Long Beach Blvd., Lynwood	388.18	3754.75
HS05	3367 Beechwood Ave., Lynwood	388.25	3754.83
HS06	3340 Sanborn Ave., Lynwood	388.20	3754.70
HS07a	11330 Bullis Ave., Lynwood, 50 ft. elev.	389.26	3754.60
HS07b	11330 Bullis Ave., Lynwood, 100 ft. elev.	389.26	3754.60
HS07c	11330 Bullis Ave., Lynwood, 150 ft. elev.	389.26	3754.60
HS08	3366 E. Imperial Hwy., Lynwood	388.15	3754.95
HS09	10821 Capistrano Ave., Lynwood	387.57	3755.50
HS10	10700 San Luis Ave., Lynwood	388.90	3755.47
HS11	3801 Cortland St., Lynwood	389.06	3754.00
HS12	11817 State St., Lynwood	387.50	3753.85
HS13	9603 Croesus Ave., Lynwood	386.03	3757.05
HS14	9329 Hildreth Ave., South Gate	390.37	3756.74
HS15	5300 Clark St., Lynwood	390.40	3752.63
HS16	13824 N. Pausen Ave., Compton	385.75	3752.12
LTS	3300 Century Blvd., Lynwood	389.30	3754.60
VTS	3375 Fruitland Ave., Vernon	388.20	3762.30
Tracer Sites			
TA-PMCP	Washington at I-5	394.00	3762.00
TB-PMCH	Firestone at I-605	398.00	3754.20
TC-PDCH	Central Ave. at Freeway 91	384.60	3748.60
TD-PTCH	Century Blvd. at Freeway 110	381.80	3756.70
Traffic Measurement Sites			
TRANS1	La Cienega near 120th, Hawthorne		
TRANS2	Firestone Blvd. near John Ave., Los Angeles		
TRANS3	Atlantic Ave. North of Firestone Blvd (Dec), South Gate		
	Atlantic Ave. South of Firestone Blvd (Jan), South Gate		
TRANS4	Imperial Hwy. near Long Beach Blvd., Lynwood		
TRANS5	Long Beach Blvd. near Imperial Hwy and Mulford, Lynwood		
TRANS6	Rosecrans Ave. near Long Beach Blvd., Compton		
CALTRANS Sites			
I210-STA	I-210 at Santa Anita Ave. (westbound)		
I405-VENI	I-405 at Venice Blvd. (northbound)		
I405-I10	I-405 at I-10 (eastbound)		
I405-CMP	I-405 at Compton Blvd. (northbound)		
I605-SGR	I-605 at San Gabriel River (northbound)		
I5-I10	I-10 at I-5 (southbound)		

AQMD AND CC MONITORING SITES

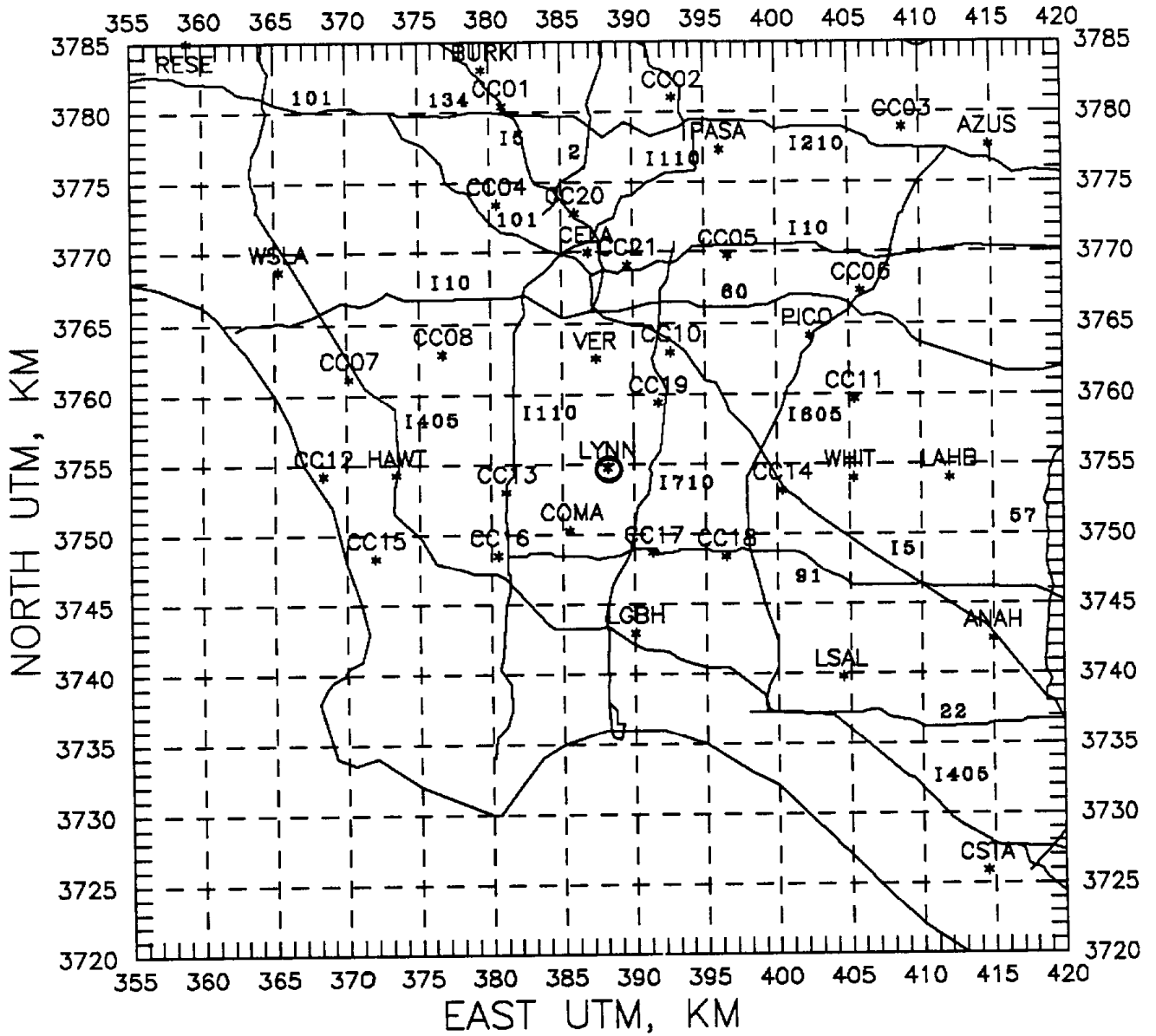


Figure 1-1. Locations of SCAQMD and CC Sample Sites. Freeway system also shown.

SITES WITHIN 15 KM OF LYNWOOD

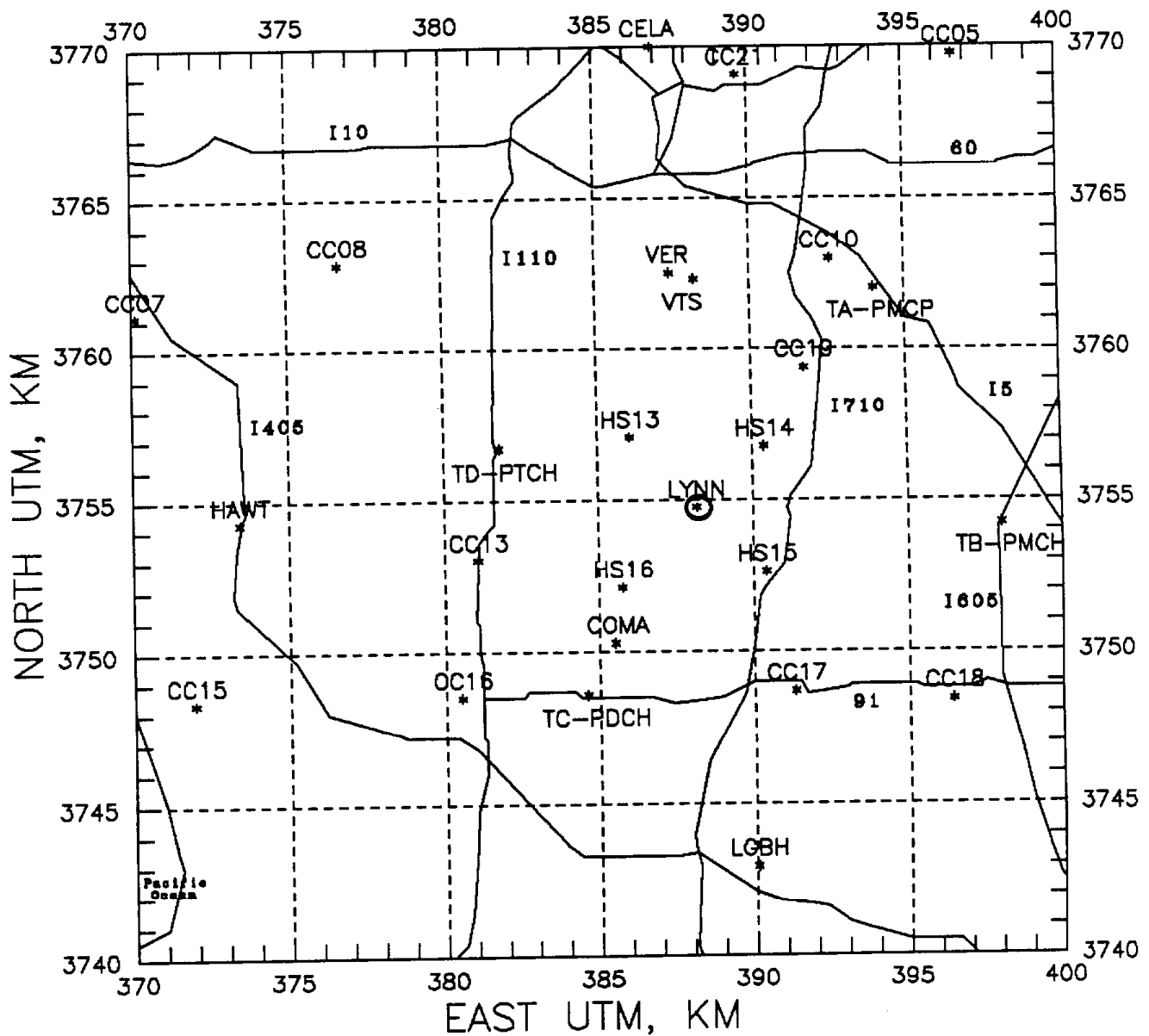


Figure 1-2. Locations of SCAQMD and AV Sites 1 to 15 km of LYNN.

SITES WITHIN 1 KM OF LYNWOOD AQMD

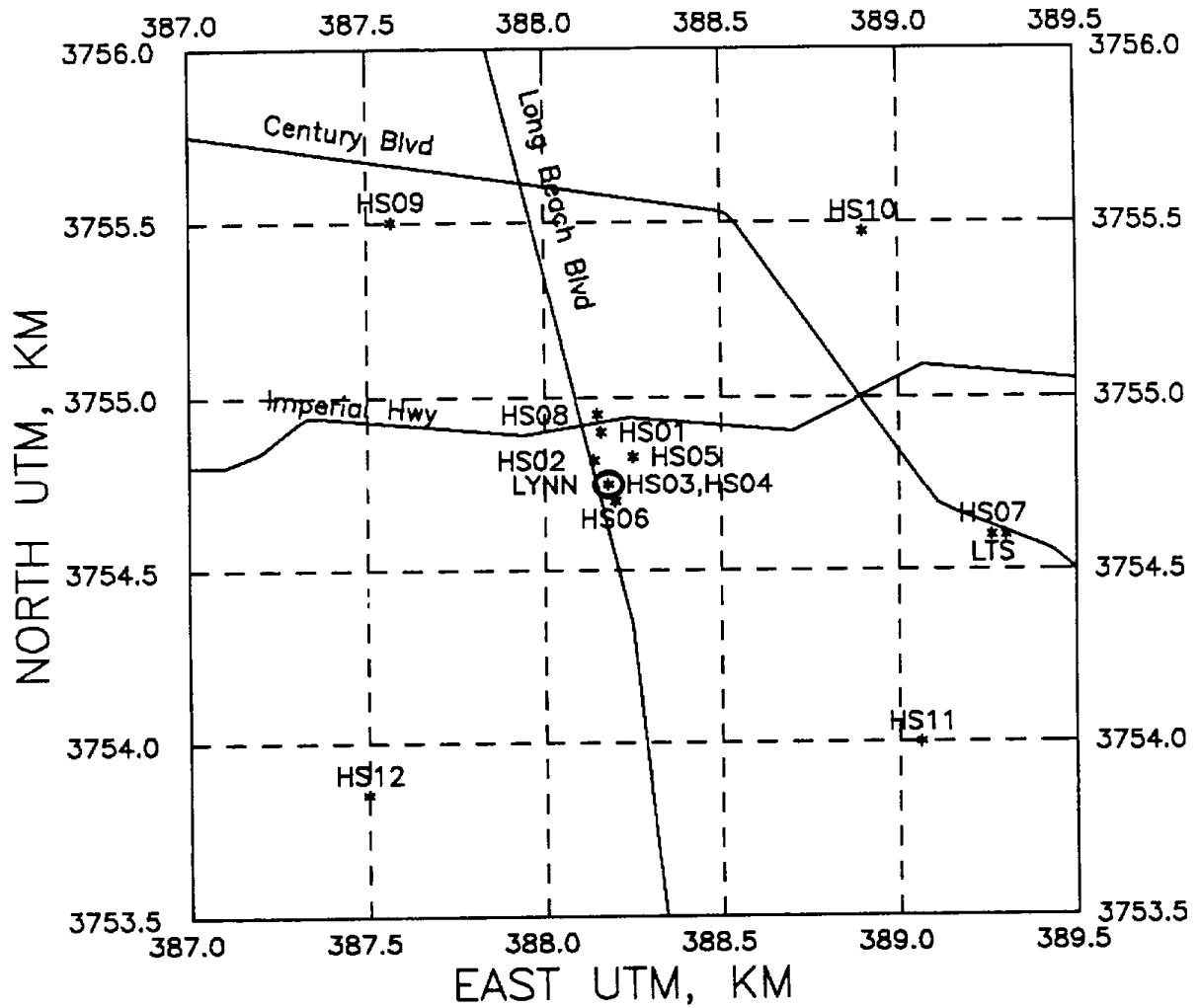


Figure 1-3. Locations of Sample Sites Within 1 km of LYNN.

increase in CO was not just the result of low wind-speed conditions. However, the monitoring report did not differentiate between locally generated CO and CO transported to the Lynwood site; determine specific meteorological conditions that are conducive to high CO concentrations; or determine the relative importance among sources, meteorology, or terrain as causes of high CO concentrations.

1.1 Objectives

The overall objectives of this study were to 1) determine why CO concentrations are higher at Lynwood than at any other monitoring location, 2) determine the relative contributions of local and areawide sources, and 3) determine the relative influence of meteorology, topography, and motor vehicle fleet characteristics on the CO concentrations at Lynwood.

To accomplish these objectives, this report addresses the following specific items:

- Identify source regions of CO (local and areawide) and their relative contributions to CO concentrations at Lynwood for each study period;
- Identify potential transport routes from source regions that contribute to CO at Lynwood during intensive periods, along with non-study periods when GMRL vehicle data are available;
- Identify topographic factors affecting CO concentrations at Lynwood for each episode and relative importance of these;
- Identify key meteorological parameters or scenarios responsible for high CO concentrations;
- Identify subperiods where source types, meteorological conditions, or other factors are shown to play a significant role in high CO concentrations, and characterize the relative importance of these factors.

These objectives were to be accomplished through an evaluation of the available data and analysis of those data considered valid.

2.0 EVALUATION OF DATA

2.1 CO and Tracer Bag Samples

Bag samplers were deployed at CC and HS sites to collect 1- and 2-hour samples during intensive measurement periods. At the end of each intensive, bags were returned to AV's laboratory where CO concentrations in the bags were measured with a nondispersive infrared CO analyzer. Bags were then sent to Tracer Technology, Inc., for perfluorocarbon analysis.

CO concentrations for AV's bag sample sites are summarized in Table 2-1 for the December intensive and Table 2-2 for the January intensive. CO data from the SCAQMD sites for the same periods are listed in Tables 2-3 and 2-4.

The initial evaluation of bag sample data by AV and ARB pointed to possible problems in the data collection. Some sites had tracer material appearing in samples before the time of release.

A review of AV's sampling and analytical procedures and field documentation did not uncover any systematic problems that would necessitate the adjustment of sampling times. A review of the data did, however, confirm that bag sample data from some sites were questionable because of a lack of temporal consistency in these data compared to data from SCAQMD sites and because of differences between bag samples and GM rover data when the vehicle was nearby.

The typical temporal variation of CO concentrations consists of one peak of CO associated with the morning rush hour and a second peak associated with, but often several hours later than, the evening rush hour. This pattern can be seen in Figures 2-1 and 2-2 for data collected at SCAQMD sites in the western part of the SoCAB on intensive days in December, 1989 and January, 1990. The vertical lines on the plots mark the hours of 0600 and 1800 PST to facilitate timing of peaks. Points below the zero line indicate missing data. These data show that, while some differences occurred in the times of evening peaks, the diurnal pattern of maxima during mid-morning and early-to-late evening hours and minima during midday and early morning hours occurred at all SCAQMD sites in the western part of the SoCAB. Such a pattern should also be evident at locations between SCAQMD sites even if it is partially masked by the contribution of local sources at other times.

Time series of CO data for bag samples are shown in Figures 2-3 and 2-4 for CC sites and in Figures 2-5 and 2-6 for HS sites. A detailed inspection of these figures shows that the expected evening and morning maxima in CO concentration were not present at a number of sites. Thus, these data become highly suspect with the possible cause of problems being the timing of data. Most of the CC sites, as well as the HS sites closest to LYNN (HS01, HS02, HS03, HS05, HS06, HS08), had diurnal variations similar to those at other SCAQMD sites. The variations of the data from the other HS sites, however, did not conform with the two maxima

Table 2-1

**Summary of AeroVironment CO Data for December, 1989 Intensive Period
December 19, 1200 to 20, 1100**

<u>Site</u>	<u>Obs.</u>	<u>CO Concentration in PPM</u>			
		<u>Mean</u>	<u>Std. Dev.</u>	<u>Min.</u>	<u>Max.</u>
<u>2-Hour Samples</u>					
AQ02	0	--	--	--	--
AQ03	1	23.97	1.40	1.90	6.13
CC01	1	14.63	1.74	1.63	7.25
CC02	0	--	--	--	--
CC03	9	2.82	0.67	2.00	4.00
CC04	11	4.72	1.27	2.75	6.88
CC05	0	--	--	--	--
CC06	0	--	--	--	--
CC07	11	5.18	2.64	1.56	9.88
CC08	12	3.51	1.82	1.56	7.56
CC09	0	--	--	--	--
CC10	12	3.75	1.60	1.88	7.50
CC11	0	--	--	--	--
CC12	12	3.89	2.78	1.25	8.38
CC13	12	1.87	0.22	1.63	2.50
CC14	6	6.59	2.45	2.75	9.13
CC15	12	3.00	1.85	1.13	5.75
CC16	12	5.67	3.17	1.75	10.2
CC17	7	8.76	3.68	2.88	12.75
CC18	12	5.73	2.75	1.50	9.38
CC19	9	4.74	2.74	1.63	10.00
CC20	11	4.66	1.53	2.50	7.63
CC21	0	--	--	--	--
HS01	3	2.88	0.33	2.63	3.25
HS07a	7	7.14	1.80	4.25	9.13
HS07b	11	4.57	1.75	1.60	7.25
HS07c	12	3.90	1.38	1.80	6.13
HS13	11	5.44	5.21	1.75	16.25
HS14	9	4.57	1.79	2.50	7.25
HS15	12	6.64	4.48	1.63	15.50
HS16	0	--	--	--	--
<u>1-Hour Samples</u>					
HS02	23	6.93	3.71	2.50	14.75
HS03	0	--	--	--	--
HS04	0	--	--	--	--
HS05	23	7.86	3.87	2.63	14.13
HS06	0	--	--	--	--
HS08	0	--	--	--	--
HS09	20	7.30	4.25	2.00	16.38
HS10	24	6.80	3.69	2.13	14.25
HS11	0	--	--	--	--
HS12	22	7.71	5.00	2.00	20.63

Table 2-2

**Summary of AeroVironment CO Data for January, 1990 Intensive Period
January 8, 1200 to 10, 0300**

<u>Site</u>	<u>Obs.</u>	<u>CO Concentration in PPM</u>			
		<u>Mean</u>	<u>Std Dev.</u>	<u>Min.</u>	<u>Max.</u>
<u>2-Hour Samples</u>					
AQ02	17	7.58	4.41	2.13	17.00
AQ03	12	4.90	1.64	2.43	7.25
CC01	10	5.71	1.40	3.90	8.35
CC02	0	--	--	--	--
CC03	9	3.19	0.98	1.83	4.38
CC04	12	5.78	1.73	3.20	9.75
CC05	9	5.65	2.01	2.75	8.75
CC06	10	5.33	1.64	3.18	7.38
CC07	0	--	--	--	--
CC08	18	5.34	2.33	1.40	9.90
CC09	0	--	--	--	--
CC10	18	5.69	2.68	2.50	11.63
CC11	0	--	--	--	--
CC12	0	--	--	--	--
CC13	18	7.11	2.83	2.75	12.25
CC14	12	5.94	1.98	3.38	10.38
CC15	0	--	--	--	--
CC16	17	6.32	3.07	1.75	12.88
CC17	12	5.62	2.48	1.58	8.50
CC18	12	6.01	2.49	2.38	10.13
CC19	18	7.04	3.25	2.50	12.75
CC20	0	--	--	--	--
CC21	12	5.50	1.88	3.55	9.08
HS01	17	8.95	4.62	2.63	18.55
HS07a	18	8.57	4.02	4.15	17.50
HS07b	16	6.38	1.57	4.13	9.13
HS07c	18	5.80	1.98	3.25	10.75
HS13	12	6.11	3.57	1.88	15.00
HS14	15	5.56	1.44	3.75	8.63
HS15	16	8.96	3.79	3.00	15.95
HS16	16	8.60	4.94	3.50	19.00
<u>1-Hour Samples</u>					
HS02	32	9.15	4.38	3.50	20.43
HS03	33	9.36	4.44	3.25	20.13
HS04	0	--	--	--	--
HS05	34	8.89	4.20	2.63	16.68
HS06	34	9.32	4.99	2.50	21.50
HS08	35	10.49	5.26	4.00	25.00
HS09	0	--	--	--	--
HS10	29	7.44	4.59	3.25	22.25
HS11	0	--	--	--	--
HS12	28	6.47	3.83	1.63	17.13

Table 2-3

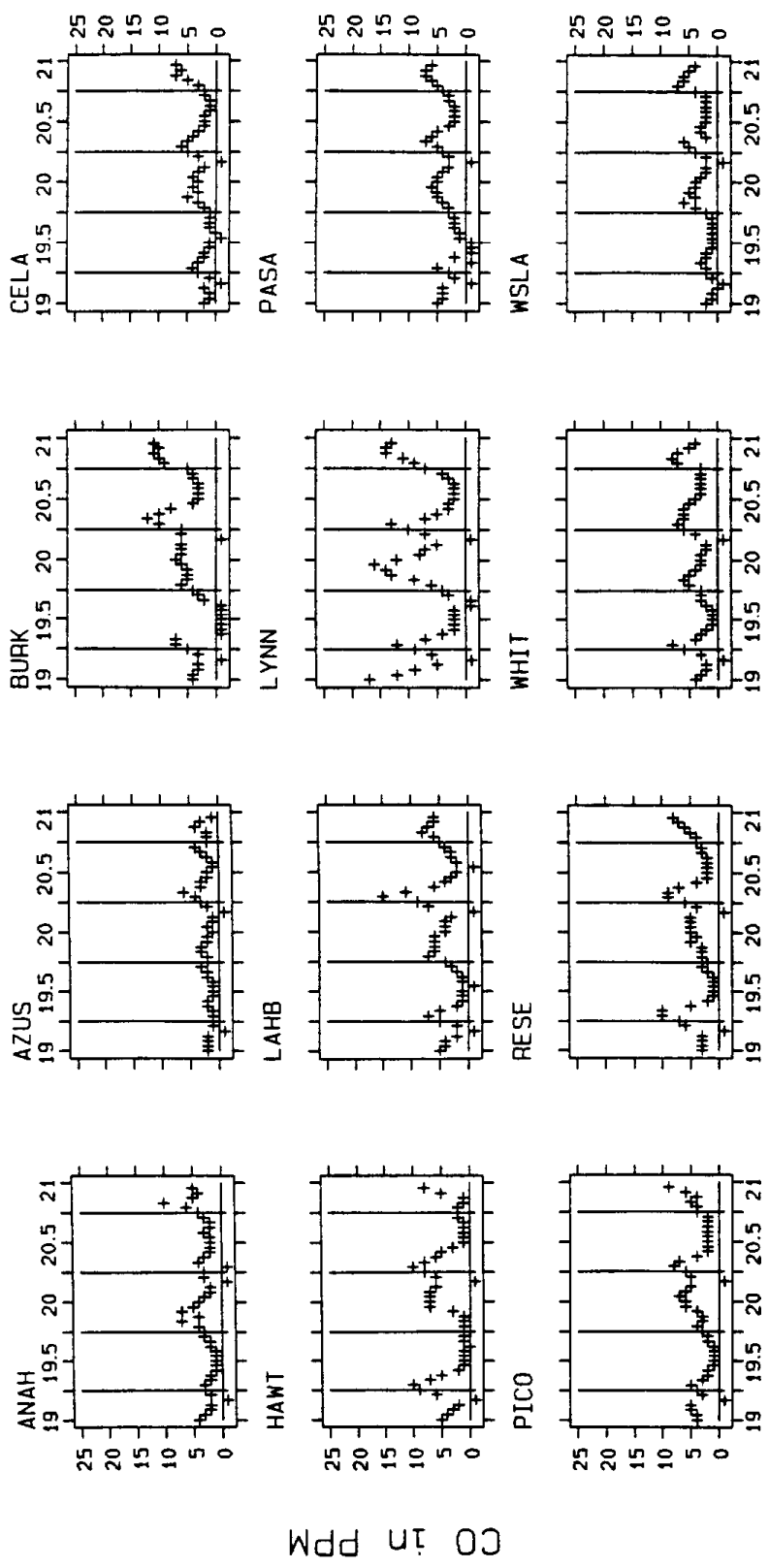
**Summary of South Coast AQMD CO Data for December, 1989 Intensive Period
December 19, 1200 to 20, 1100**

<u>Site</u>	<u>Obs.</u>	<u>CO Concentration in PPM</u>			
		<u>Mean</u>	<u>Std Dev.</u>	<u>Min.</u>	<u>Max.</u>
ANAH	22	3.09	1.66	1	7
AZUS	23	2.26	1.18	1	6
BURK	19	6.16	2.46	2	12
CELA	22	2.82	1.62	0	6
HAWT	23	4.00	3.13	0	10
LAHB	22	5.14	3.37	1	15
LGBH	23	5.07	2.25	2	9
LYNN	21	7.19	4.37	2	16
PASA	22	3.82	1.65	1	7
PICO	23	3.87	2.20	1	8
RESE	23	3.91	2.33	1	9
WHIT	23	3.78	1.86	1	7
WSLA	23	2.91	1.65	1	6

Table 2-4

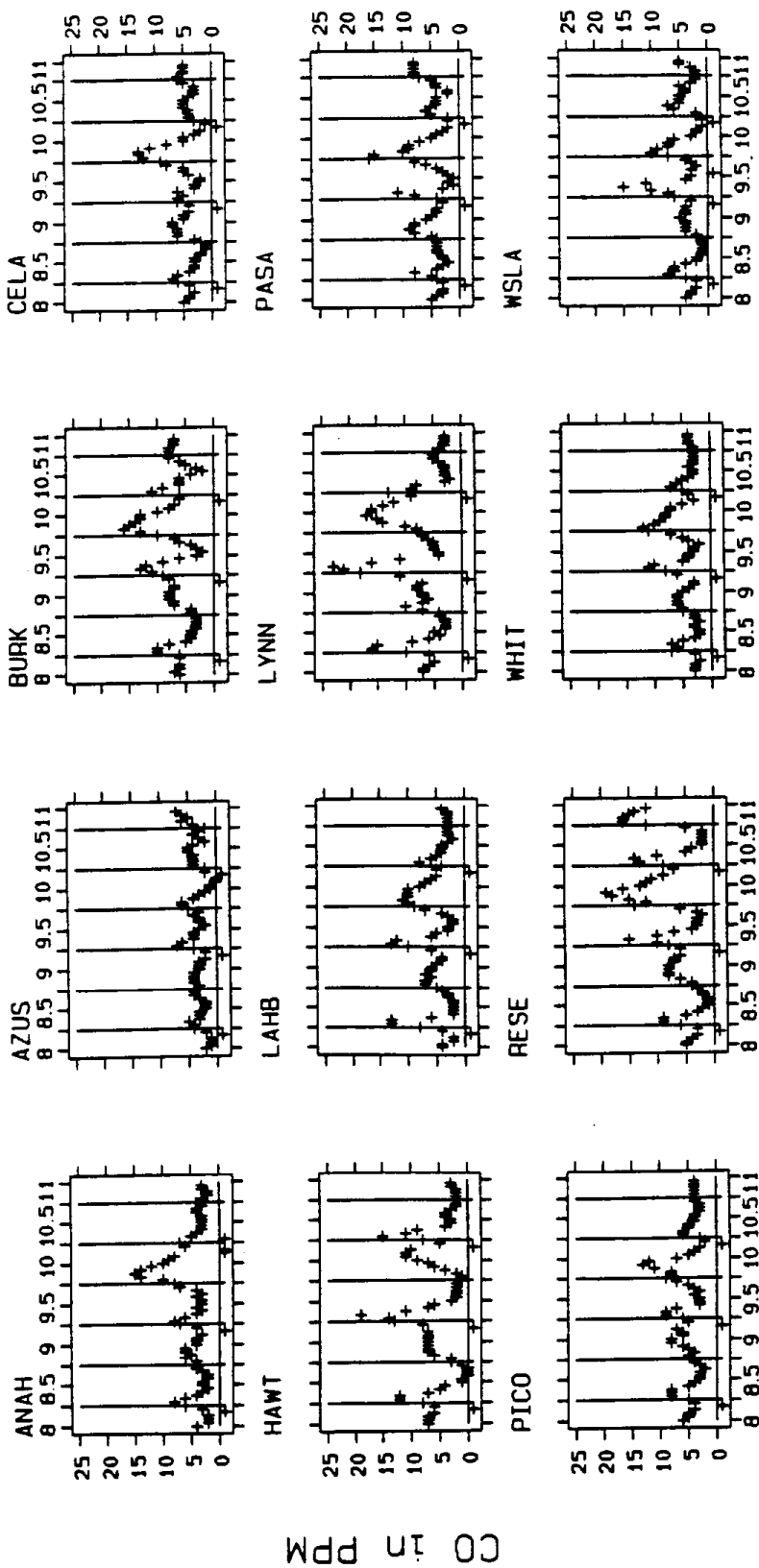
**Summary of South Coast AQMD CO Data for January, 1990 Intensive Period
January 8, 1200 to 10, 0300**

<u>Site</u>	<u>Obs.</u>	<u>CO Concentration in PPM</u>			
		<u>Mean</u>	<u>Std Dev.</u>	<u>Min.</u>	<u>Max.</u>
ANAH	38	5.87	3.48	2	15
AZUS	39	3.28	1.54	0	7
BURK	39	7.56	3.91	2	16
CELA	39	5.21	3.13	1	13
HAWT	39	5.56	4.44	0	19
LAHB	39	6.03	3.05	2	13
LGBH	39	6.05	2.18	2	10
LYNN	39	9.15	5.36	3	23
PASA	39	5.62	3.48	1	16
PICO	39	5.77	2.72	2	13
RESE	39	7.56	4.96	1	19
WHIT	39	5.56	2.74	2	12
WSLA	38	4.45	3.24	1	15



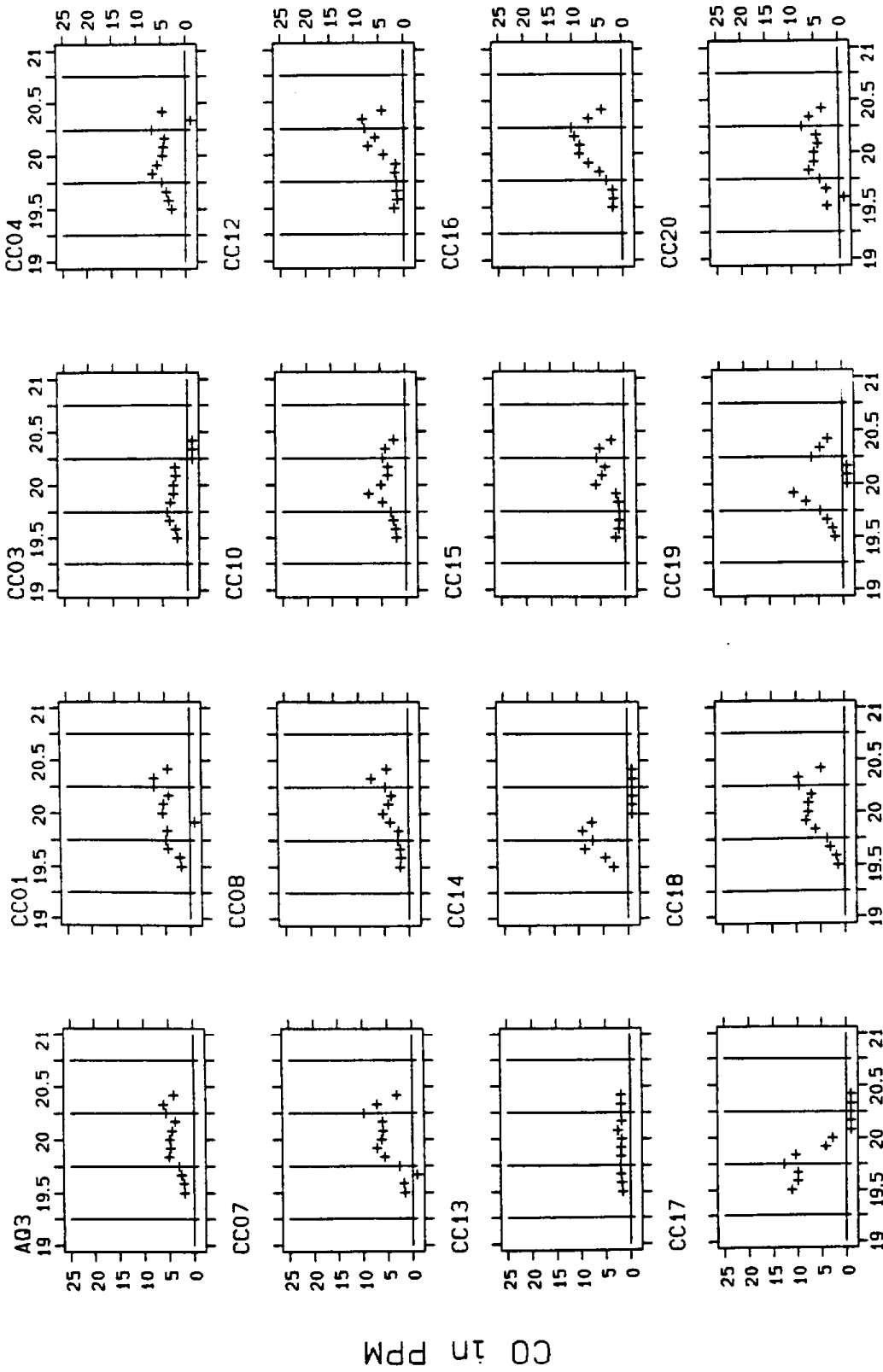
DAY - DECEMBER INTENSIVE, 1989

Figure 2-1. CO Concentrations at SCAQMD Sites during December, 1989 Intensive Period. Symbol at -1 denotes missing data.



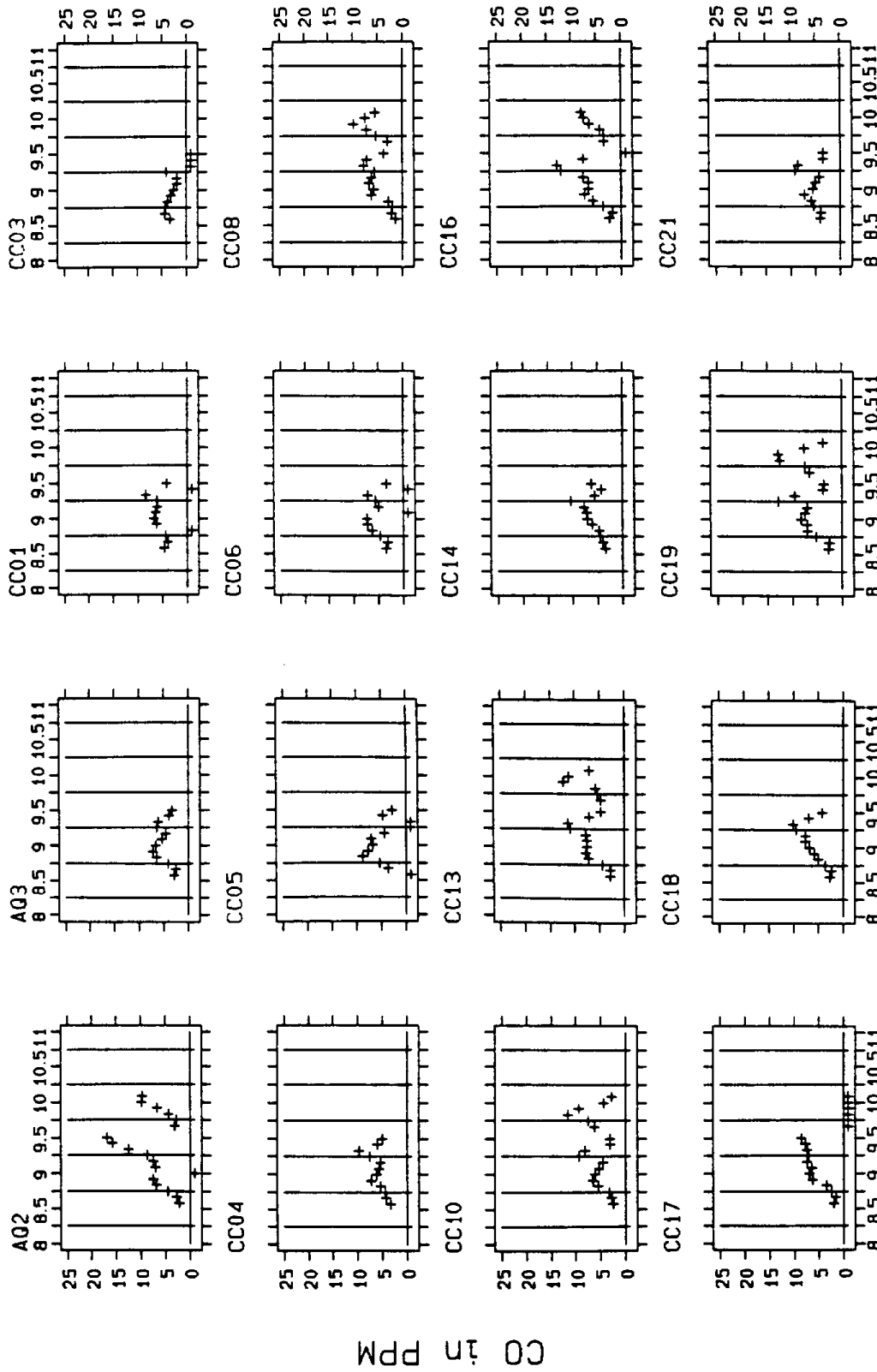
DAY - JANUARY, 1990 INTENSIVE

Figure 2-2. CO Concentrations at SCAQMD Sites during January, 1990 Intensive Period. Symbol at -1 denotes missing data.



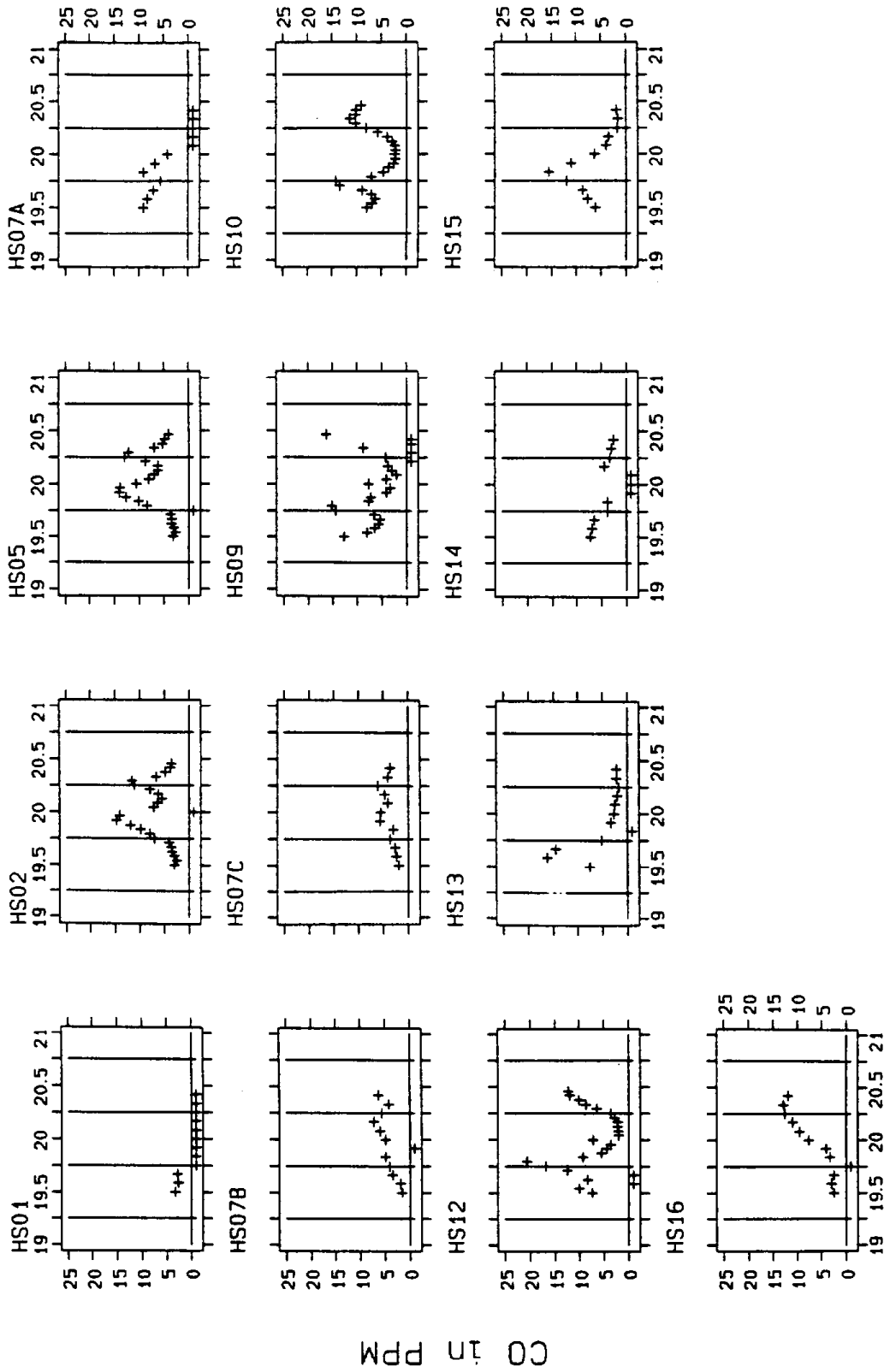
DAY - DECEMBER INTENSIVE, 1989

Figure 2-3. CO Concentrations at CC Sites during December, 1989 Intensive Period. Sites with no data are not included. Symbol at -1 denotes missing data.



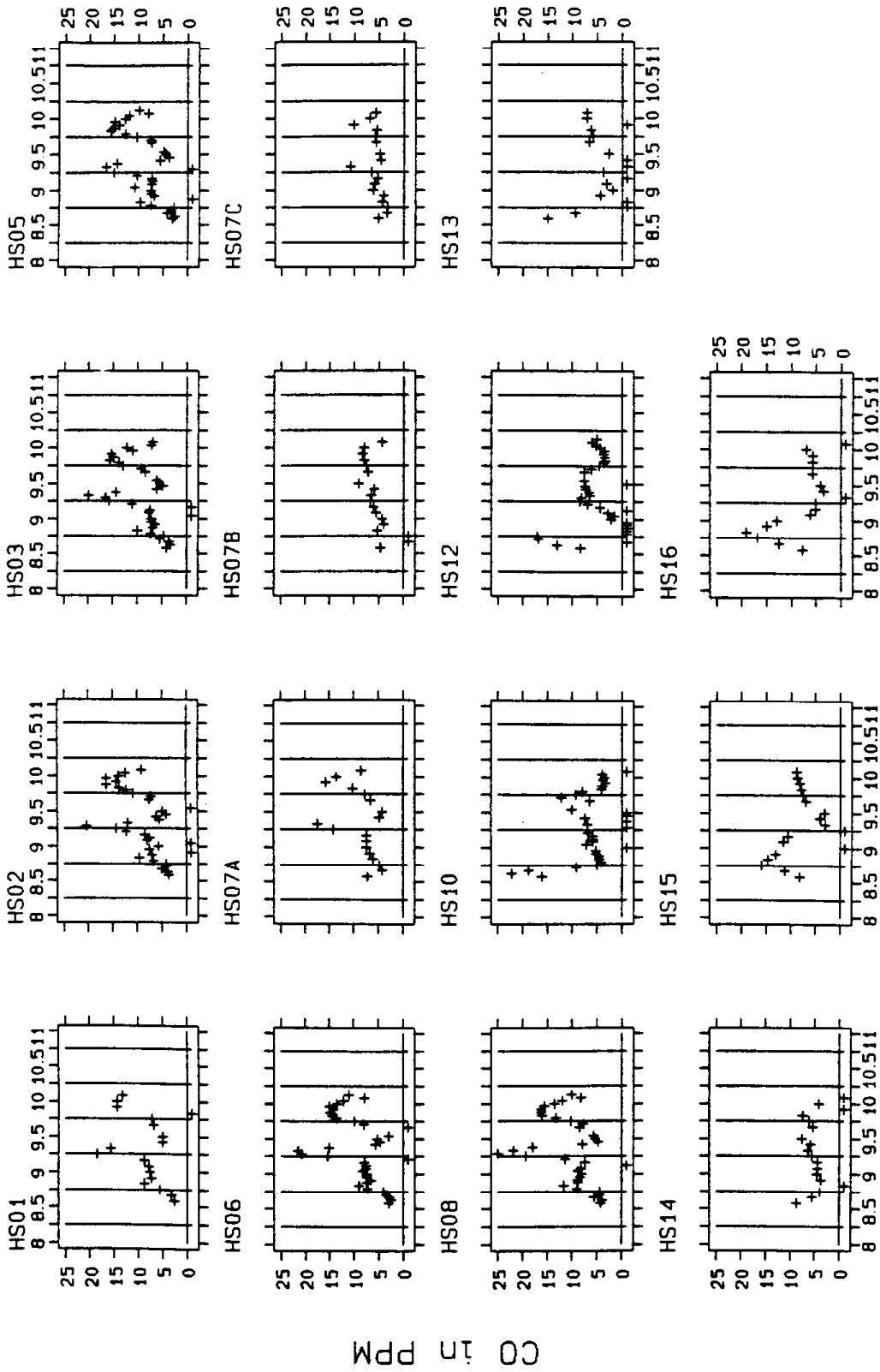
DAY - JANUARY INTENSIVE, 1990

Figure 2-4. CO Concentrations at CC Sites during January, 1990 Intensive Period. Sites with no data are not included. Symbol at -1 denotes missing data.



DAY - DECEMBER INTENSIVE, 1989

Figure 2-5. CO Concentrations at HS Sites during December, 1989 Intensive Period. Sites with no data are not included. Symbol at -1 denotes missing data.



DAY - JANUARY INTENSIVE, 1990

Figure 2-6. CO Concentrations at HS Sites during January, 1990 Intensive Period. Sites with no data are not included. Symbol at -1 denotes missing data.

pattern. These were the sites located 1 km (HS09, HS10, HS12, no data at HS11) and 4 km (HS13, HS14, HS15, HS16) from LYNN. Table 2-5 evaluates the similarity of the evening and morning maximum CO concentrations at bag sample sites to those at nearby SCAQMD sites.

As an additional check on the temporal variation of the bag samples, data from HS sites were compared to data collected by GM's Pontiac rover vehicle on 19-20 December, 1989 (Section 2.2, below). Concentrations from the vehicle were averaged when it was within half a kilometer of a sampling site and compared to the corresponding bag samples for the hour. Figure 2-7 shows CO data for the LYNN site and selected HS sites and for the Pontiac in the vicinity of those sites. Open circles indicate hourly concentrations for bag samples at the beginning of the sample while pluses are data from the Pontiac for the shorter times while it was near the site. At the LYNN and HS05 sites, vehicle data showed similar magnitude and temporal variation as the continuous data. Concentrations ranged from 15 to 25 ppm between 2000 and 2400 PST and then decreased during the next several hours. While differences between vehicle and stationary data were evident, the trends in the data were similar. In contrast, CO from sites HS09, HS10, HS12, and HS13 peaked and decreased before the vehicle CO. CO at site HS14, with several missing hours, showed little variation. CO at site HS15 had an evening peak similar to that at LYNN but no morning peak. CO at HS16 had a broad morning peak but no evening peak.

Analysis of the patterns in CO concentrations by empirical orthogonal functions (EOF) presented in Section 3.9, below, confirms that data from several supplemental sites were not consistent with data from SCAQMD sites. While one might speculate that several unusual sources of CO exist within 1 to 4 km of the SCAQMD site, it is expected that the typical diurnal pattern should still be present in the samples.

Most of the sites for which CO compared poorly to SCAQMD sites also indicated the presence of tracer material before the time of tracer release. Table 2-6 compares times of samples with tracer to times of tracer release. The early appearance of tracer material could indicate other sources of the material, contamination of samples during handling or analysis, or mistimed samples. Other sources and contamination might be expected to appear in more than just a few samples. The supposition that samples were mistimed is consistent with above comparisons to SCAQMD data. It appears that some bag samplers did not operate in the intended sequence. Given the available information, no method has been devised to correct the times of bag samples.

2.2 GM Rover Data

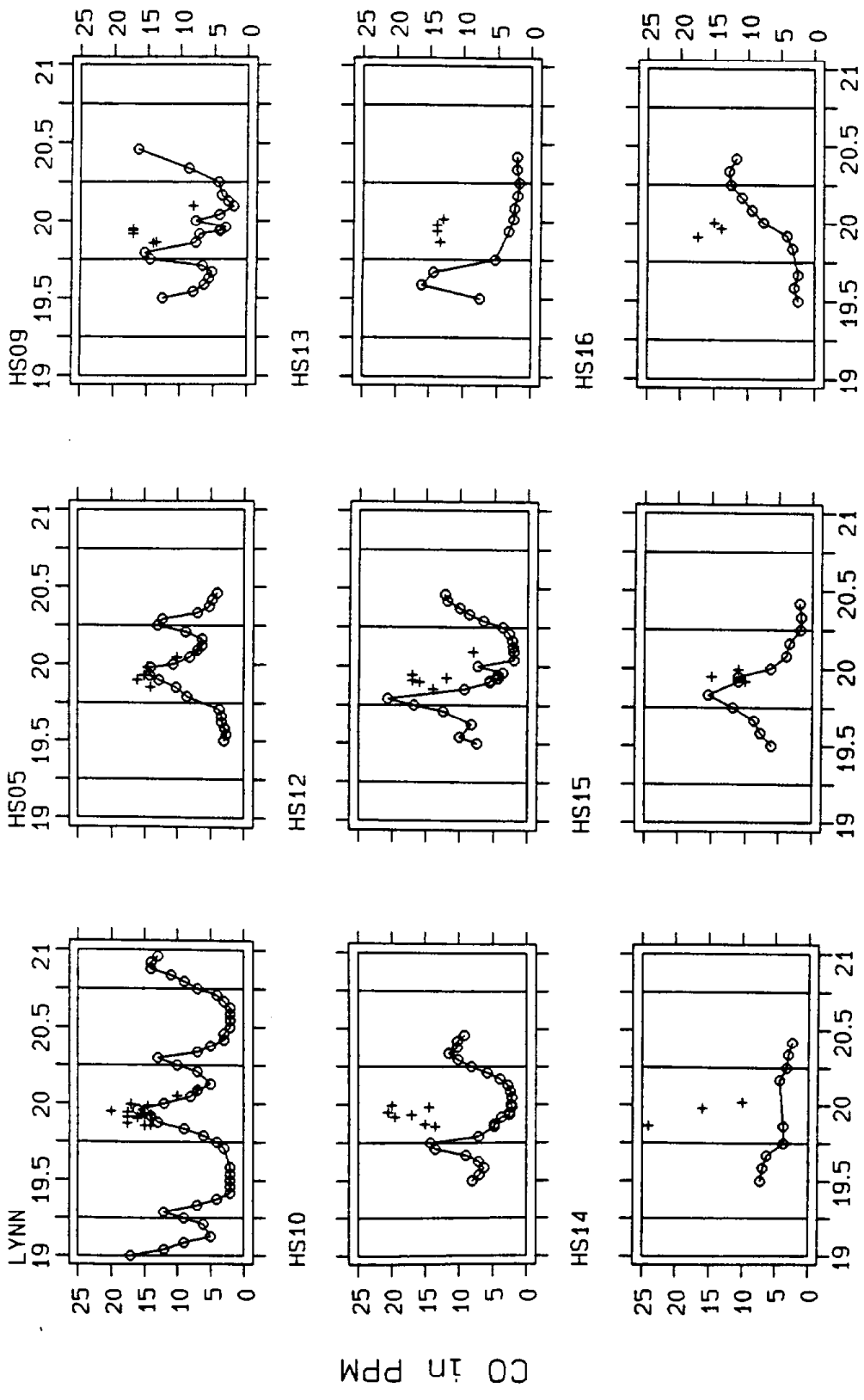
General Motors Research Laboratories collected ambient CO data in the vicinity of Lynwood from 1 December to 20 December 1989 using instruments that were installed in two vehicles. A Pontiac contained a standard Monitor Labs Model 8310 CO analyzer, while an Oldsmobile contained a Draeger CO instrument. For the Pontiac, data were collected through a sample tube installed outside the car at the top of the rear window for all days except 19-20 December, when the samples were collected inside the car from the heater vent. All Oldsmobile

Table 2-5

Evaluation of CO Bag Samples by Similarity to Nearby SCAQMD Sites

<u>Site</u>	<u>December</u>	<u>January</u>	<u>SCAQMD Site</u>
AQ02	No Data	Good	HAWT
AQ03	Good	Good	CELA
CC01	Good	Good	BURK
CC02	No Data	No Data	-
CC03	Good	Good	AZUS
CC04	Good	Good	CELA
CC05	No Data	Good	CELA
CC06	No Data	Good	PICO
CC07	Good	No Data	HAWT/WSLA
CC08	Good	Good	HAWT/WSLA
CC09	No Data	No Data	-
CC10	Good	Good	LYNN/PICO
CC11	No Data	No Data	-
CC12	Good	Good	HAWT
CC13	Poor	Good	LYNN/HAWT
CC14	Good	Good	WHIT
CC15	Good	Good	HAWT
CC16	Good	Good	HAWT/LYNN
CC17	Poor	Good	LYNN/LGBH
CC18	Good	Good	LYNN/LGBH
CC19	Poor	Good	LYNN
CC20	Good	No Data	CELA
CC21	No Data	Good	CELA
HS01	3 Samples	Good	LYNN
HS02	Good	Good	LYNN
HS03	No Data	Good	LYNN
HS04	No Data	No Data	-
HS05	Good	Good	LYNN
HS06	No Data	Good	LYNN
HS07a	Poor	Good	LYNN
HS07b	Poor	Poor	LYNN
HS07c	Good	Good	LYNN
HS08	No Data	Good	LYNN
HS09	Poor	No Data	LYNN
HS10	Poor	Poor	LYNN
HS12	Poor	Poor	LYNN
HS13	Poor	Poor	LYNN
HS14	Poor	Poor	LYNN
HS15	Poor	Poor	LYNN
HS16	Poor	Poor	LYNN

Hourly CO Concentration + Pontiac CO Concentration



DAY - DECEMBER INTENSIVE

Figure 2-7. Pontiac CO Measurements Near LYNN and HS Sites.

Table 2-6
Time of Tracer Sample Relative to Release - 1700 through 2300

Site	December				January			
	PMCP	PMCH	PDCH	PTCH	PMCP	PMCH	PDCH	PTCH
AQ02(HAWT)	N	N	N	N	A	A	A	A
AQ03(CELA)	Z	Z	Z	Z	Z	Z	Z	Z
CC01	Z	Z	Z	Z	Z	Z	Z	Z
CC02	N	N	N	N	N	N	N	N
CC03	Z	Z	Z	Z	Z	Z	Z	Z
CC04	Z	Z	Z	Z	Z	Z	Z	Z
CC05	N	N	N	N	Z	Z	Z	Z
CC06	N	N	N	N	A	A	Z	Z
CC07	Z	E	E	Z	N	N	N	N
CC08	Z	Z	Z	Z	A	A	A	A
CC09	N	N	N	N	N	N	N	N
CC10	Z	Z	Z	Z	A	A	A	A
CC11	N	N	N	N	N	N	N	N
CC12	A	A	A	A	N	N	N	N
CC13	Z	Z	Z	Z	A	A	Z	A
CC14	E	EA	E	E	A	Z	A	Z
CC15	EA	E	E	A	N	N	N	N
CC16	A	A	A	A	A	A	A	A
CC17	E	E	E	E	A	A	A	Z
CC18	A	A	Z	Z	A	A	A	Z
CC19	A	Z	Z	Z	A	A	A	Z
CC20	N	N	N	N	N	N	N	N
CC21	N	N	N	N	Z	Z	Z	Z
HS01	E	E	E	Z	A	A	Z	A
HS02	A	A	A	A	N	N	N	N
HS03(LYNN)	N	N	N	N	A	Z	Z	A
HS04	N	N	N	N	N	N	N	N
HS05	N	N	N	N	N	N	N	N
HS06	N	N	N	N	A	A	Z	A
HS07a	E	E	Z	E	Z	Z	Z	Z
HS07b	EA	EA	A	A	N	N	N	N
HS07c	A	A	Z	A	EA	EA	A	Z
HS08	N	N	N	N	N	N	N	N
HS09	E	E	Z	EA	N	N	N	N
HS10	EA	Z	Z	A	A	Z	Z	Z
HS11	N	N	N	N	N	N	N	N
HS12	E	E	Z	EA	EA	EA	Z	E
HS13	Z	Z	Z	Z	EA	EA	Z	Z
HS14	E	Z	Z	Z	EA	EA	Z	Z
HS15	E	E	Z	Z	EA	EA	Z	Z
HS16	EA	EA	Z	A	EA	EA	EA	EA

E - Earlier than release
A - During or after release
EA - Appearance before release and after start of release
Z - No samples with concentrations above zero
N - No samples collected and/or analyzed

samples were collected inside the car from the heater vent. Both instruments had morning and afternoon calibrations at 0 and 45 ppm concentrations. CO, mileage, and time data were collected every two seconds and recorded on data acquisition systems in the cars. Voice records of locations and unusual occurrences were also made during the sample runs.

Most data were collected along the same paths. Four loops were repeated in the vicinity of LYNN near the intersection of Long Beach Blvd. and Imperial Hwy., the corner common to all loops. For each sampling run, the end points of each leg of each loop have been determined from voice tapes and mileage locators and data tagged with loop, sector identification, and leg numbers to identify the location of the data collection. Table 2-7 lists the sector and leg designations. Figure 2-8 shows a map of the streets covered, the location of the LYNN site, and the directions of travel. Average CO concentrations along each leg have been computed for both vehicles and are available on request.

Vehicle CO data were compared to hourly CO data from LYNN. For each loop, data collected in the vicinity of LYNN were combined into an estimate of the hourly CO concentrations while hourly SCAQMD data at the same times were compiled. Data used in this comparison are listed in Tables A-1 and A-2 in Appendix A. Paired differences were computed and a t-test applied. The t-statistic was computed from the mean of the differences between vehicle CO and its standard deviation for N pairs:

$$t = [\text{Mean}(\text{CO}_{\text{PONT}} - \text{CO}_{\text{OLDS}})] / [\text{Std}(\text{CO}_{\text{PONT}} - \text{CO}_{\text{OLDS}}) / N^{1/2}] \quad (1)$$

For a total of 46 loops, the data collected outside the Pontiac averaged 6.3 ppm higher than data from LYNN with a standard deviation of the paired differences of 3.4 ppm. The t-test on the paired differences gave a t-statistic of 12.51, which implies a highly significant statistical difference between the Pontiac and LYNN data. For the samples collected from the heater vent of the Pontiac, the vehicle data averaged 3.5 ppm higher than the LYNN data, with a standard deviation of 2.6 ppm. A t-test on the paired differences gave a t-statistic of 3.75, which indicates a difference that is also statistically significant at the 1% significance level. Figure 2-9 compares Pontiac and LYNN data. The circles are for data collected outside the vehicle, while the triangles are for data collected inside the vehicle. The regression line is only for data collected outside the vehicle. Collecting data inside the vehicle appears to be a better method although only a few samples were made.

A similar comparison was made between data collected by the Oldsmobile and at LYNN, the data from which are given in Table A-3 in Appendix A. For a total of 68 loops, the Oldsmobile data averaged 5.5 ppm higher than data at LYNN, with a standard deviation of the paired differences of 4.5 ppm. The t-test on the paired differences gave a t-statistic of 10.04 and a highly significant statistical difference between the two samples. Figure 2-10 shows the comparison between Oldsmobile and LYNN data.

The higher vehicle measurements probably resulted from the influence of traffic near the vehicles. CO would have had some chance to disperse before reaching sample inlet at LYNN.

Table 2-7

GM Vehicle Paths - Loop and Segment Flags

Northwest - Loop #1

- 1 Long Beach (Northbound)
- 2 Firestone (Westbound)
- 3 Central (Southbound)
- 4 Imperial (Eastbound)

Northeast - Loop #2

- 1 Long Beach (Northbound)
- 2 Firestone (Eastbound)
- 3 I-710 (Southbound)
- 4 Imperial (Westbound)

Southwest - Loop #3

- 1 Long Beach (Southbound)
- 2 Rosecrans (Westbound)
- 3 Wilmington (Northbound)
- 4 Imperial (Eastbound)

Southeast - Loop #4

- 1 Imperial (Eastbound)
- 2 I-710 (Southbound)
- 3 Alondra (Westbound)
- 4 Long Beach (Northbound)

Airport Inbound - Leg #5

Hughes Garage to Lynwood via Imperial

Airport Outbound - Leg #6

Lynwood to Hughes Garage via Imperial



Figure 2-8. Paths of General Motors Vehicles during Collection of Ambient CO Concentration in Vicinity of Lynwood.

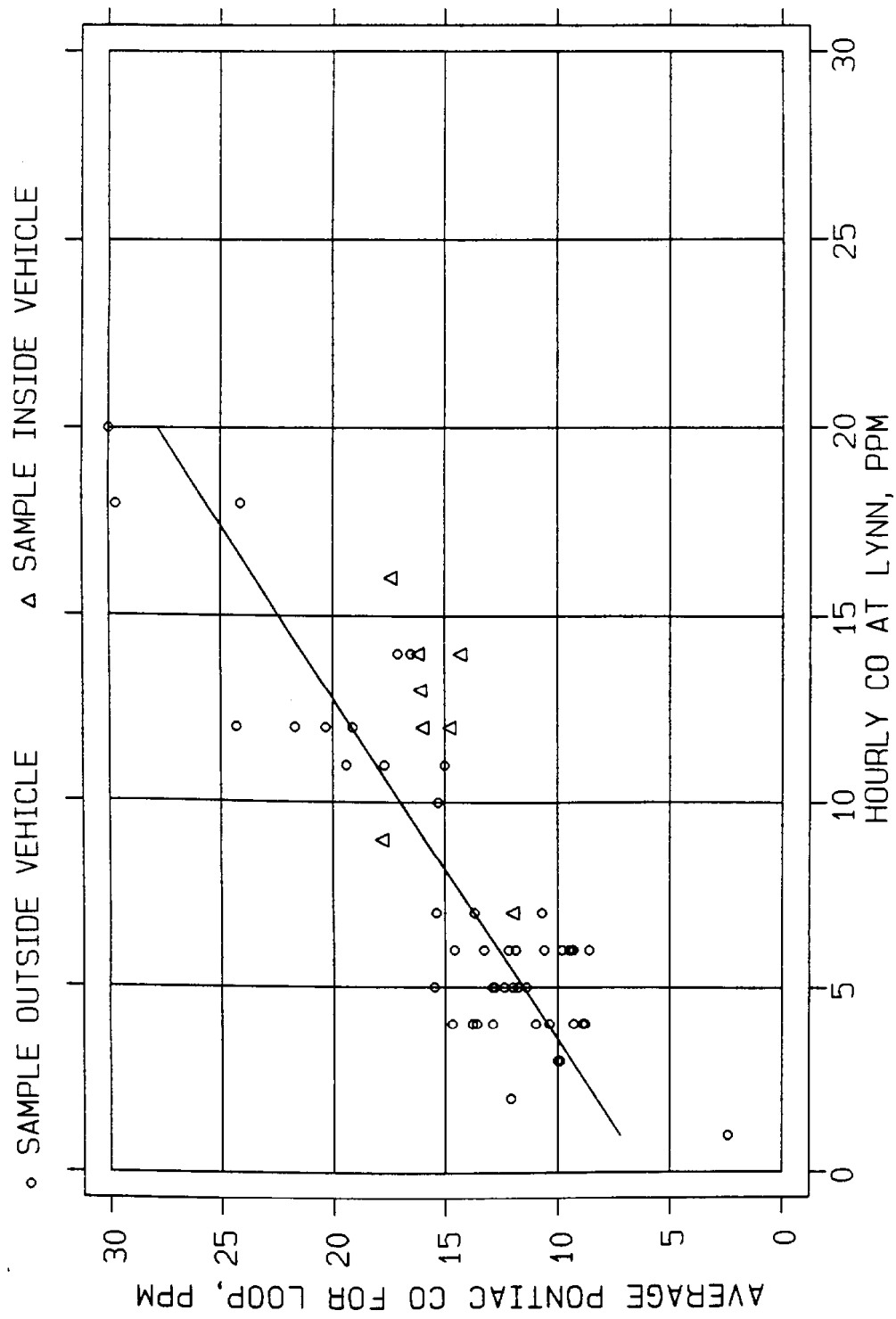


Figure 2-9. Pontiac CO Concentrations Near LYNN.
 Linear Regression, outside data: $CO_{PONT} = 1.088 CO_{LYNN} + 6$
 $R = 0.880$

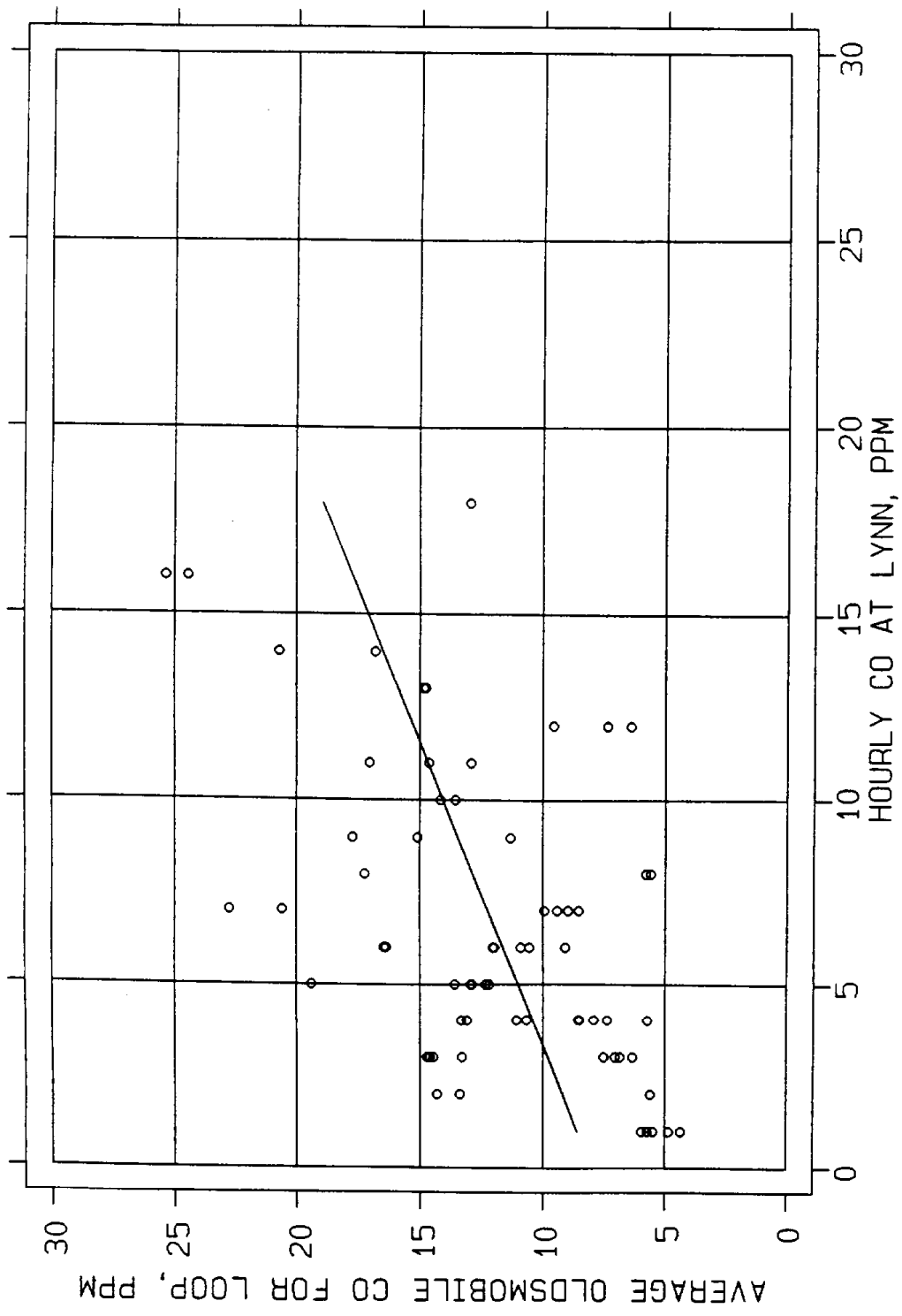


Figure 2-10. Oldsmobile CO Concentrations Near LYNN.
 Linear Regression: $CO_{OLDS} = 0.608 CO_{LYNN} + 8$
 $R = 0.515$

Most of the vehicle data were collected at times of relatively high vehicle counts, but not necessarily during the highest CO concentrations. Most of the vehicle operation occurred near the end of the morning rush hour when CO concentrations were decreasing and during the evening rush hour before CO concentrations reached their peak. Data collected by the Pontiac between 2000 and 2400 PST on 19 December 1989, when CO concentrations were high and after traffic counts decreased, compared much better to SCAQMD data.

Additional problems developed in the Oldsmobile data near the end of the study when the data had very little variation. It is likely that the instrument had some response problems.

Early in the study, there were some comparisons made between data collected by the two vehicles. They were driven together along the same paths and their simultaneous data compared. The t-test of the paired differences was applied to a total of 53 comparison legs. With a mean of paired differences of 0.2 ppm and standard deviation of 3.9 ppm, the resulting t-statistic was 0.35. A statistically significant difference at the 5% significance level (95% chance that the differences are real) requires a t-statistic for 53 degrees of freedom to exceed 2.01. Thus the difference between the Pontiac and Oldsmobile data had no statistically significant difference. The data did, however, have a large variation and relatively poor correlation as shown in Figure 2-11.

Data for mileage for the two vehicles were also compared. For the 53 runs, the mean of the differences between the paired Pontiac and Oldsmobile mileage data was 0.6 mi with a standard deviation of 0.9 mi. The t-test gave a t-statistic of 5.04, which shows a statistically significant difference at a level that exceeds the 1% significance level.

An attempt was made to use the vehicle data to calculate the flux of CO into and out of the area defined by the vehicle paths to try to determine the relative effects of locally generated CO and transported CO. Vehicle data were used to calculate the flux of CO out of each loop by combining the average CO concentration along each leg with the estimated component of wind velocity normal to the leg. Within a loop, the change in CO concentration should have depended on the difference between the net flux from the loop and any source of CO inside the loop. Data from LYNN were used to estimate the change in CO levels during the measurements as a measure of change of CO inside the loops. The vehicle measurements, however, were too contaminated by nearby traffic, as noted above, to provide reliable data along the paths that would have been representative of CO being transported into a loop. The results of this work are not reported here.

2.3 Terrain Data

Terrain elevations in the western part of the SoCAB were obtained from U.S. Geological Survey (USGS) 7.5 minute topographic maps. Elevations were manually digitized on a 1 km by 1 km grid spacing using the Universal Transverse Mercator (UTM) coordinate system. Gridded terrain covered UTM coordinates 355 to 420 km East and 3720 to 3785 km North, all in Zone 11. Contoured terrain in the various maps were generated with Surfer software from Golden West, Inc.

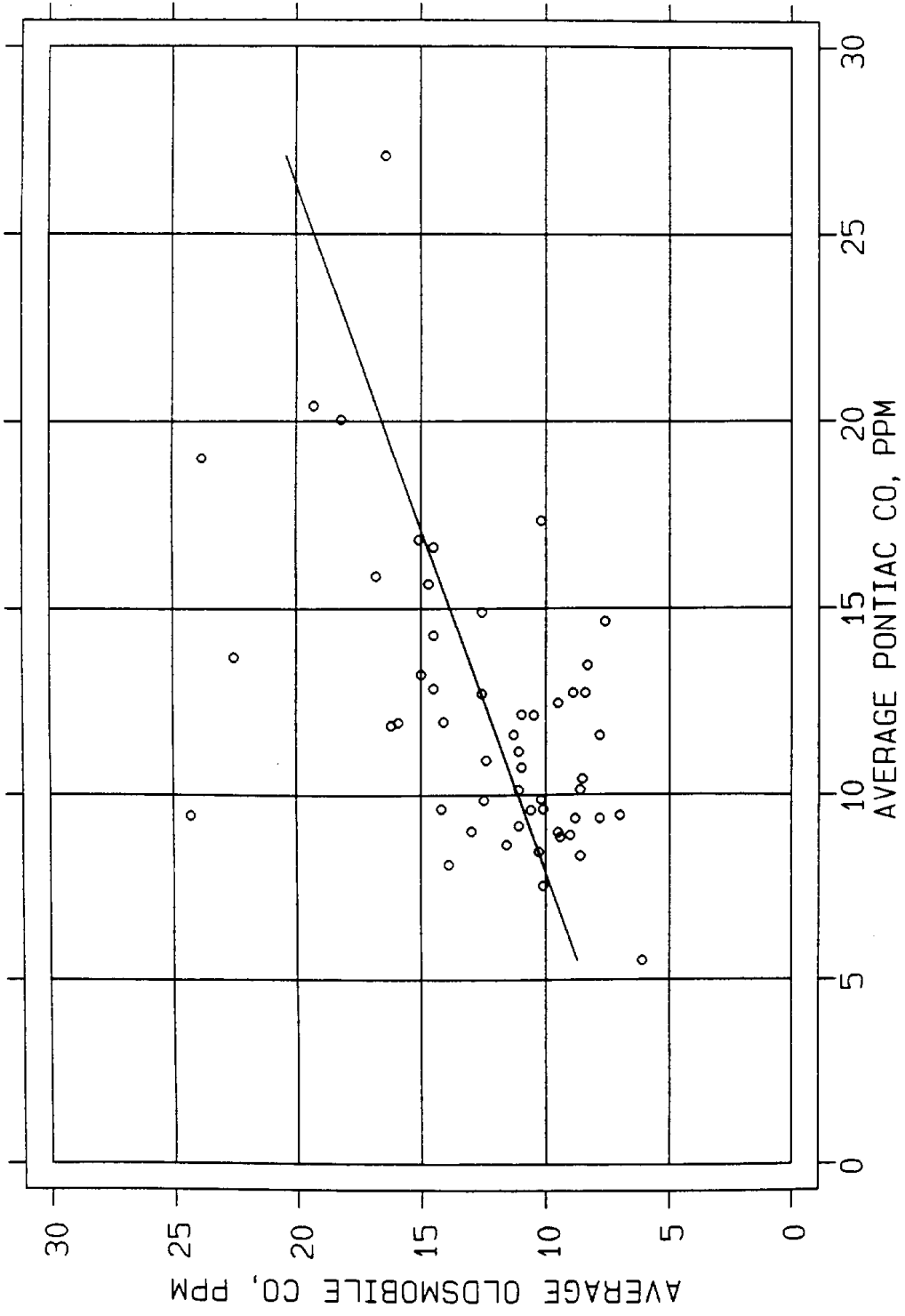


Figure 2-11. CO Concentrations from GM Rover Vehicles on Concurrent Legs.
 Linear Regression: $CO_{OLDS} = 0.544 CO_{PONT} + 6$
 $R = 0.510$

2.4 Meteorological Data

Routinely collected meteorological data consisted of hourly averaged surface data from several SCAQMD sites, upper air data from one sounding per day (at 0600 PST) by the SCAQMD at Loyola Marymount University (LMU), and surface data from the National Weather Service (NWS) for several airports in the SoCAB. Surface and upper air data included wind speed, wind direction, and temperature. These data were supplemented during the intensive periods with tether sondes at Lynwood and Vernon. Soundings were made at a frequency of about two per hour. Wind speed and direction, wet- and dry-bulb temperatures, and pressure were collected up to an altitude of 60 m above the ground. Height and relative humidity were computed.

During intensive periods, the data had good spatial and temporal resolution. These data were used to define hourly wind fields to quantify the change in winds during the intensives. Tether sonde instruments were better able to measure low wind speeds typical at night than the instruments at the SCAQMD sites, which often reported zero wind speeds at night when the speed was less than the instrument threshold of 1.75 mi/hr (Cassmassi et al., 1988). The sensors at LYNN and several other SCAQMD sites were particularly prone to reporting zero wind speeds. The tether sondes provided good data during low wind speed conditions.

2.5 Traffic Count Data

Traffic counts were obtained from California Department of Transportation (CALTRANS) at five freeway locations for four days (19-20 December 1989 and 8-9 January 1990) and one location for two days (19-20 December 1989). CALTRANS data were for one direction of travel on each freeway. Traffic counts on surface streets were collected by Newport Traffic Studies for five locations on 19 December 1989 and 10 January 1990. Newport traffic counts were for both directions.

Traffic data for the intensive periods were evaluated for their consistency to determine if traffic volumes had significant day-to-day variations. Differences among counts for each day were generated for each hour. A total of six differences were generated for the CALTRANS data, and one difference was generated for the Newport data. A t-test was applied to each mean difference to determine if significant differences existed among the various days.

Time series of CALTRANS data are given in Figure 2-12. Counts at all locations had minimum values near 0300 PST followed by rapid increases to maximum values between 0600 and 0800 PST. Traffic counts generally remained high throughout the day but had some day-to-day variation. Evening maxima occurred at some locations between 1600 and 1800 PST. The differences in morning and evening peaks at some locations were probably caused by dominant traffic directions associated with either morning or afternoon rush hours. The evening peaks were generally spread over more hours than the morning peaks and the evening rate of decrease was less than that of the morning.

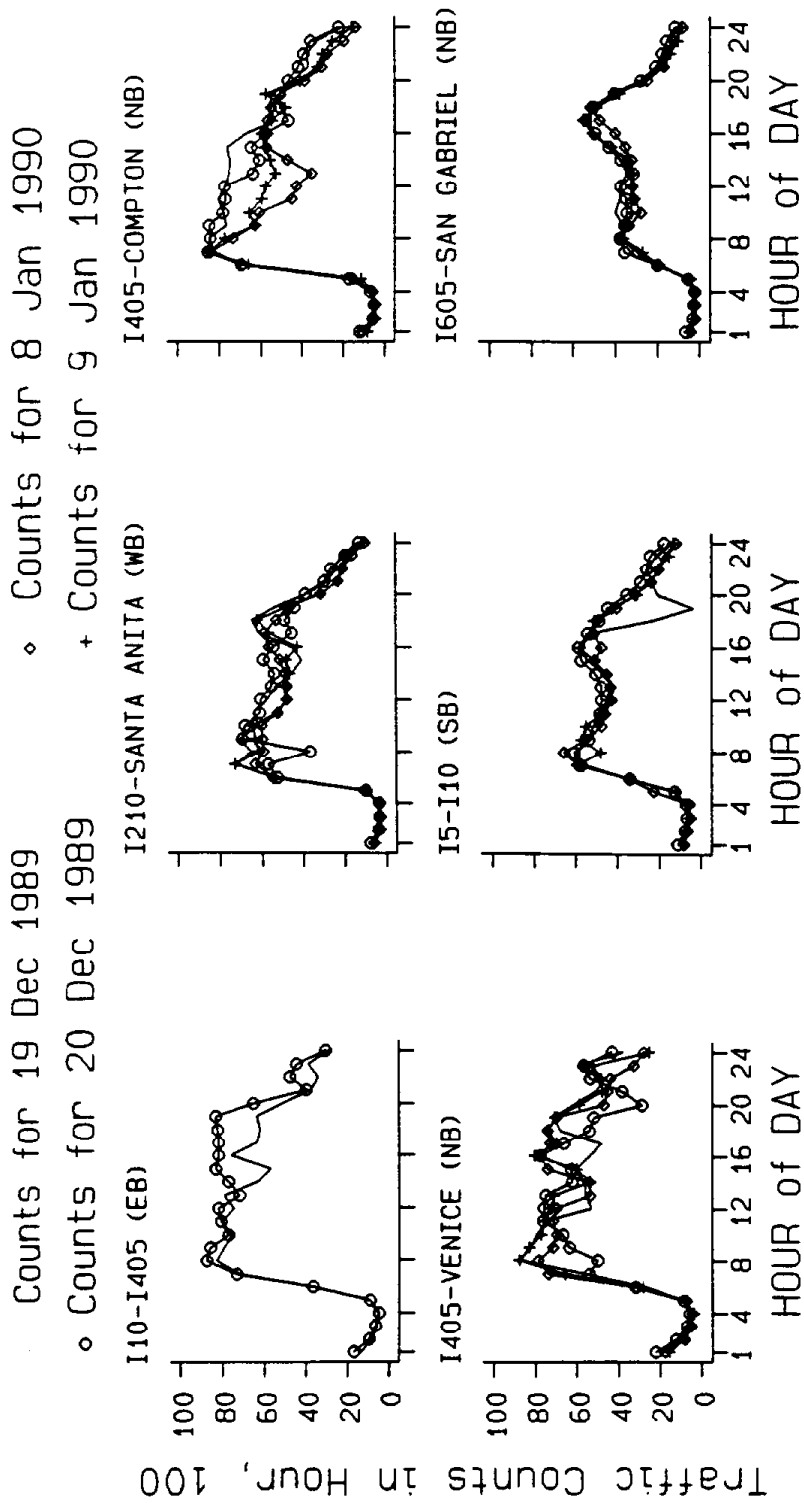


Figure 2-12. Traffic Counts from CALTRANS Sites.

Results of t-tests for CALTRANS data are given in Table 2-8. Included as a measure of the difference between days is the probability that there was no difference. A 5% probability corresponds to a statistically significant difference at a 5% significance level. Of the 31 comparisons, 16 had probabilities of no difference that were greater than 5%. Counts for days from the same intensive tended to be more alike than counts for different intensives. No overall difference is evident although some sites, such as I-405 at Compton, had statistically significant differences among most days.

Time series of Newport data are given in Figure 2-13. Counts at all locations showed morning peaks between 0600 and 0800 PST and afternoon peaks between 1600 and 1900 PST. Rates of increase in morning were slightly greater than rates of decrease at night. The rush hours had some differences in the amounts of traffic counts.

Results of t-tests for Newport data are given in Table 2-9. Two sites (Long Beach Blvd. and La Cienega) had high probability of no differences. Two sites (Firestone and Imperial Hwy) had moderate differences. Different locations for the Atlantic counters resulted in different counts. As with the CALTRANS data, no overall difference is evident in local traffic counts.

2.6 On-Road Remote Sensing of CO Emissions

Emissions of CO from on-road vehicles were measured by the University of Denver (Stedman et al., 1991) using an infra-red (IR) remote monitoring system at 7 locations on 11 days during December, 1989. As a vehicle passed through the IR beam, the ratio of CO to CO₂ in the vehicle's exhaust was measured, and the percentage of CO in the exhaust of the vehicle was determined. Vehicles were recorded on video tape as they passed through the IR beam. License plate numbers were used to determine make, model, and age of the vehicles. The intent of the study was to observe the wide variability of emissions in the Los Angeles area with particular emphasis on those vehicles in the vicinity of Lynwood. With the limited number of locations, the measurements were not necessarily representative of the entire vehicle fleet in the Los Angeles area although they seem to fall within the population found for all fleets measured in the US and Canada.

Measurements were made on surface streets in the vicinity of LYNN for 6 days, on freeway on- and off-ramps near Lynwood for 2 days, on a freeway on-ramp in Los Alamitos for one day, and on a surface street near HAWT for 2 days. Table 2-10 contains the time and location of the measurements and brief descriptions of the traffic. Measurements generally started near the end of the morning traffic peak and continued until the middle of the evening traffic peak. All were made during daylight hours. Most of the data were collected between 09:00 and 16:00 PST with the earliest time at about 07:30 PST and latest at about 17:30 PST. These data were collected between the morning and afternoon rush hours when the local traffic count would have been about 75 to 80% of the peak traffic counts during the rush hours. All data were collected on week days except at Willow/Katella where data were collected on a Saturday. The Willow/Katella site was also intended to supply information from an area in which the vehicles were expected to be newer.

Table 2-8

Comparisons of Vehicle Counts - CALTRANS

Site	Days	Difference		Probability of No Difference	
		Mean Counts	Std. Dev. Counts	t-STAT	%
I-405/Compton (Northbound)	12/19-12/20	161	552	1.43	16.55
	12/19-01/08	1057	1255	4.13	0.04
	12/19-01/09	774	767	4.94	0.01
	12/20-01/08	896	1150	3.82	0.09
	12/20-01/09	612	732	4.09	0.04
	01/08-01/09	-283	602	-2.30	3.07
I-10/I-405 (Eastbound)	12/19-12/20	-668	827	-3.95	0.06
I-405/Venice (Northbound)	12/19-12/20	137	1568	0.73	67.26
	12/19-01/08	-22	1226	-0.09	93.15
	12/19-01/09	-270	935	-1.41	17.07
	12/20-01/08	-159	1329	-0.59	56.41
	12/20-01/09	-407	1315	-1.52	14.33
	01/08-01/09	-248	761	-1.60	12.39
I-605/San Gabriel (Northbound)	12/19-12/20	5	231	0.11	91.02
	12/19-01/08	327	354	4.53	0.02
	12/19-01/09	215	244	4.32	0.03
	12/20-01/08	322	285	5.53	0.00
	12/20-01/09	210	232	4.43	0.02
	01/08-01/09	-112	333	-1.63	11.43
I-5/I-10 (Southbound)	12/19-12/20	-487	951	-2.51	1.96
	12/19-01/08	-236	1005	-1.15	26.19
	12/19-01/09	-244	1042	-1.15	26.29
	12/20-01/08	251	435	2.83	0.96
	12/20-01/09	243	380	3.13	0.47
	01/08-01/09	-8	512	-0.08	93.74
I-210/Santa Anita (Westbound)	12/19-12/20	158	960	0.81	42.73
	12/19-01/08	306	590	2.54	1.83
	12/19-01/09	256	388	3.23	0.37
	12/20-01/08	147	775	0.93	36.12
	12/20-01/09	97	909	0.52	60.48
	01/08-01/09	-50	430	-0.57	57.47

o Counts for 19 Dec 1989 + Counts for 10 Jan 1990

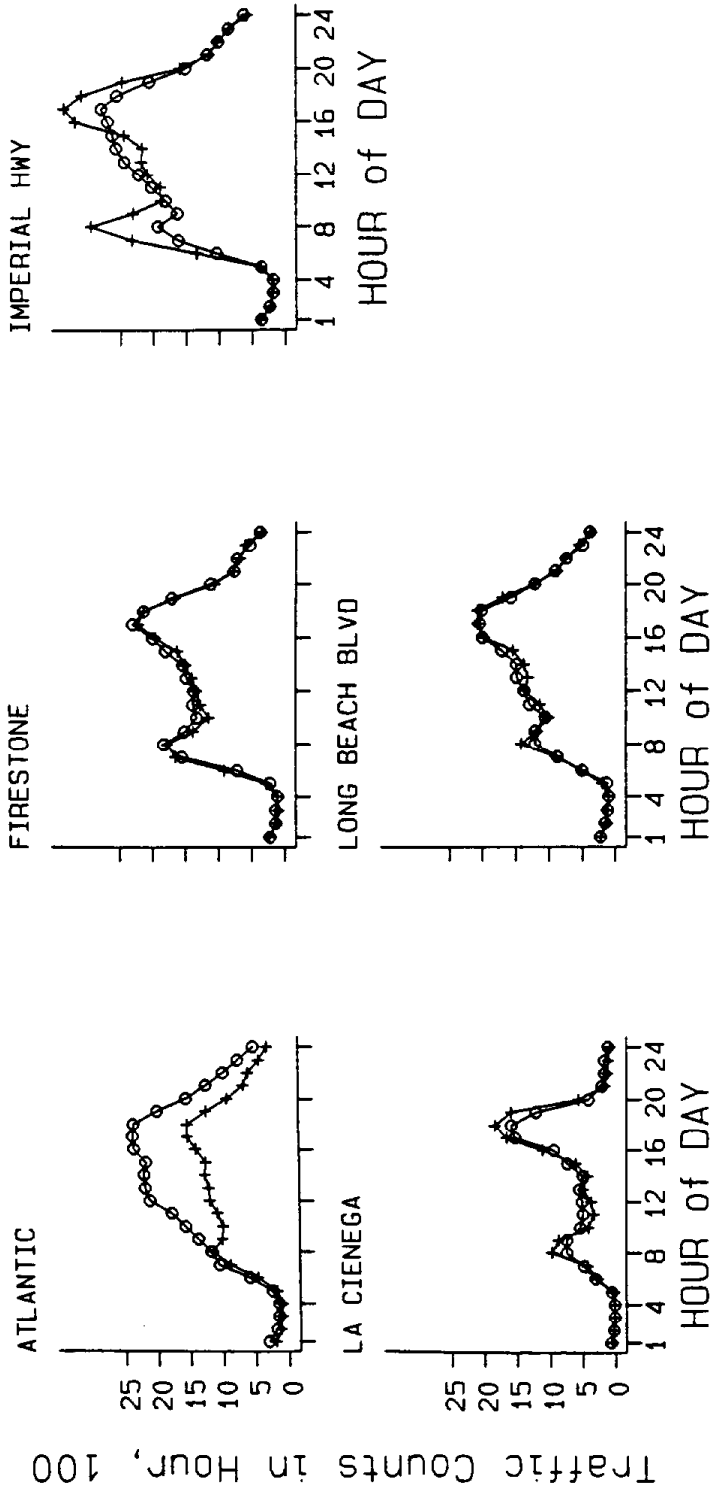


Figure 2-13. Traffic Counts from Newport Traffic Sites.

Table 2-9

Comparisons of Vehicle Counts - Newport Traffic Studies

Site	Days	Difference		Probability of No Difference	
		Mean Counts	Std. Dev. Counts	t-STAT	%
La Cienega South of 120th St.	12/19-01/10	-19	135	-0.68	50.26
Firestone between Alameda and Central	12/19-01/10	-31	84	1.82	8.20
Atlantic North of Firestone (12/19) South of Firestone (01/10)	12/19-01/10	477	351	6.67	0.00
Imperial Hwy. at Long Beach Blvd.	12/19-01/10	-155	351	-2.16	4.14
Long Beach Blvd. near Mulford/ Imperial Hwy.	12/19-01/10	6	85	0.34	73.59

Table 2-10

On-Road CO Measurements

<u>Site</u>	<u>Day/Time</u>	<u>Location/Traffic Description</u>
Long Beach Blvd.	12/06 13:36-17:29	Southbound one block north of Norton. Traffic restricted to single lane. Speeds between 10 and 25 mph, except last hour when traffic backed up at stop light.
Imperial Highway	12/07 08:45-14:40	Westbound 100 m east of Long Beach Blvd. Two open lanes, one measured. Traffic depended on traffic light with light acceleration. Maximum speeds near 30 mph.
Long Beach Blvd.	12/08 09:17-15:11	Southbound 75 m south of 12/06 site. Traffic backed up more often than on 12/06.
Long Beach Blvd.	12/11 10:54-16:42	Southbound 100 m north of location on 12/08 (25 m north of location on 12/06). Less traffic back up than 12/08.
Long Beach Blvd.	12/12 10:06-15:55	Same location as 12/11.
I-710 (On-ramp)	12/13 07:32-14:08	On-ramp to southbound I-710 from eastbound Imperial Hwy. Vehicles accelerating and fast moving.
I-710 (Off-ramp)	12/14 08:43-16:34	Off-ramp from northbound I-710 to westbound Imperial Hwy. Vehicles travelling up 3% grade and decelerating. Frequent backups.
Long Beach Blvd.	12/15 08:58-14:58	Same location as 12/11.
Willow/Katella	12/16 09:14-15:05	On-ramp from Willow/Katella St to southbound I-605.
La Cienega Blvd.	12/18 09:22-17:24	Southbound 100 m north of 120th St. Measurements on left of two lanes. Both lanes open to traffic. Vehicles travelling under deceleration and light cruise. Speeds near 20 mph.
La Cienega Blvd.	12/19 09:20-15:26	Same location as 12/18.

Table 2-11 summarizes the age of the vehicles and the percent CO in the vehicle emissions. The vehicles in Lynwood were consistently older and had higher emissions than vehicles at other locations. While some differences have been attributed to vehicles having different operating conditions such as acceleration and deceleration, the main factor controlling the CO emission is vehicle age. The vehicles at the Lynwood sites are considerably older than those at other sites, both in Los Angeles and in other cities.

These measurements showed that the vehicles in Lynwood were older and have higher emissions than those in some other parts of Los Angeles. They did not, however, delineate the areal extent of the older, higher emitting vehicles. They also did not show the emissions during peak traffic periods nor at the time of highest CO concentrations. The vehicle mix on surface streets at other times was likely similar to that measured because it was probably dominated by local rather than through traffic. The vehicle mix at the freeway on- and off-ramps may have been somewhat different unless they were used mainly by local vehicles.

Table 2-11

On-Road CO Measurements

<u>Site</u>	<u>Day</u>	<u>Number of Vehicles</u>	<u>Mean Age Years</u>	<u>% CO Mean</u>
Long Beach Blvd.	12/06	824	8.31	1.94
Long Beach Blvd.	12/08	1736	8.86	1.70
Long Beach Blvd.	12/11	1419	8.91	2.13
Long Beach Blvd.	12/12	1513	8.91	2.00
Long Beach Blvd.	12/15	1661	9.14	2.24
Imperial Highway	12/07	1056	<u>7.71</u>	<u>1.67</u>
	Cumulative Site Averages		8.64	1.95
	Standard Deviation		0.23	
I-710 (On-ramp)	12/13	2144	6.09	1.56
I-710 (Off-ramp)	12/14	2936	<u>6.63</u>	<u>1.09</u>
	Cumulative Site Averages		6.36	1.33
	Standard Deviation		0.33	
Willow/Katella	12/16	1367	4.86	0.76
La Cienega Blvd.	12/18	998	5.55	1.17
La Cienega Blvd.	12/19	791	<u>5.66</u>	<u>1.04</u>
	Cumulative Site Averages		5.36	0.99
	Standard Deviation		0.21	

3.0 ANALYSIS OF DATA

3.1 Maximum CO Concentrations

While a number of the bag samples cannot be used in temporal analysis, the bag sample data along with SCAQMD data can be used to indicate the locations of high CO within the SoCAB. Our analysis assumed that bag samples were collected during the time of maximum CO concentrations. This assumption might not be appropriate at sites with missing samples.

Maximum CO concentrations for the hours of the December intensive period are shown in Figures 3-1 to 3-3. Most of the bag sample sites within 4 km of LYNN had maximum CO concentrations that were similar to the 16 ppm at LYNN. HS12 has a value of 21 ppm. In general, concentrations were 8 to 10 ppm less at other sites than at LYNN. The only sites outside the 4 km distance with concentrations approaching LYNN's were La Habra SCAQMD (15 ppm) and CC17 (13 ppm).

Maximum CO concentrations for the hours of the January intensive period are shown in Figures 3-4 to 3-6. The extent of bag sample sites with maximum concentrations similar to LYNN's 23 ppm were within 1 km of the AQMD site. Maximum concentrations for January were generally greater than those in December, but concentrations at most other locations were still 8 to 10 ppm less than at LYNN. The sites outside the 1 km distance from LYNN with the highest concentrations were Hawthorne and Reseda with 19 ppm and Burbank with 16 ppm.

The bag samples near LYNN do confirm that the high CO concentrations measured at that site are representative of concentrations in the immediate vicinity.

3.2 Wind Speeds at SCAQMD Sites

One factor governing the concentration of CO is wind speed. For with areas with similar emissions, the one having consistently lower wind speeds should have higher CO concentrations. Tables 3-1 and 3-2 summarize the maximum CO concentrations and the average wind speeds at SCAQMD sites in the western part of the SoCAB during the December and January intensive periods, respectively. The wind speeds were averaged during the morning and evening hours associated with increasing CO concentrations with the maxima listed. Two evening periods are listed for January since the intensive period included the evening of January 8-9 and January 9-10. Several sites, including LYNN, had low wind speeds with averages less than 1 mi/hr. The wind speed values at very low speeds are somewhat suspect since some reported values were zero. The zero wind speeds were at or below the instrument threshold value stated to be 1.75 mi/hr (Cassmassi et al., 1988).

While higher CO concentrations tend to occur at all sites during low wind speed conditions, a direct relation between wind speed and CO concentration that would be valid at all sites is not apparent in Tables 3-1 and 3-2. Other sites had wind speeds as low as LYNN had but usually did not have as high CO concentrations. It should be noted that during the evening

Table 3-1

**Summary of Maximum CO Concentrations and Scalar Wind Speeds at SCAQMD Sites
December 19, 1200 to 20, 1100**

<u>SITE</u>	<u>Evening Hours 1700 - 0100 PST</u>				<u>Morning Hours 0400 - 0900 PST</u>			
	<u>CO</u>	<u>Wind Speed</u>			<u>CO</u>	<u>Wind Speed</u>		
	<u>Max ppm</u>	<u>Ave mph</u>	<u>Max mph</u>	<u>Min mph</u>	<u>Max ppm</u>	<u>Ave mph</u>	<u>Max mph</u>	<u>Min mph</u>
ANAH	7	1.1	4	0	4	4.2	5	3
AZUS	3	2.5	5	0	6	1.6	4	0
BURK	7	0.6	3	0	12	0.4	2	0
CELA	5	3.0	6	0	6	6.6	7	6
HAWT	7	1.5	4	0	10	0.4	2	0
LAHB	7	0.5	2	0	15	0.6	3	0
LGBH	7	1.1	3	0	9	2.0	4	0
LYNN	16	0.5	4	0	12	0.0	0	0
PASA	6	0.5	2	0	7	0.4	1	0
PICO	7	1.9	4	0	8	3.4	5	2
RESE	5	1.4	4	0	8	0.0	0	0
WHIT	6	0.8	1	0	5	1.0	3	0
WSLA	6	1.5	4	0	6	2.6	4	0

Table 3-2

**Summary of Maximum CO Concentrations and Scalar Wind Speeds at SCAQMD Sites
January 8, 1200 to 10, 0400**

SITE	Date	Evening Hours 1700 - 0100 PST				Morning Hours 0400 - 0900 PST			
		CO	Wind Speed			CO	Wind Speed		
		ppm	mph	mph	mph	ppm	mph	mph	mph
ANAH	8-9	6	1.1	3	0	8	1.2	4	0
	9-1	15	0.3	2	0				
AZUS	8-9	3	1.0	5	0	7	0.4	2	0
	9-10	6	2.3	7	0				
BURK	8-9	7	1.9	5	0	13	0.4	2	0
	9-10	16	0.3	2	0				
CELA	8-9	7	3.3	6	0	6	7.2	9	5
	9-10	13	5.0	9	1				
HAWT	8-9	7	1.9	4	0	18	0.8	2	0
	9-10	10	0.4	3	0				
LAHB	8-9	7	0.6	2	0	13	0.6	3	0
	9-10	10	0.5	2	0				
LGBH	8-9	6	1.4	3	0	10	1.6	4	0
	9-10	10	2.3	5	0				
LYNN	8-9	10	0.6	3	0	23	0.0	0	0
	9-10	17	0.9	4	0				
PASA	8-9	9	0.4	1	0	11	1.0	2	0
	9-10	15	1.1	3	0				
PICO	8-9	8	2.5	4	0	9	4.0	5	3
	9-10	13	3.0	4	0				
RESE	8-9	8	0.4	2	0	15	0.2	1	0
	9-10	19	0.0	0	0				
WHIT	8-9	6	0.1	1	0	11	0.2	1	0
	9-10	12	0.1	1	0				
WSLA	8-9	5	3.0	4	2	15	1.6	5	0
	9-10	10	1.8	6	0				

MAX CO CONCENTRATION — DEC INTENSIVE

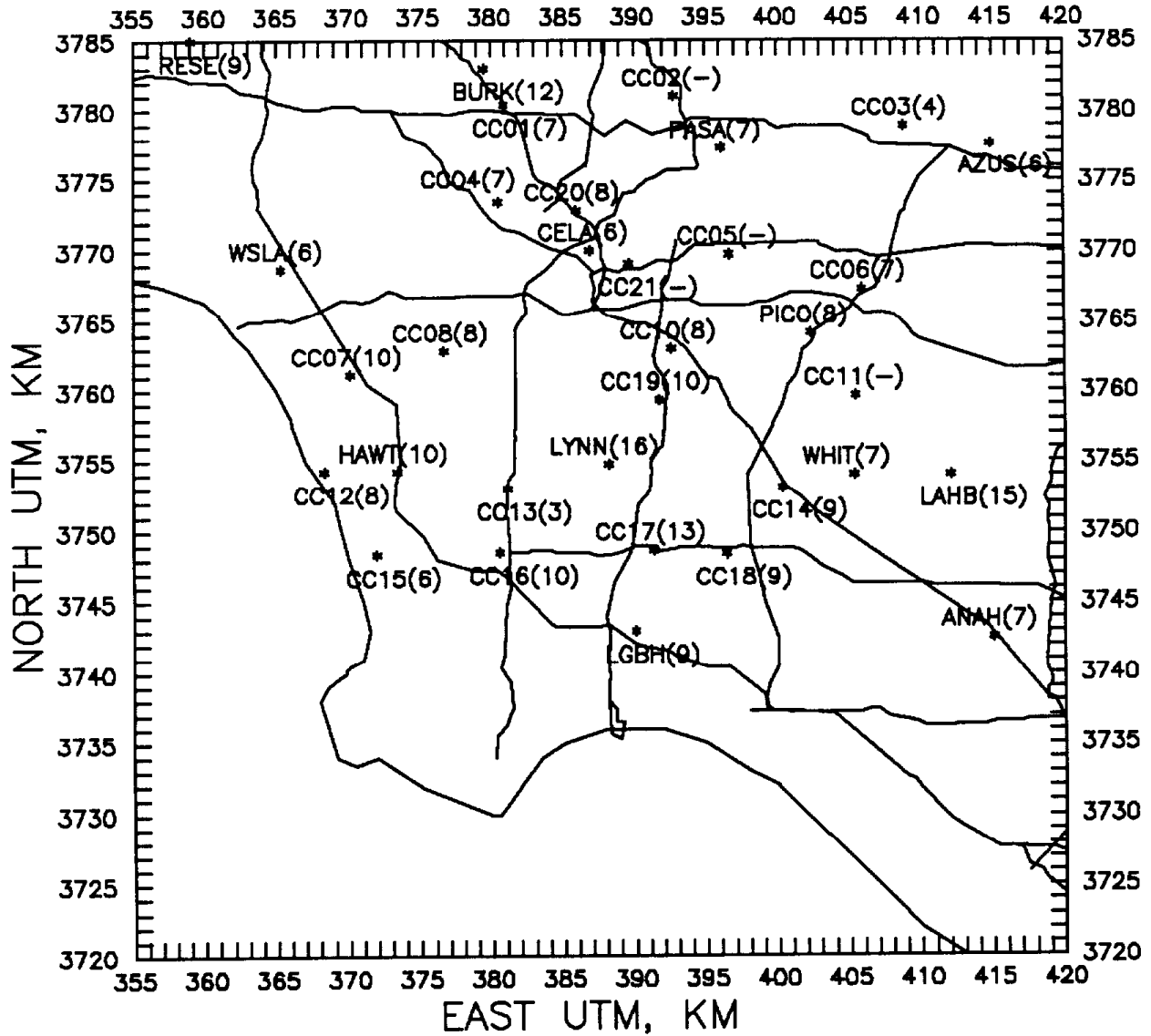


Figure 3-1. Maximum CO Concentrations at SCAQMD and CC Sites for December, 1989 Intensive Period.

MAX CO CONCENTRATION – DEC INTENSIVE

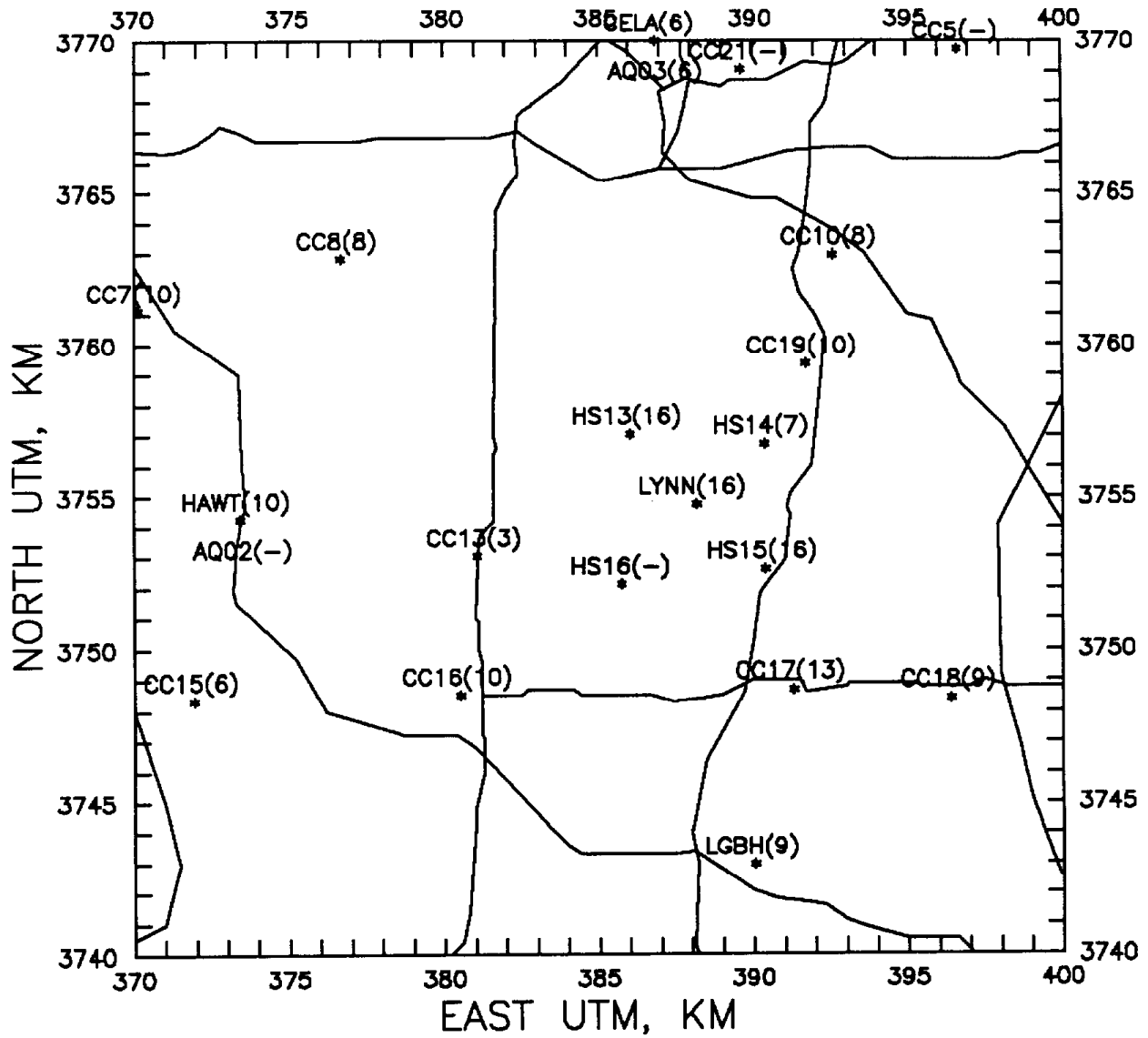


Figure 3-2. Maximum CO Concentrations at Sites Within 15 km of LYNN for December, 1989 Intensive Period.

MAX CO CONCENTRATION – DEC INTENSIVE

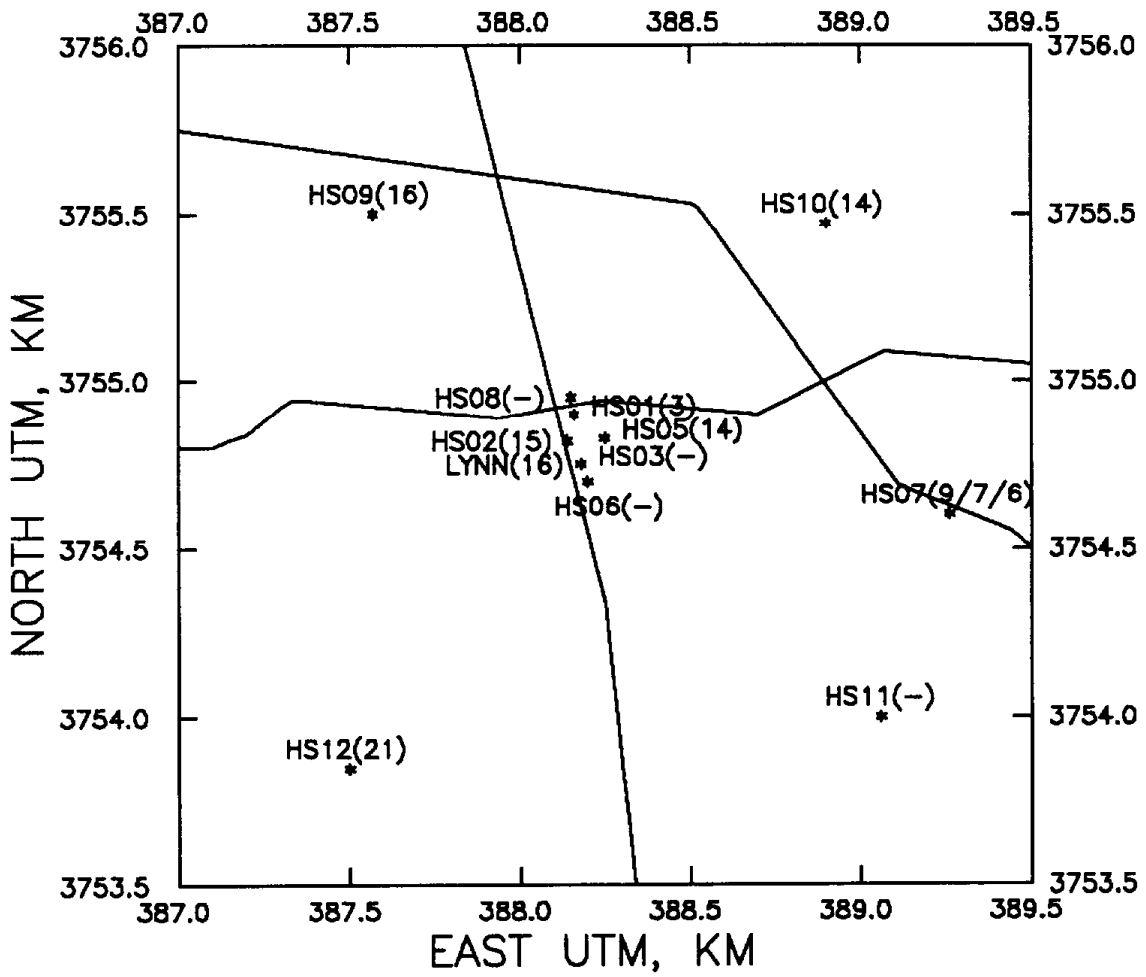


Figure 3-3. Maximum CO Concentrations at Sites Within 1 km of LYNN for December, 1989 Intensive Period.

MAX CO CONCENTRATION — JAN INTENSIVE

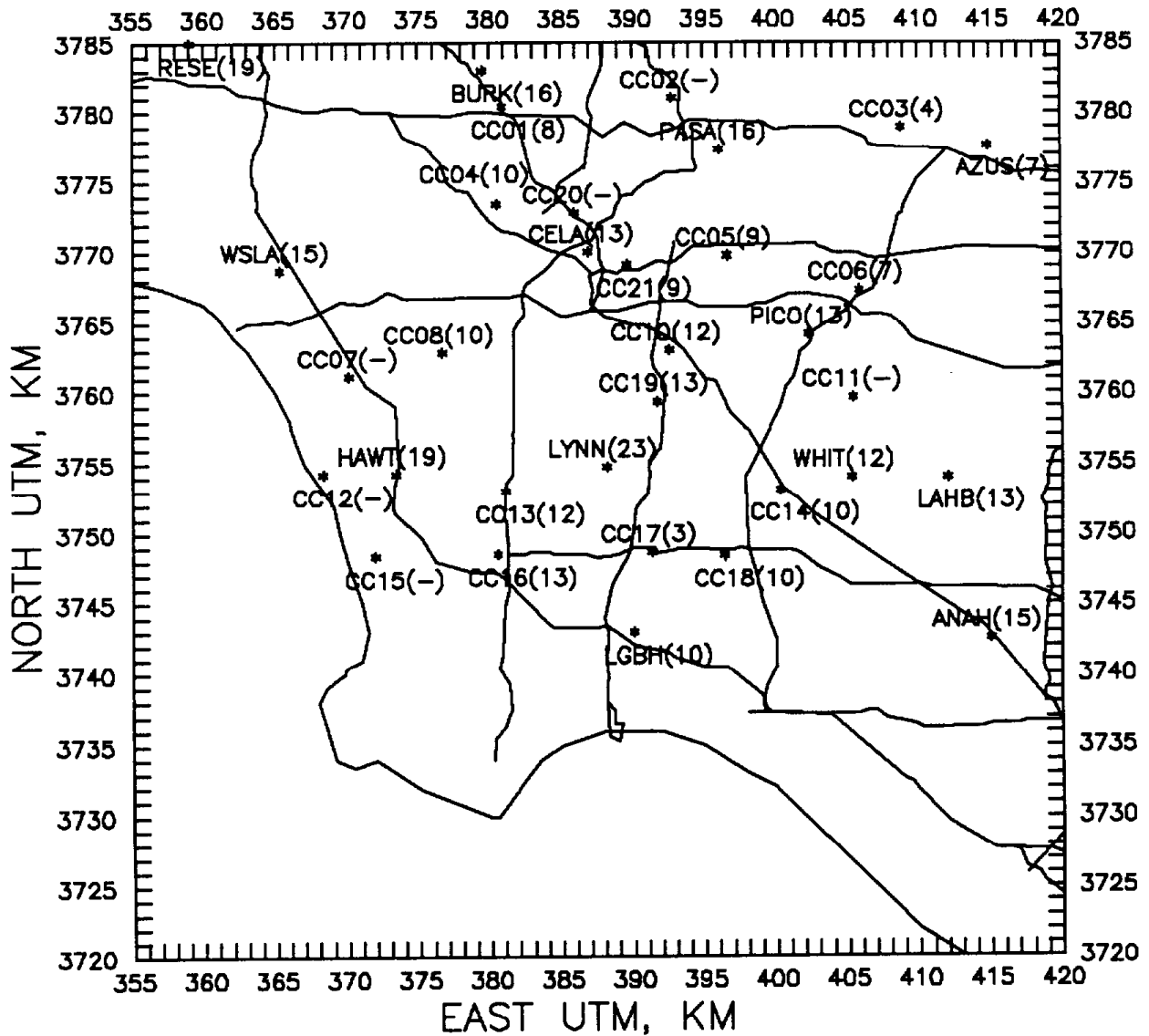


Figure 3-4. Maximum CO Concentrations at SCAQMD and CC Sites for January, 1990 Intensive Period.

MAX CO CONCENTRATION – JAN INTENSIVE

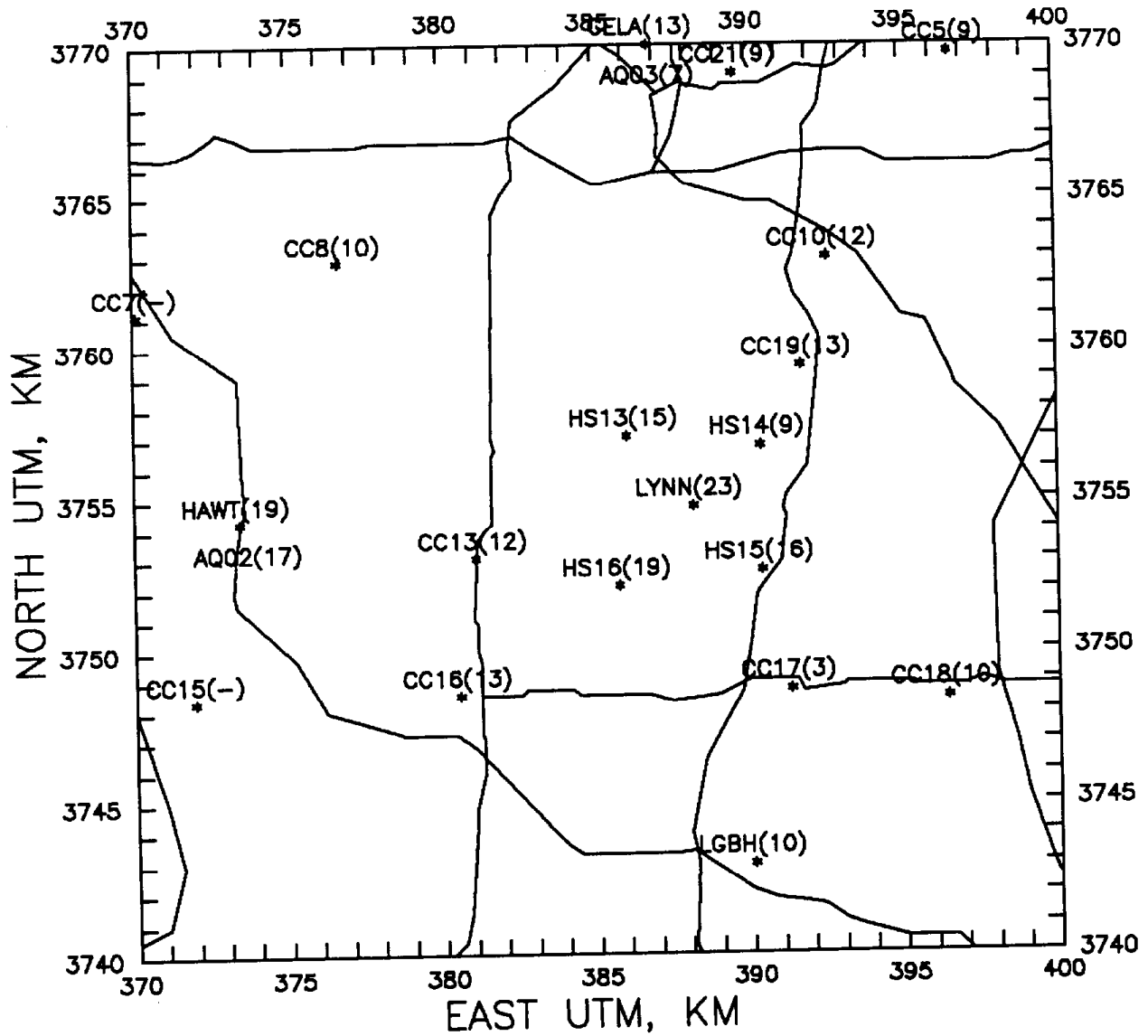


Figure 3-5. Maximum CO Concentrations at Sites Within 15 km of LYNN for January, 1990 Intensive Period.

MAX CO CONCENTRATION – JAN INTENSIVE

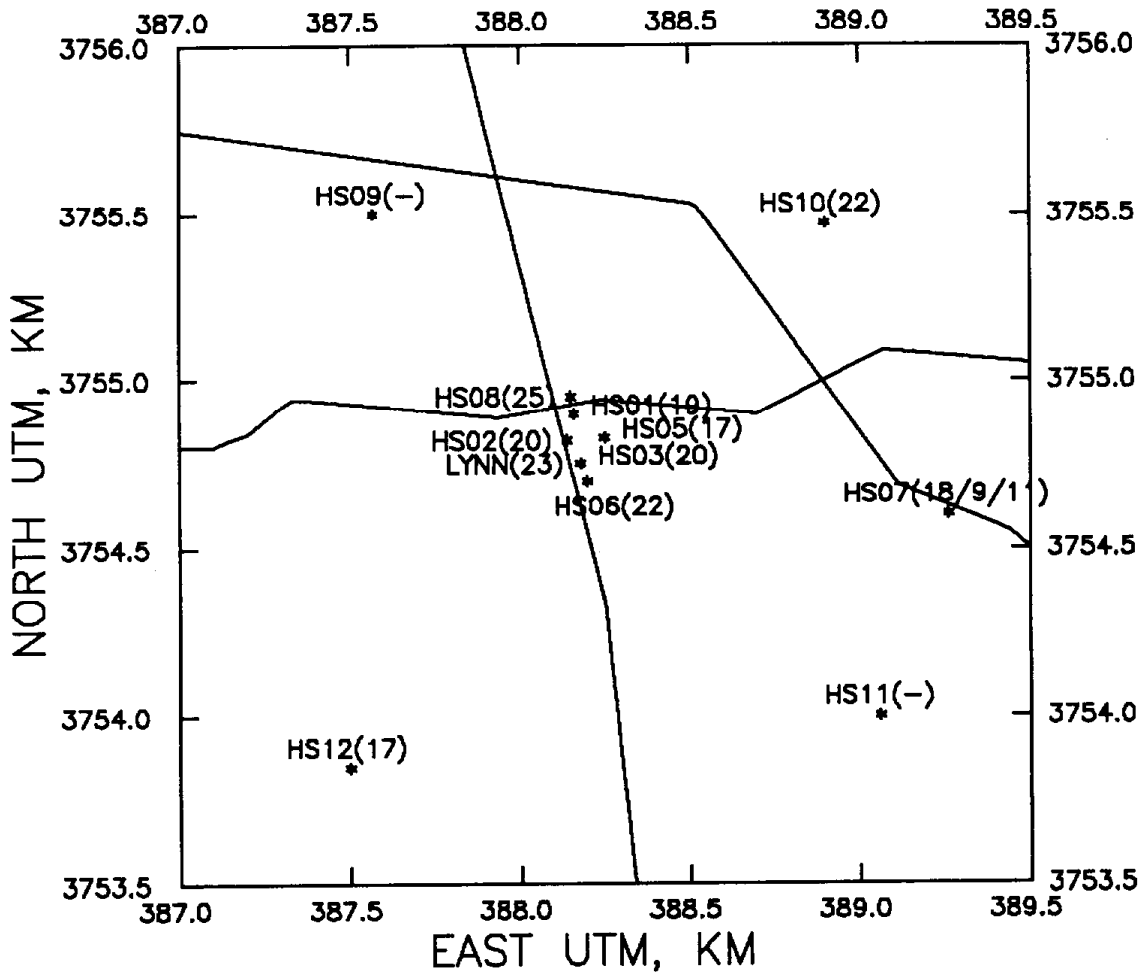


Figure 3-6. Maximum CO Concentrations at Sites Within 1 km of LYNN for January, 1990 Intensive Period.

and morning periods another site sometimes had higher maximum CO than LYNN did although highest values were at LYNN.

3.3 Wind Field Generation

Wind fields for each hour were computed using the Diagnostic Wind Model (Douglas et al., 1990) that was developed as part of the Urban Air Shed model (Morris and Myers, 1990). This model uses an objective analysis method to generate wind fields in the region of interest in a two-step process. The first step generates a wind field from physical processes. The second step adjusts this wind field using measured winds. The model starts with initial inputs for mean wind, stability, and terrain elevations. Gridded wind fields are then developed by adjusting the initial mean winds for local effects such as lifting and acceleration of airflow over terrain obstacles, thermodynamically generated slope flows, and blocking by elevated terrain using iterative methods that conserve mass by minimizing the three-dimensional divergence of the wind. Temporal variations of the wind field and stability are included in the model by defining the initial winds and stabilities for each hour. Inaccuracies from the first step are removed by adjusting the wind field in the vicinity of available measurement stations to approximate the measured winds while retaining the mass-consistent character of the wind field.

Wind fields were generated over a 61 km by 61 km grid centered on Lynwood. The grid covered UTM Easting coordinates 360 to 420 km and Northing coordinates 3725 to 3785 km. This grid covered all the intensive sample sites and SCAQMD monitoring sites in the western part of the SoCAB. Terrain heights obtained from USGS topographic maps as described in Section 2.3 were used as inputs to the model.

The initial wind speeds and directions and average lapse rates for each hour of the intensive periods were obtained from tethersonde data at LYNN. Surface winds from 12 SCAQMD sites were formatted for input into the model as were winds from the two tethersondes at elevations of 20 and 40 m above the ground.

Wind components were generated at each grid point for each hour for wind at the surface (effectively at 10 m) and at an elevation between 20 and 40 m. Typical plots of vector winds for near the times of maximum CO concentrations during morning and evening hour are shown in Figures 3-7 and 3-8 to illustrate the wind fields that are generated. The entire set of surface wind fields generated during the intensive periods is included in Appendix B.

3.4 Trajectory Analysis

Several trajectories of air parcels were computed from wind fields generated by the Diagnostic Wind Model. Estimates of the paths of air reaching the LYNN site during each hour of the intensive periods were made with backward trajectories. Backward trajectories were also computed for several other SCAQMD sites for the December intensive. Forward trajectories were used to estimate the paths of air parcels leaving the locations of tracer releases and the vicinity of downtown Los Angeles.

891220 HOUR 08 - LEVEL 1 WINDS

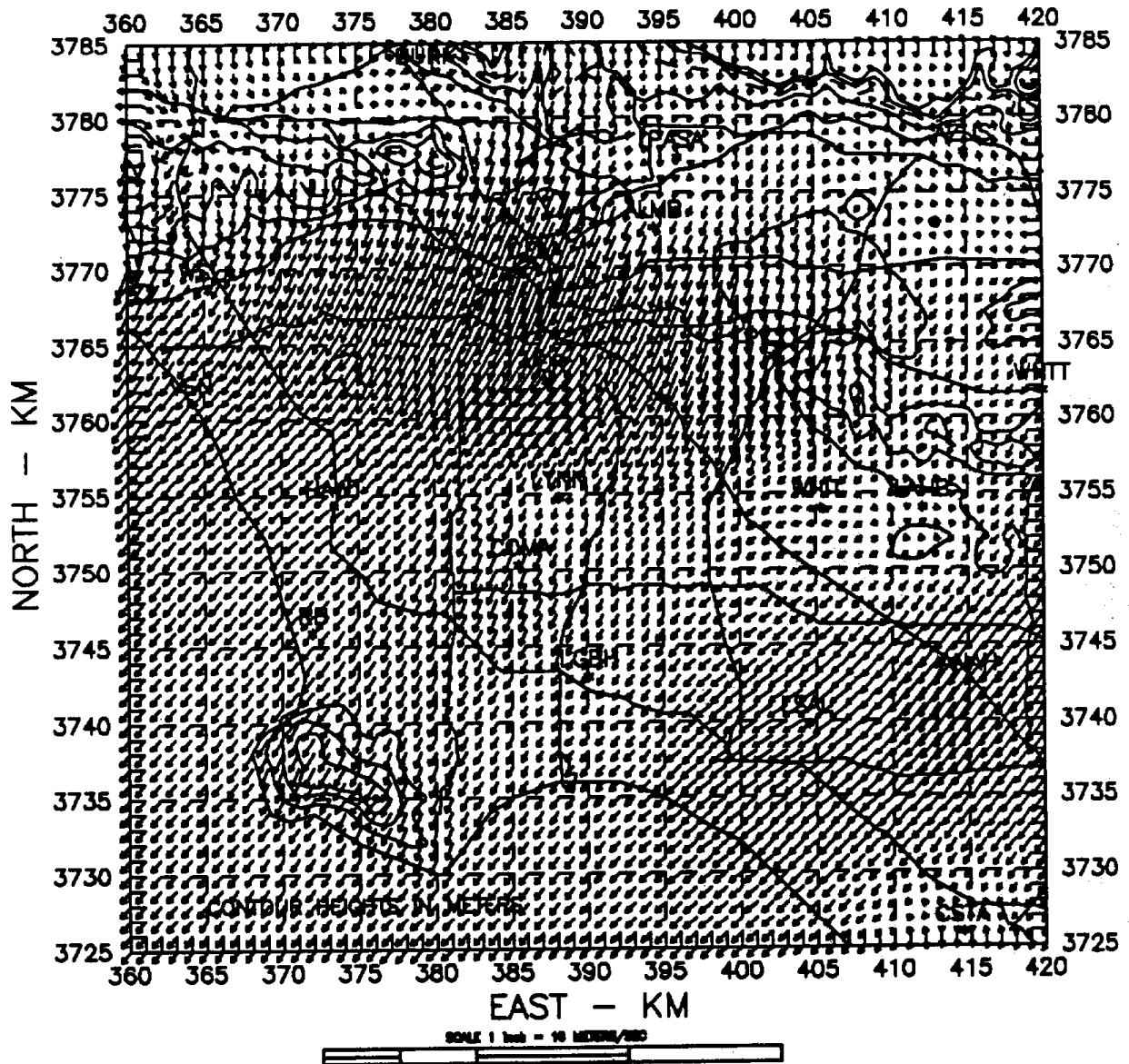


Figure 3-7. Example of Wind Field Generated by Diagnostic Wind Model for Morning Hours: 0800 PST, Dec. 20, 1989.

891219 HOUR 20 - LEVEL 1 WINDS

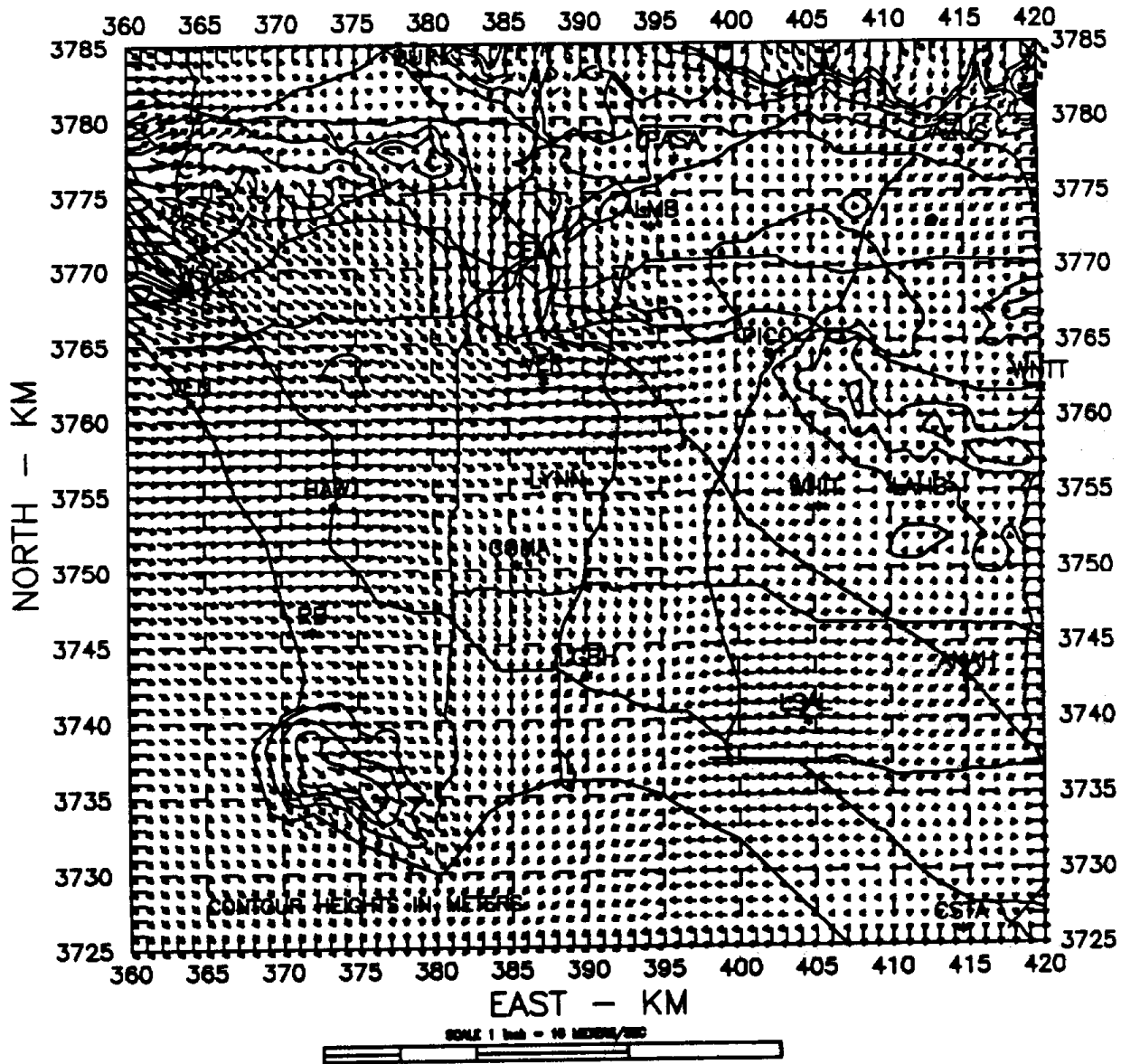


Figure 3-8. Example of Wind Field Generated by Diagnostic Wind Model for Evening Hours: 2000 PST, Dec. 19, 1989.

The location of an air parcel at the previous hour for backward trajectories or at the next hour for forward trajectories was computed from the wind speed and direction for that particular hour. Wind speed and direction at the starting locations were estimated by a linear interpolation of the DWM wind components at the surrounding UTM coordinates and used to compute the travel distance of an air parcel for that hour and the location of the air parcel at the end of the hour. Succeeding computations started at each new point with interpolated wind speed and direction for the appropriate hour.

The uncertainty in the trajectories can be estimated from results the application of the DWM to air motions in the SoCAB during the Southern California Air Quality Study in 1987 (Douglas et al., 1991). In this study, wind fields were generated over a 320 km by 180 km area encompassing the SoCAB. Hourly velocity components were computed at a 5 km by 5 km grid spacing. Backward and forward trajectories were computed using interpolated 15-minute wind vectors. The uncertainty of these computed trajectories was investigated by introducing random fluctuations in the wind vectors to the trajectory calculations and determining the variation in the paths of air parcels. In particular, the root mean square errors (RMSE) values that were introduced were 0.2 m/sec for wind speed and 10° for wind direction. Using these values, Douglas et al. found the RMSEs for the deviations of surface trajectories from the computed paths after 12 hours to be 5.7 km during a summer period and 1.7 km during a winter period. Plots of possible trajectory paths showed that parcel paths were less divergent in winter than in summer. The uncertainties in this study are likely of similar magnitude with a RMSE of about 2 km.

3.4.1 Lynwood Trajectories

Examples of the backward trajectories for air arriving at LYNN are shown in Figures 3-9 and 3-10. All figures showing backward trajectories for air arriving at the LYNN site at each hour are contained in Appendix C. Each figure is labelled with the day and hour that an air parcel arrives at LYNN. The location of an air parcel at previous hours is labelled along each trajectory. Labels follow the hour-beginning naming convention associated with air quality data, e.g., hour 06 indicates time between 0600 and 0700 PST. The hour label indicates where the air parcel would be at the end of an hour (at 0700 PST for hour 06).

A review of the trajectories shows the expected dependence of the variation in air parcel transport on the variation in wind field. Late afternoon trajectories show the eastward transport under the influence of westerly winds. As the evening progresses, the transport gradually shifts toward the south as winds change to northerly throughout the night. Transport eventually changes back toward the east near noontime as the westerly sea breeze commences. Transitions in transport direction during evening hours can be of two types: 1) change through the southwest as the wind shifts from westerly to northwesterly to northerly (veering); and 2) change through the northeast as the wind shifts from westerly to southerly to northerly (backing).

During the evening of 19-20 December, the transition from eastward transport to southward transport occurred as winds gradually veered from westerly at 1700 to northwesterly

TRAJECTORY — ARRIVE LYNN — 1220/08

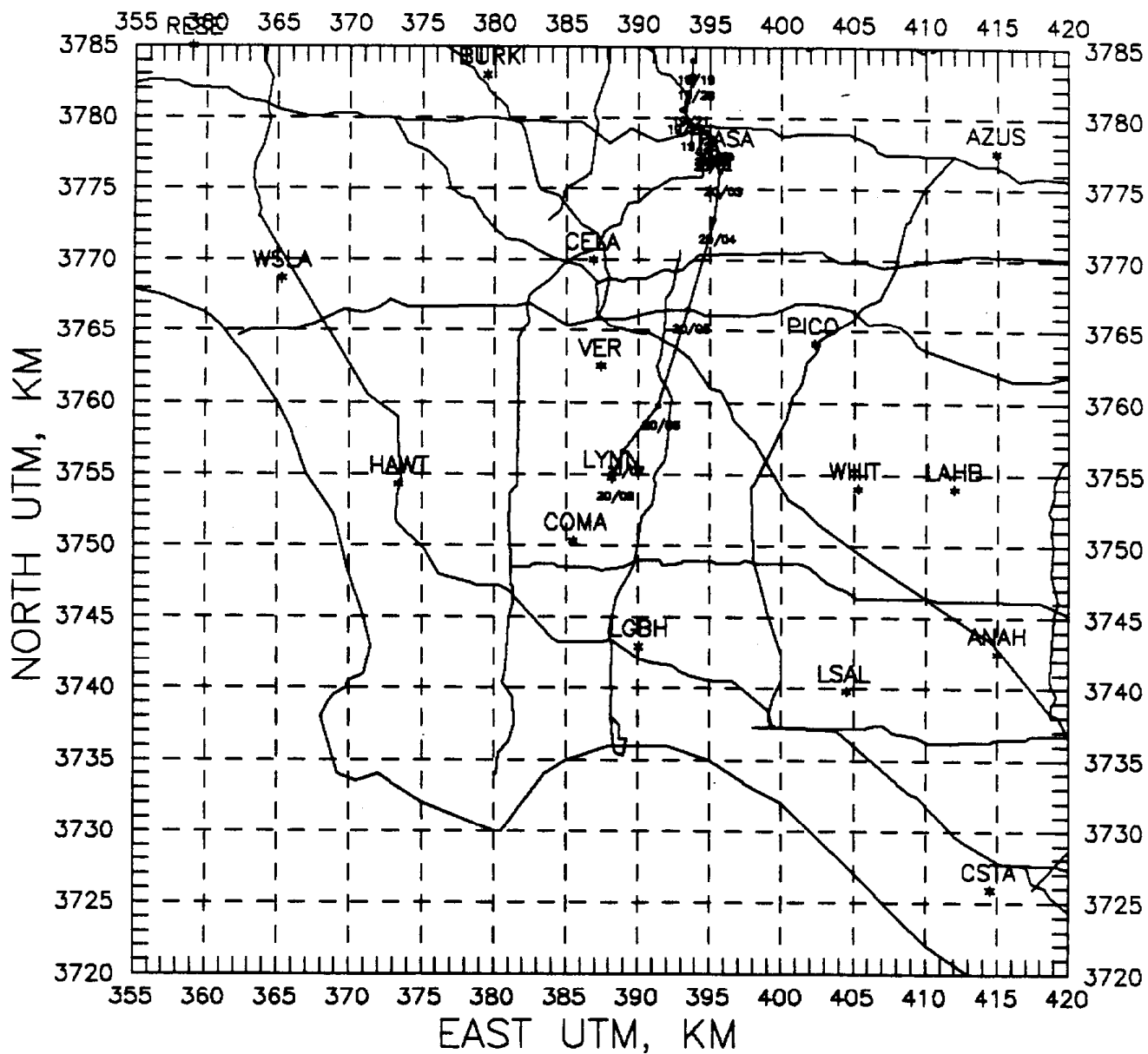


Figure 3-9. Example of Trajectory of Air Arriving at LYNN for Morning Hours: 0800 PST, Dec. 20, 1989.

TRAJECTORY - ARRIVE LYNN - 1219/23

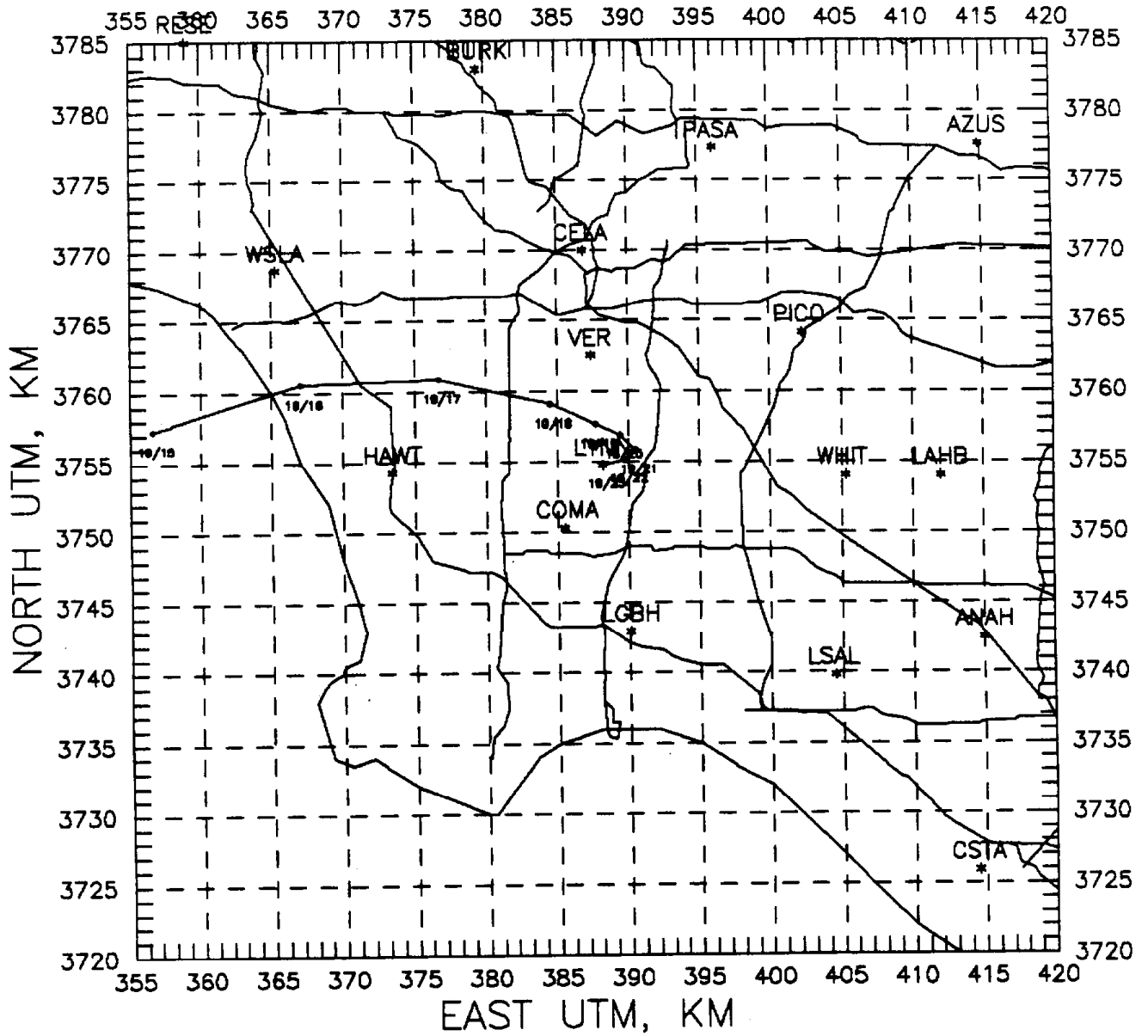


Figure 3-10. Example of Trajectory of Air Arriving at LYNN for Evening Hours: 2300 PST, Dec. 19, 1989.

at 2000 to northeasterly at 2100 with CO concentrations at Lynwood starting to increase. There was very little transport from 2000 to 2300 when CO concentrations peaked. During this time, air parcels moved only a few kilometers from their locations at 1800. Air that arrived at LYNN at 0000, when the CO concentration started to decrease, followed a path that passed a few kilometers south of the I-10/I-5 freeway system (but not over it) before turning southwestward towards Lynwood. Only after 0000 did air arrive at LYNN that had passed in the vicinity of emission sources near downtown Los Angeles. Air that might have been expected to have higher concentrations of CO because it passed in the vicinity of major sources at the time of maximum emissions arrived at the site as concentrations were starting to decrease.

During the evening of 8-9 January, air initially arrived at LYNN from the west. At 2000 a shift in winds brought air to LYNN from the southwest and then from the east. The CO concentration reached a maximum at 1800 and then decreased.

During the evening of 9-10 January, trajectories were similar to those of 19-20 December, although speeds were somewhat higher and air that passed in the vicinity of sources near downtown Los Angeles arrived at Lynwood 1 to 2 hours earlier. The CO concentration at Lynwood began to increase during the midafternoon while transport was still from the west. The CO level reached a maximum at 2300, coinciding with the arrival of air from downtown Los Angeles.

For the morning of 20 December, southward trajectories show that air parcels arriving at Lynwood during hours 0500 to 0700 (when CO concentrations at Lynwood were increasing) were in the vicinity of downtown Los Angeles 2 to 3 hours earlier. By hour 0800, as the CO level reached a maximum, air arriving at Lynwood had been near the I-710 freeway 2 hours earlier and near other freeways 3 to 4 hours earlier. A decrease in wind speed near Lynwood is evident for hours 0700 and 0800. Air parcels that would have been near freeways at times of peak traffic counts (0600-0800) arrived at Lynwood during hour 0800 and after. The increase in morning CO concentration at Lynwood appears to have preceded the arrival of air at Lynwood from source regions associated with peak freeway traffic.

On the morning of 9 January, trajectories were similar to those of 20 December after hour 0300. The transport distance was slightly greater during hour 0700 and slightly less during hour 0900. Direction of transport during later hours was more from the north rather than the northeast. On this day, air parcels that would have been near freeways at times of peak traffic counts arrived at Lynwood during hour 0900 and after. The morning maximum CO concentration as well as the increase in CO level occurred before the arrival of air from major source regions associated with peak freeway traffic.

3.4.2 Other SCAQMD Trajectories

Appendix C also contains trajectories to SCAQMD sites at Central Los Angeles, Hawthorne, and Long Beach for the evening hours of the 19-20 December intensive. All trajectories for each site are shown on a single map. The hour designation refers to the hour

(using hour beginning convention) the air parcel arrived at a site. It is necessary to count back one hour from the site at each mark on the trajectory lines to determine the earlier locations of the air parcels.

At Central Los Angeles, air arrived from the west until hour 1900 and from the north after hour 1900. The path crossed several freeways between hours 1600 and 2300. Winds were higher than at Lynwood during the evening hours. The maximum CO concentration occurred during hour 2100 when air was being transported from the north.

At Hawthorne, air arrived from the west until hour 2200. After hour 2200, air arrived from the north to northeast but followed a path that started off-shore, penetrated inland 15 km, and returned to Hawthorne. This coincided with the increase in CO concentration at the site which reached a maximum after 0000, when the air, coming from the northeast, would have passed over the nearby I-405 freeway. Not until hour 0600 did air reach Hawthorne that passed near downtown Los Angeles. Transport in the vicinity of Hawthorne slowed markedly after hour 2200. The CO concentration, near zero until hour 1900, reached a maximum during hour 2200.

At Long Beach, air arrived from the west until hour 2000. As with other sites, air arriving after hour 2000 continued to come from the west of the site. Maximum concentrations occurred at hours 0000, 0100, and 0300 as air was reaching the site from the northeast under moderately slow transport conditions.

3.4.3 Tracer Trajectories

As a check on the generation of wind fields, forward trajectories of tracers were computed. For each hour of release, the track of each tracer was determined for subsequent hours. Maps of the trajectories are included in Appendix C. Each map shows the trajectories of the four tracers for the same release hour. The time that each tracer was in the vicinity of Lynwood is shown in Table 3-3. The times correspond fairly well with times that tracers appear in bag samples at HS02 in December and HS01 in January.

3.5 Terrain

In order to quantify the effect of terrain, the gradient or slope of the terrain was computed from terrain elevations obtained from USGS topographic maps. The gradient was computed by numerical differentiation in the east-west (x) and north-south (y) directions (Kunz, 1957). At each grid point, terrain elevations were fitted in the x and y directions with a polynomial using Stirling's formula, a polynomial interpolation formula using differences. Differentiation of the x and y polynomials then gave the gradient or slope of the terrain. Two terms were retained in the polynomials to give better results than found with one term. With the differences reduced

Table 3-3

**Arrival of Tracers in Vicinity of Lynwood -
Trajectory Analysis**

<u>Release Time</u>		<u>Day/Hour of Arrival</u>			
		<u>PCMP</u>	<u>PMCH</u>	<u>PDCM</u>	<u>PTCH</u>
1219	1700	20/03	---	---	19/18
	1800	20/02	---	---	19/19
	1900	20/01	--	--	---
	2000	20/01	---	---	---
	2100	20/00	---	---	---
	2200	20/00	---	---	---
	2300	20/01	---	---	---
Measured at HS02		19/22-20/03	---	19/22, 20/08	19/20-23
0108	1700	9/02	9/01	---	8/21
	1800	---	8/23	---	8/20
	1900	---	8/22	---	---
	2000	---	8/23	---	---
	2100	---	8/23	---	---
	2200	---	---	---	---
	2300	9/01	---	---	---
Measured at HS01		8/22-9/08	8/20-9/04	---	---

to values at the grid points, the components of the gradient in the east-west, H_x , and north-south, H_y , directions computed from

$$H_x(x_0,y) = [-H(x_2,y) + 8H(x_1,y) - 8H(x_{-1},y) + H(x_{-2},y)]/(12h) \quad (2)$$

$$H_y(x,y_0) = [-H(x,y_2) + 8H(x,y_1) - 8H(x,y_{-1}) + H(x,y_{-2})]/(12h) \quad (3)$$

where 0 subscript denotes location of gradient

1, -1 subscripts denote locations one grid space from location of gradient

2, -2 subscripts denote locations two grid spaces from location of gradient

h is the spacing between points (1 km)

Topography gradients at SCAQMD and CC sites are shown in Table 3-4. Sites have been ranked by magnitude of gradient. Of the SCAQMD sites with CO measurements, LYNN has the smallest gradient, followed by Hawthorne and Anaheim. Gradients at other SCAQMD sites are at least twice as large as at Lynwood. The downslope direction of the gradient is toward the south at LYNN which would tend to reinforce the northerly nocturnal land breeze. The amount of this reinforcement, however, would be limited by the small magnitude of slope and would lead to low wind speeds in the vicinity of LYNN when external forcing is weak.

The gradient of the slope is small within several kilometers of LYNN. Figure 3-11 shows the downslope vector of gradient at grid points with magnitude less than 10 m/km. The gradient vectors are smaller, and the areal extent of small magnitude is greater near LYNN than at other SCAQMD CO sites.

The SCAQMD meteorological sites at Vernon and Compton have relatively small gradients that are not quite twice as large as that at LYNN. Both routine and tethered measurements at these sites showed higher wind speeds than at LYNN. The tethersondes also showed that the lower atmosphere was less stable at Vernon than at LYNN during the night, possibly a result of the difference in slope.

Several CC sites to the south of LYNN had smaller gradients than at LYNN. One site, CC16, was in the same drainage basin as Hawthorne, while the CC17 and CC18 were in the drainages of the Los Angeles River and San Gabriel River, respectively. All sites were near freeways. CC17 and CC18 were down slope from the Artesia Freeway and might have been expected to be impacted by emissions from traffic. CC16 was near, but up slope, from the junction of the Harbor and Redondo Beach Freeways. Concentrations at these sites were less than at LYNN.

The Diagnostic Wind Model develops a slope flow as one component of the generated wind field. This slope flow depends on the terrain slope and the thermal stability. Model calculations of average and maximum magnitudes of the slope flows are shown in Table 3-5 for SCAQMD sites. Shown are values for non-zero magnitudes. For sites with small slopes, the model determined that the slope flow was zero for the daytime hours. At a number of sites, the

Table 3-4

Gradient of Topography at Sampling Sites

Site	UTM E Km	UTM Y Km	Down Slope Gradient	
			Magnitude m/Km	Direction Deg
LYNN	388.2	3754.8	2.11	179.9
HAWT	373.4	3754.3	2.73	80.6
ANAH	415.0	3742.5	3.69	233.5
CELA	386.9	3770.0	6.48	187.9
AZUS	414.9	3777.6	9.96	212.8
LGBH	390.0	3743.0	11.36	200.8
LAHB	412.0	3754.0	11.53	223.9
ALMB	374.5	3772.7	15.01	179.0
WHIT	405.3	3754.0	15.39	210.8
PICO	402.3	3764.1	19.67	343.3
PASA	396.1	3777.3	22.82	159.1
WSLA	365.3	3768.7	26.74	167.4
BURK	379.5	3783.0	33.11	201.5
LSAL (Met)	404.5	3739.8	1.73	232.7
VER (Met)	387.4	3762.5	3.42	164.4
COMA (Met)	385.5	3750.3	3.91	64.9
CSTA (Met)	414.5	3725.9	4.53	332.9
CC16	380.5	3748.5	1.38	56.9
CC17	391.3	3748.7	1.85	205.9
CC18	396.4	3748.4	1.90	180.9
CC10	392.6	3763.0	2.36	165.3
CC01	380.9	3780.4	2.40	59.3
CC19	391.7	3759.4	2.93	152.9
CC14	406.3	3753.1	3.04	198.3
CC05	396.6	3769.7	6.86	73.0
CC21	389.6	3769.1	7.35	306.6
CC15	371.9	3748.4	10.80	65.9
CC07	370.1	3761.2	12.93	353.3
CC06	405.9	3767.3	15.58	195.8
CC12	368.3	3754.2	17.00	256.8
CC13	381.1	3753.0	17.19	192.6
CC04	380.5	3773.4	20.61	181.2
CC02	392.8	3781.0	22.61	225.3
CC08	376.7	3762.8	33.11	65.3
CC11	405.4	3759.7	43.27	212.2
CC03	408.8	3778.9	70.50	194.1
CC20	386.0	3772.8	77.24	50.6

DOWNSLOPE GRADIENT (< 10 M/KM)

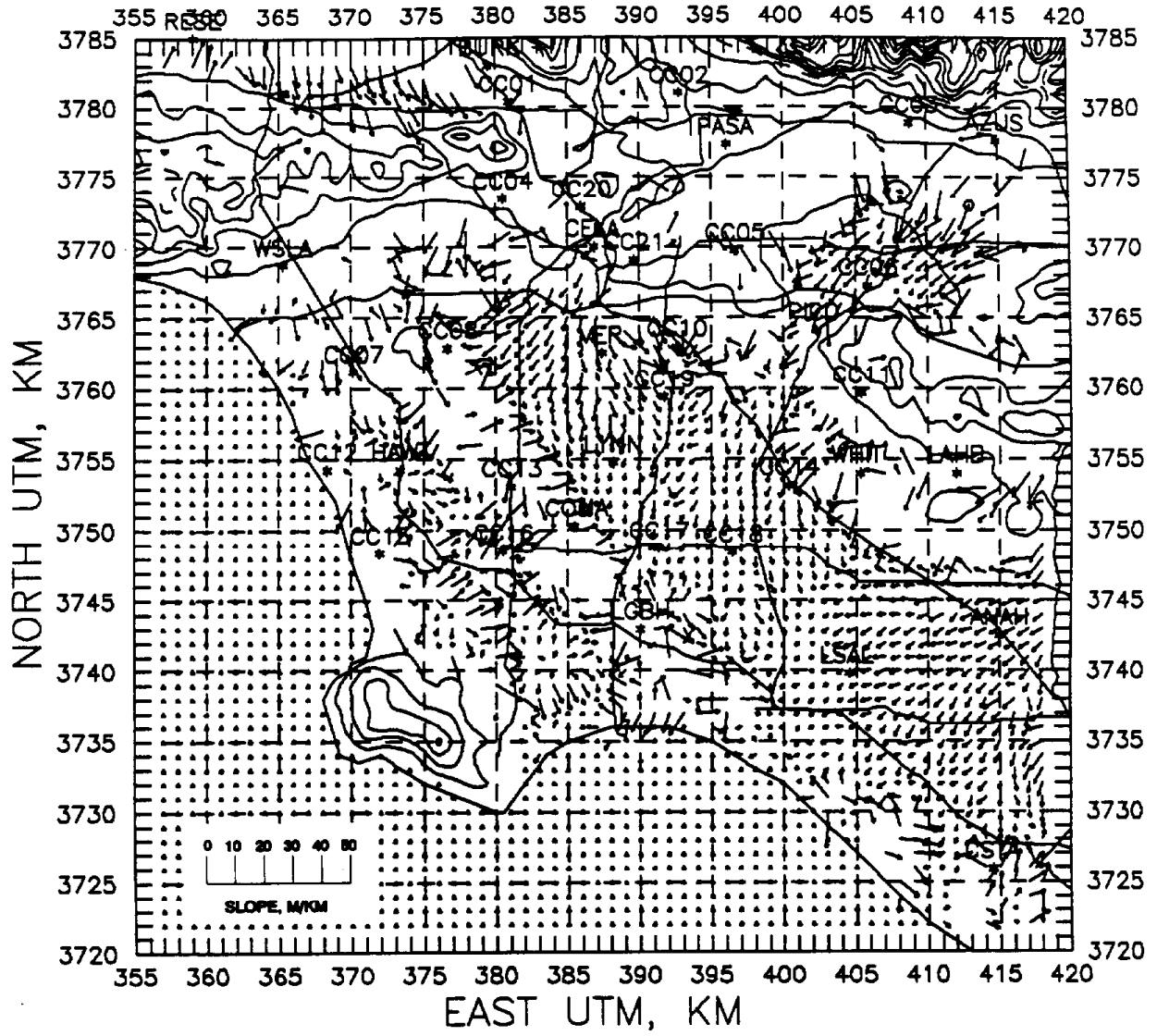


Figure 3-11. Gradient of Topography at Locations Where Magnitude is < 10 m/km.

Table 3-5

Magnitude of Slope Winds from Diagnostic Wind Model

Site	December, 1989 Intensive			January, 1990 Intensive		
	Number Non-Zero Points	Average Speed (m/sec)	Maximum Speed (m/sec)	Number Non-Zero Points	Average Speed (m/sec)	Maximum Speed (m/sec)
ANAH	16	0.17	0.54	20	0.29	0.64
BURK	24	1.27	2.22	40	1.46	3.27
CELA	16	0.17	0.50	19	0.24	0.54
HAWT	15	0.18	0.51	18	0.26	0.54
LAHB	15	0.18	0.50	22	0.25	0.57
LGBH	24	0.54	1.24	40	0.60	1.50
LSAL	14	0.19	0.51	20	0.25	0.54
LYNN	15	0.19	0.50	20	0.23	0.51
PICO	15	0.17	0.40	22	0.24	0.57
WHIT	24	0.65	1.26	40	0.71	1.94

maximum magnitude of the slope flow was about 0.5 m/sec. The smallest slope flows were generated at Pico Rivera for December, 1989 and at Lynwood for January, 1990. Slope generated winds were not, however, much different for the several sites with low to moderate gradients of slope, although the gradient at Pico Rivera is fairly large. The modeled slope flows indicate that terrain in the vicinity of Lynwood contributes less to the nocturnal winds than it does at other sites.

3.6 Tethersonde Data

Several standard meteorological variables were calculated from wind speed and direction, wet- and dry-bulb temperatures, and altitude data collected by tethersonde systems in Lynwood (LTS) and Vernon (VTS). The pressures at each sample altitude were reconstructed by integration of the hydrostatic equation. Surface pressure was estimated from the surface pressure during single daily sounding made at LMU during the morning and the difference in elevation between LMU and the tethersonde sites. Virtual potential temperature was computed at each altitude as a measure of the thermal stability of the atmosphere near the ground while including the effect of water vapor on the density of the air. Virtual potential temperature is constant with altitude in a thermally neutral atmosphere, increases with altitude in a stable atmosphere, and decreases with altitude in an unstable atmosphere.

The change of virtual potential temperature with altitude or lapse rate of virtual potential temperature was used as the measure of stability to compare the various tethersonde soundings. This lapse rate is zero in a thermally neutral atmosphere, positive in a thermally stable atmosphere, and negative in a thermally unstable atmosphere. The magnitude of the lapse rate is a measure of the atmosphere's stability and instability. A second measure of stability, comparing buoyancy and mechanical forces, was also computed as the ratio of lapse rate to the square of the change of wind velocity with height. This local Richardson's Number gave similar information as the lapse rate with some amplification near the surface where the wind shear was low. Since there were fewer valid computations near the surface where the shear was often constant, only the lapse rate of virtual potential temperature has been used as a measure of stability.

Altitudes at which lapse rates had significant changes were visually determined from plots of virtual potential temperature versus altitude and lapse rate versus altitude. These altitudes defined boundaries between layers of air with different stabilities. Lapse rates for each layer were determined for each sounding. To determine a stability factor for each hour, the average lapse rates and heights of significant layer were computed from the soundings during the hour, usually four (two up and two down) soundings at LTS and two (both down) at VTS. The lapse rates and heights from the individual soundings were averaged on a layer-by-layer basis. The layer nearest the ground was used for this study because the majority of CO emissions are at the surface with little buoyancy to lift them.

Hourly values of the lapse rate and vertical extent or height above ground of this layer at LTS and VTS are shown in Figure 3-12. At both locations, lapse rates of the lowest distinct

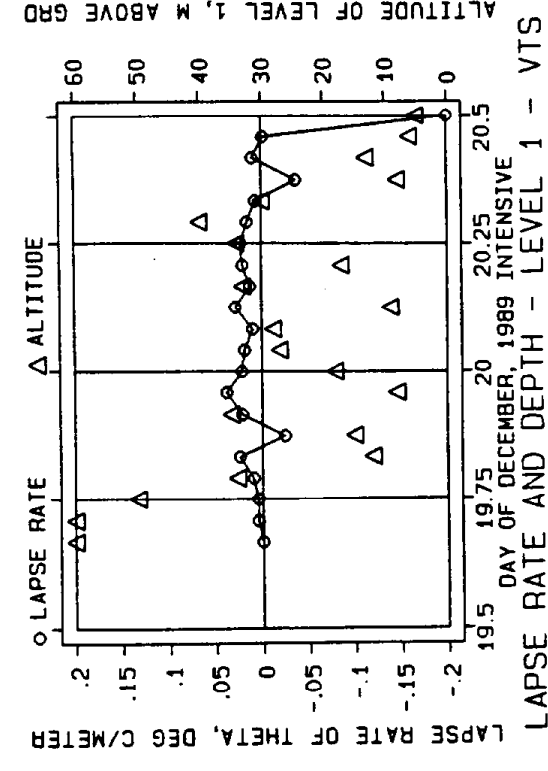
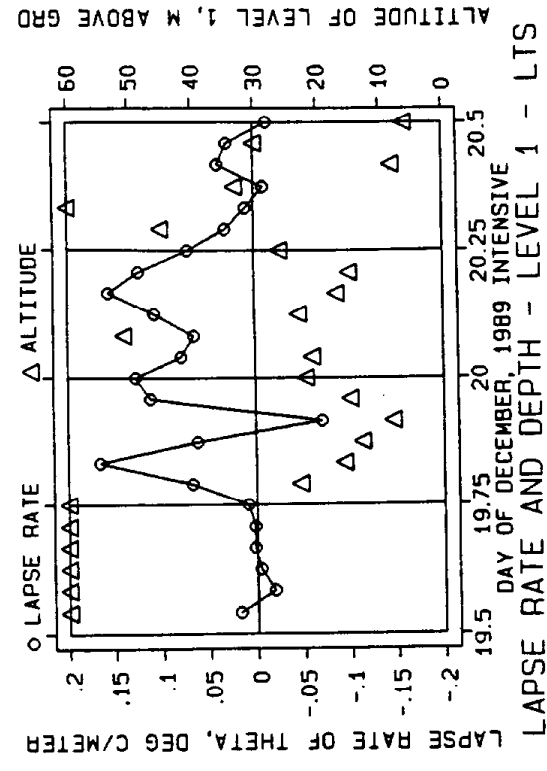
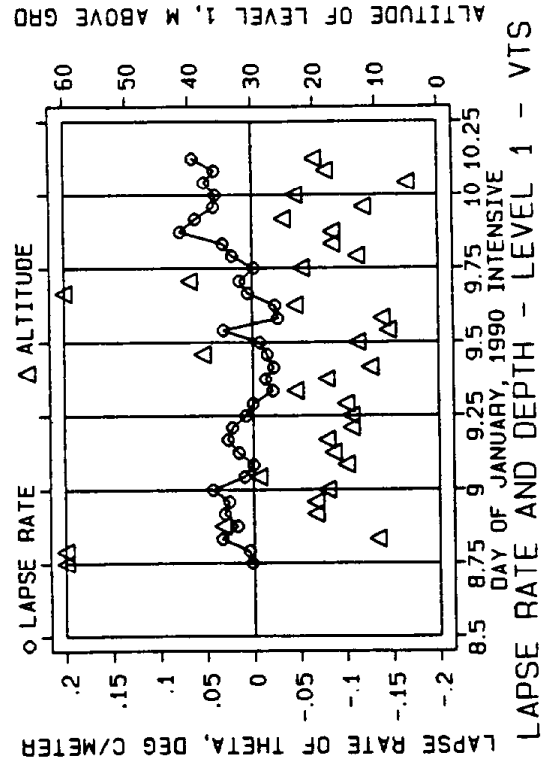
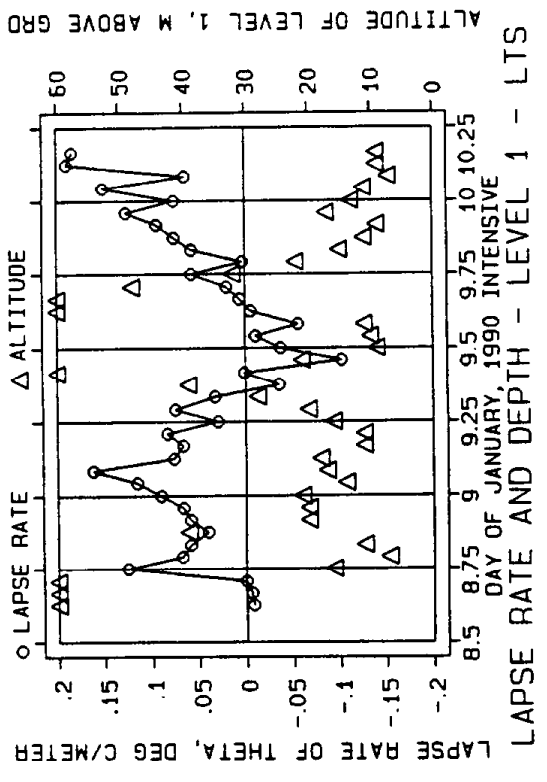


Figure 3-12. Magnitude and Depth of Lapse Rate of Potential Temperature for Lowest Significant Level at LTS and VTS.

layer were positive (stable conditions) during most nighttime hours, slightly negative (unstable conditions) during morning daylight hours under low wind speeds, and near zero (neutral conditions) during afternoon daytime hours under higher wind speeds. For 2100 PST at VTS and 2200 PST at LTS on 19 December, a shallow unstable layer did exist at the ground although the layers above the ground remained stable. In general, the depth of the surface layer was 10 to 20 m at night and during morning daylight hours. During the afternoon, the surface layer often extended past the altitude limit of 60 m for the tethersonde measurements. Nighttime lapse rates at LTS, which reached values that were several times greater than those at VTS, indicate a much higher thermal stability at LTS than at VTS.

The morning transition periods from stable to unstable conditions occurred between 0800 and 0900, while the evening transition back to stable conditions occurred between 1700 and 1900. Time of the morning transition period was similar at the two sites, while the evening transition period to stable conditions started an hour earlier at LTS on each intensive day. Average wind speeds and directions were computed for several layers: <3 m, 3 to 20 m, 20 to 40 m, and >40 m. Wind speeds and directions for the two lowest layers at LTS and VTS are shown in Figure 3-13 for December and Figure 3-14 for January. Speeds at both sites were lowest near the ground. Nighttime speeds were generally less than daytime speeds. Speeds at LTS were less than speeds at VTS. Below 3 m, nighttime speeds were less than 0.5 m/s at LTS and about 1 m/s at VTS. Between 3 and 20 m, nighttime speeds were between 0.5 and 1 m/s at LTS and between 1 and 2 m/s at VTS. Speeds at both sites decreased to minimum values between 1800 and 1900 PST with LTS's an hour earlier than VTS's. Speeds in the 3 to 20 m layer increased somewhat between 2100 and 2300 PST. Daytime speeds ranged from 1 to 4 m/s, with highest values generally in the afternoon. Wind directions reflected the change from daytime westerly sea breeze to nighttime northerly and easterly land breeze and back. As with the lapse rate and wind speed, the evening transition occurred an hour earlier at LTS than at VTS. The time of the morning transition was about the same at both sites.

3.7 Surface Mixed Layer

The surface mixed layer is the layer of the atmosphere near the ground through which vertical mixing of air occurs. Its top is defined by the altitude at which mixing is suppressed, often by an overriding layer of stable air. The surface mixing layer is generally deep under unstable and neutral conditions, while it may not exist at all under stable conditions. This depth through which pollutants are mixed is one factor that determines the magnitude of the concentrations.

Hourly surface mixing depths were estimated from tethersonde soundings when the mixed layer was shallower than 60 m and from the LMU soundings when mixing exceeded 60 m, which occurred for all daytime hours between the transition periods from stable to unstable/neutral and vice versa. Mixing height was determined from the altitude at which the stability of the air changed from neutral or unstable to stable, i.e., the lapse of potential temperature changed from zero or negative to positive. For each intensive day, the single daily sounding made at LMU at 0600 PST was plotted on a Skew T thermodynamic diagram. This sounding was assumed to be

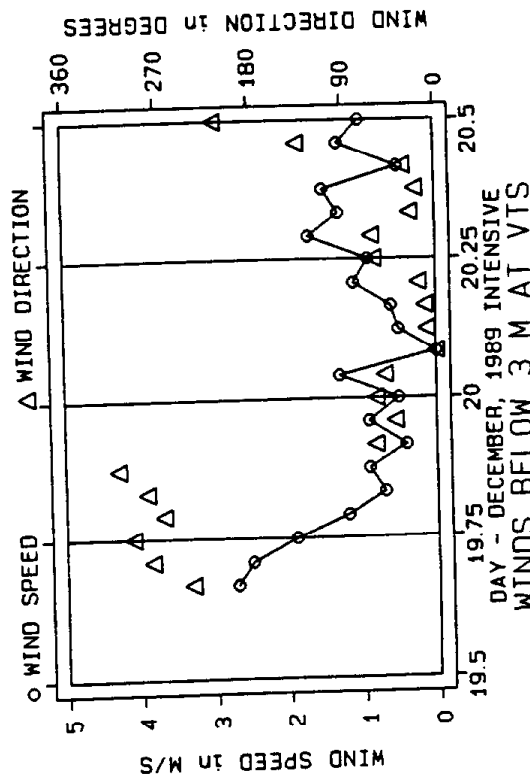
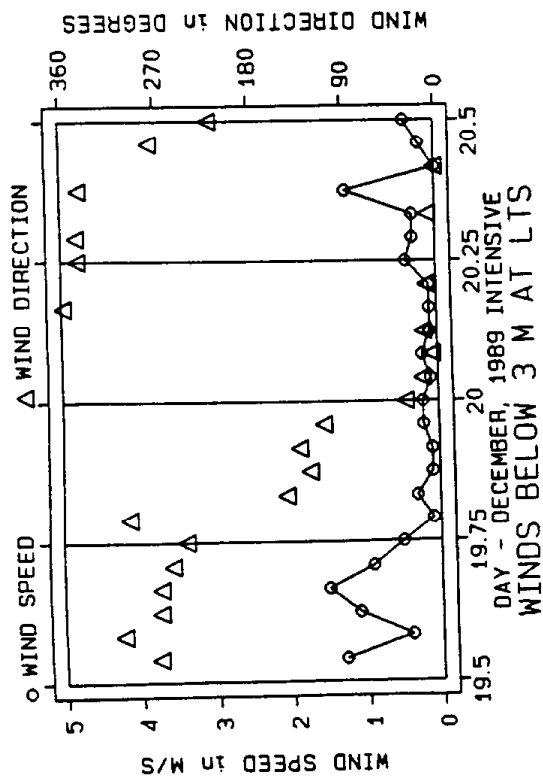
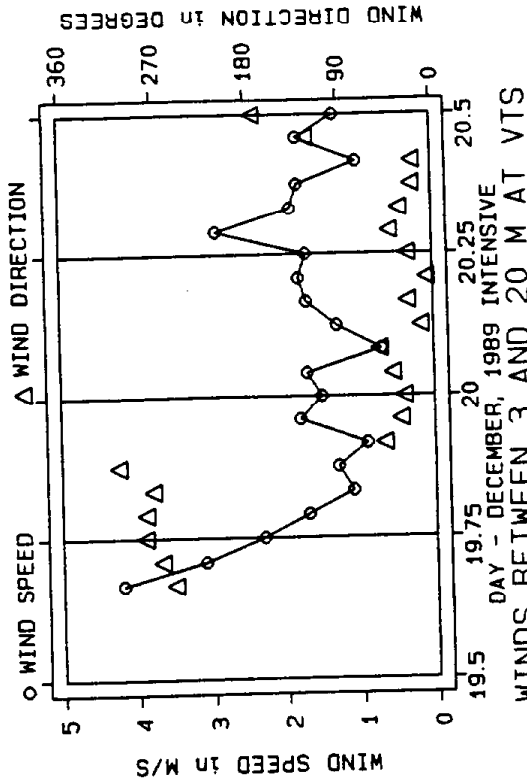
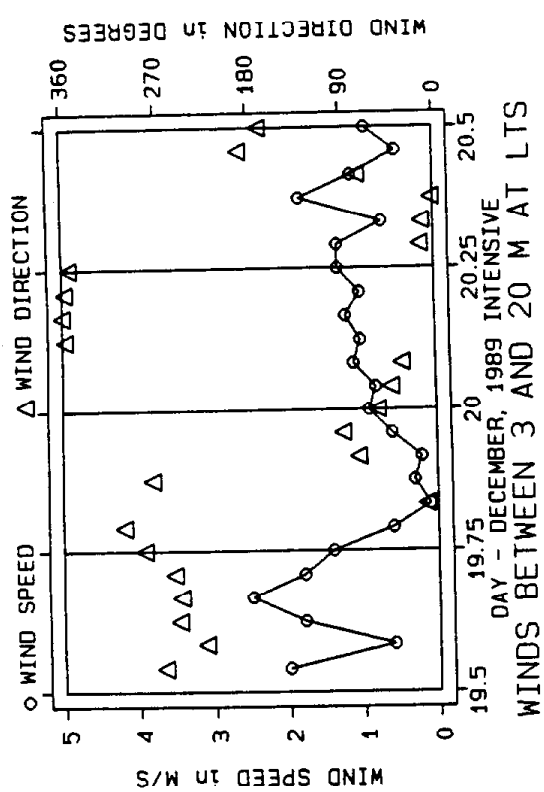


Figure 3-13. Average Wind Speed and Wind Direction at Lynwood and Vernon Tethersonde Sites for December, 1989 Intensive Period.

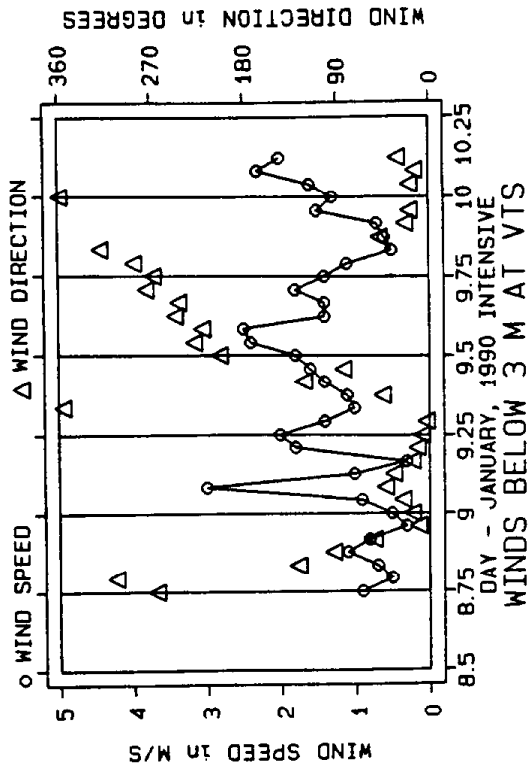
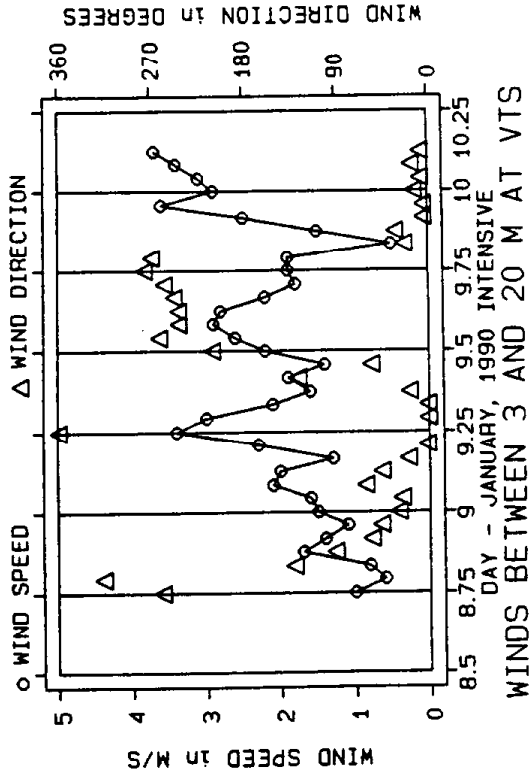
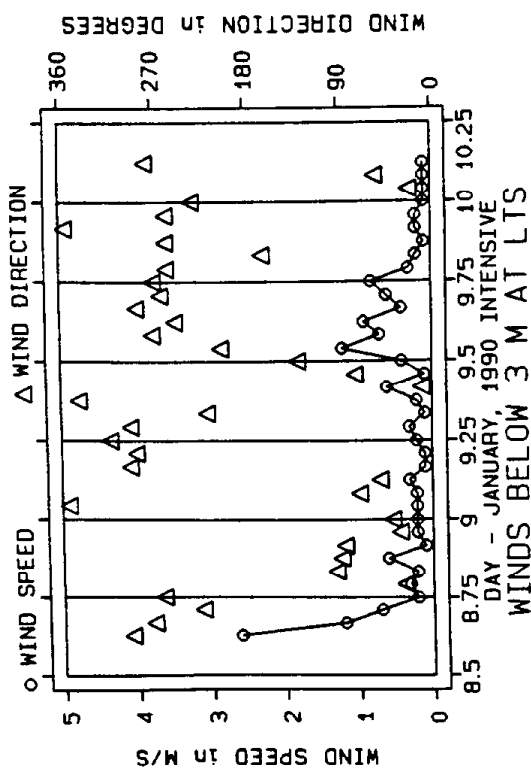
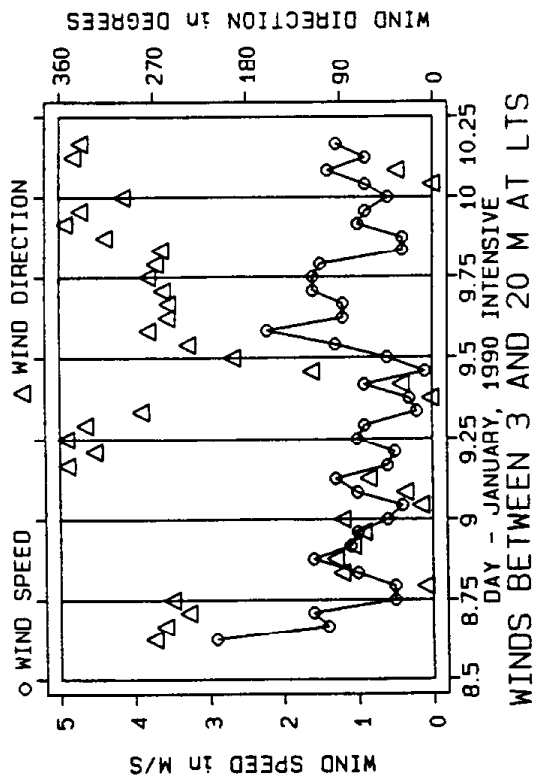


Figure 3-14. Average Wind Speed and Wind Direction at Lynwood and Vernon Tethersonde Sites for January, 1990 Intensive Period.

valid at elevations above the Lynwood area and was assumed to be valid for the entire day. When the mixing layer measured at LTS exceeded 60 m, the mixing height was determined from the LMU sounding. The surface temperature and pressure in the vicinity of Lynwood were obtained from the LTS tethersonde data. On the Skew T diagram, a line was drawn along a constant adiabat from a point at the surface temperature and pressure to a point that intersected the LMU temperature sounding. This intersection point determined the temperature and pressure at the top of the mixed layer. The height of the mixed layer was calculated from the hydrostatic equation. For stable periods, a mixing height of 20 m was used to indicate the suppression of mixing while allowing for some urban heat island effect.

Mixing heights are shown in Table 3-6, including the pressure and temperature at the top of the mixed layer and the thermal stability of the atmosphere. The maximum daytime mixing depths were about 1,250 m during the December intensive and about 550 m during the January intensive. The lower mixing depth may have contributed to the generally higher CO concentrations throughout the SoCAB during the January intensive.

3.8 Comparison of CO Concentrations, Traffic Counts, Lapse Rate, and Wind Speed and Direction

CO concentrations, traffic counts, lapse rate, and wind speed and direction have been plotted to illustrate their temporal evolution and to compare and contrast their joint changes through visualization. While this is only qualitative discussion, it does give insight into the causes of high CO concentrations at LYNN.

Figures 3-15 to 3-22 contain plots of these data for comparison with CO concentrations at LYNN. The layout of each figure is the same. The upper left-hand graph compares the CO concentration at LYNN to the traffic counts at a nearby location, either local or freeway. The upper right-hand graph compares the same CO concentration to the lapse rate of virtual potential temperature in the lowest significant layer measured at either tethersonde site. The lower left-hand graph compares the CO concentration to the wind speed in the 3 to 20 m layer measured at either tethersonde site. The lower right-hand graph compares the CO concentration to the wind direction in the 3 to 20 m layer measured at either tethersonde site.

The units and scaling of each-type of graph are the same for all sets except for the local and freeway traffic counts. The graphs have been scaled for the largest value of the particular quantity that is plotted. A direct visual comparison can be made between the same quantity measured at more than one location. The length of time covered for the two intensive period is different. The December graphs cover two days (12/19 0000 through 12/20 2300) while the January graphs cover three days (01/08 0000 through 01/10 2300). Vertical lines have been added to the graphs to delineate the hours of 0000, 0600, 1200, and 1800 PST.

December intensive data are shown in Figures 3-15 to 3-18. Figure 3-15 has traffic counts on Long Beach Blvd. and lapse rate, wind speed, and wind direction at LTS. Figure 3-16 has traffic counts on Imperial Hwy. and LTS data. Figure 3-17 has traffic counts on Long Beach

Table 3-6

Heights of Mixed Layer During Intensive Periods

<u>Date</u>	<u>Hour</u>	<u>Pressure mb</u>	<u>Temperature °C</u>	<u>Height Meters</u>	<u>Stability</u>
891219	12	875.0	6.0	1256.9	Neutral
	13	880.0	6.3	1210.3	Neutral
	14	902.0	7.8	1007.6	Neutral
	15	928.0	9.3	773.1	Neutral
	16	952.0	10.0	561.6	Neutral
	17	970.0	10.6	406.1	Neutral
	18			150.0	Transition
	891219 19 to 891220 07				20.0
	08			50.0	Transition
	09	991.0	11.7	219.4	Neutral
	10	948.0	10.0	588.4	Neutral
	11	905.0	8.9	972.6	Neutral
900108	12	957.0	13.3	552.1	Neutral
	13	955.0	13.4	569.6	Neutral
	14	955.0	13.4	569.6	Neutral
	15	958.0	13.0	543.3	Neutral
	16	970.0	12.3	439.1	Neutral
	17	980.0	12.0	353.4	Neutral
	18			180.0	Transition
	900108 19 to 900109 07				20.0
	08			60.0	Transition
	09	992.0	16.3	229.4	Neutral
	10	978.0	18.0	350.3	Neutral
	11	963.0	19.0	482.3	Neutral
	12	961.0	18.9	500.1	Neutral
	13	963.0	19.0	482.3	Neutral
	14	965.0	18.9	464.6	Neutral
	15	970.0	18.5	420.4	Neutral
	16	985.0	17.4	289.6	Neutral
	17			100.0	Transition
900109 18 to 900109 03				20.0	Stable

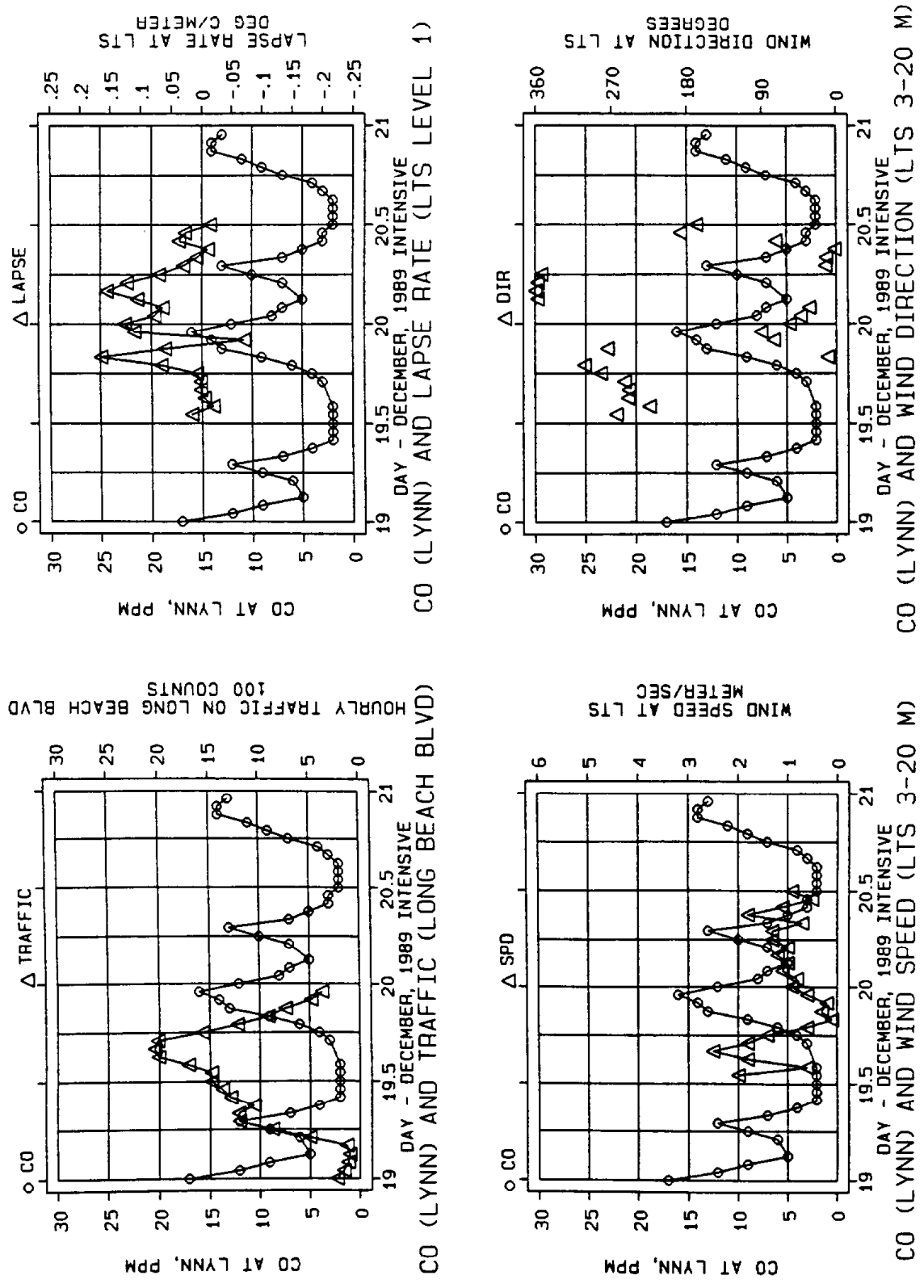


Figure 3-15. CO at LYNN; Traffic on Long Beach Blvd.; Lapse Rate, Wind Speed, and Wind Direction at LTS - December, 1989.

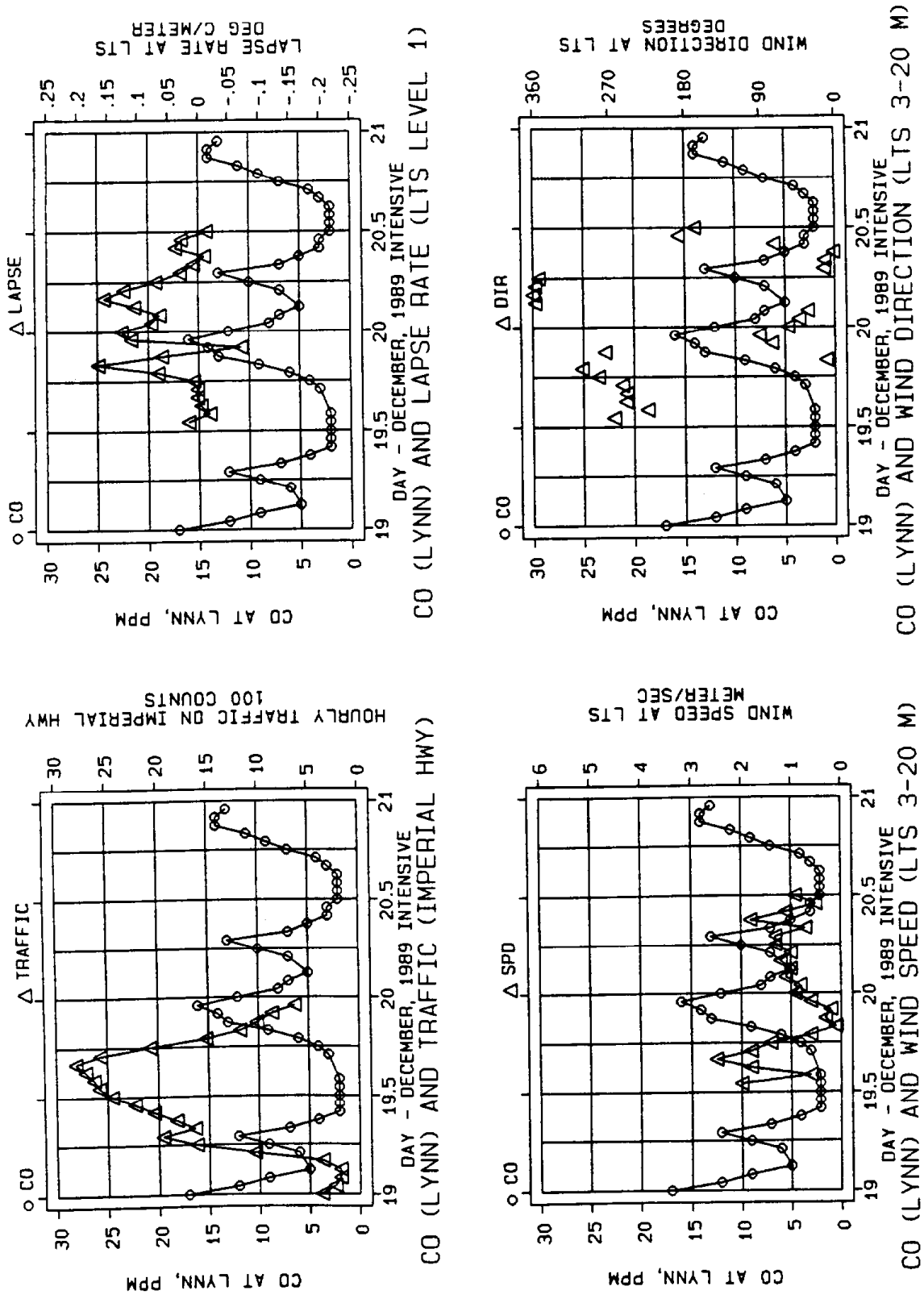
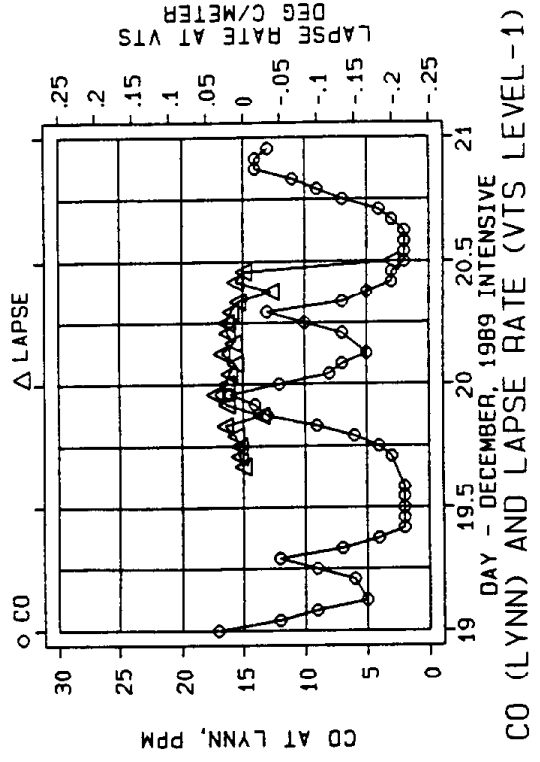
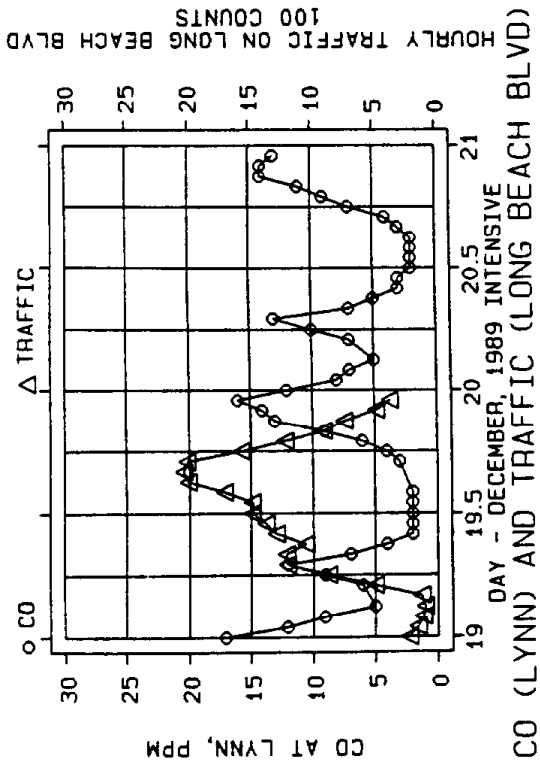


Figure 3-16. CO at LYNN; Traffic on Imperial Highway; Lapse Rate, Wind Speed, and Wind Direction at LTS - December, 1989.



3-32

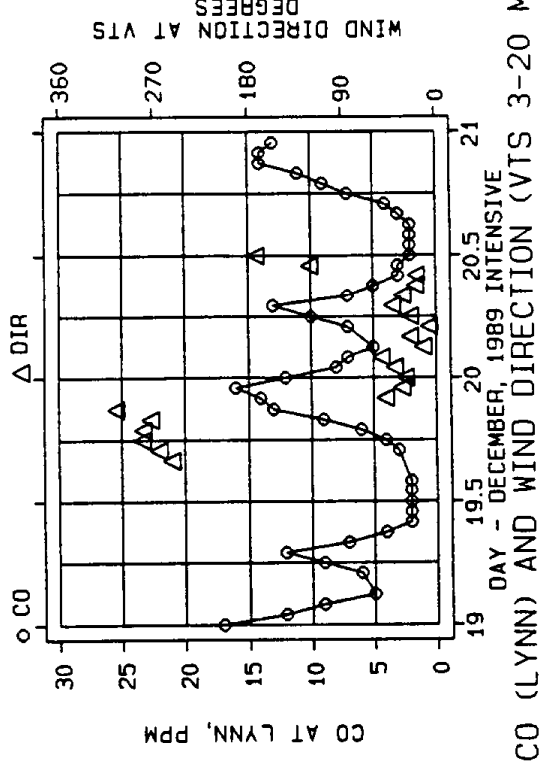
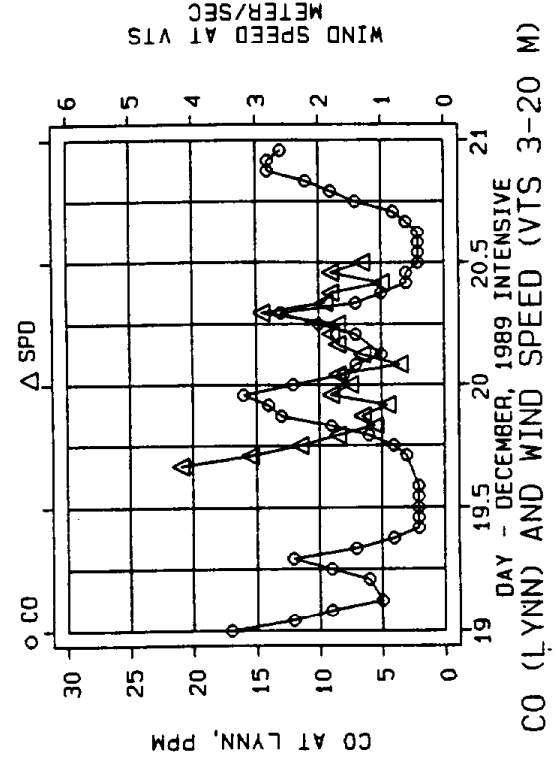


Figure 3-17. CO at LYNN; Traffic on Long Beach Blvd.; Lapse Rate, Wind Speed, and Wind Direction at VTS - December, 1989.

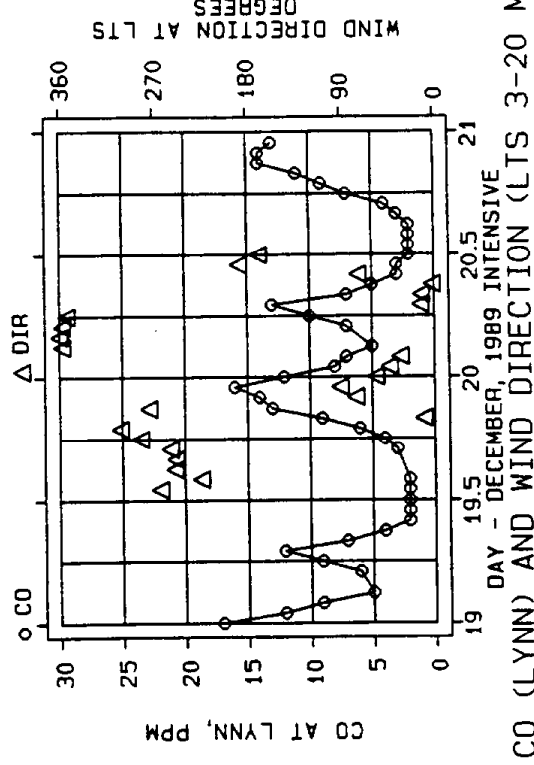
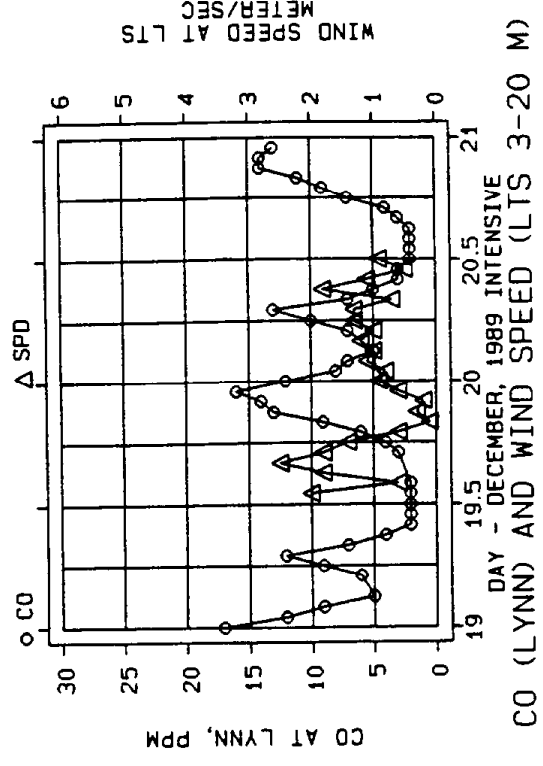
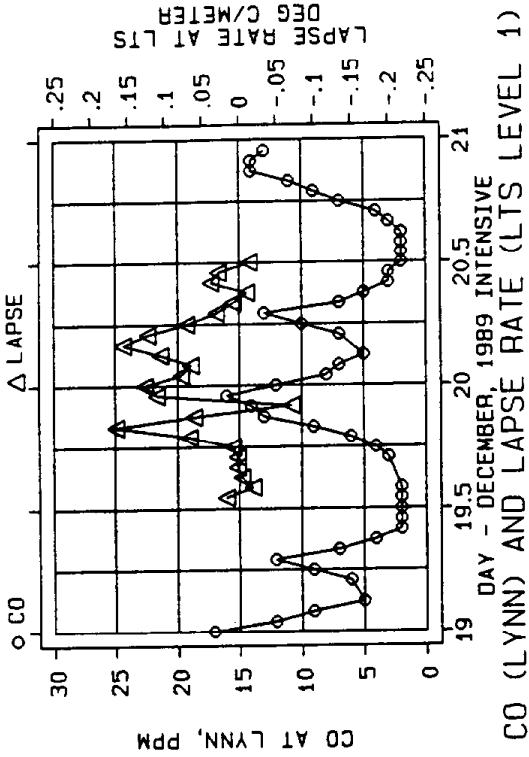
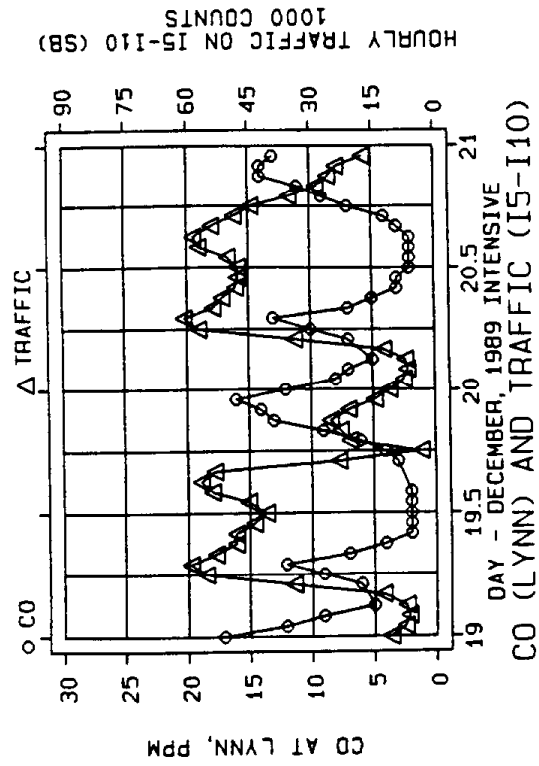
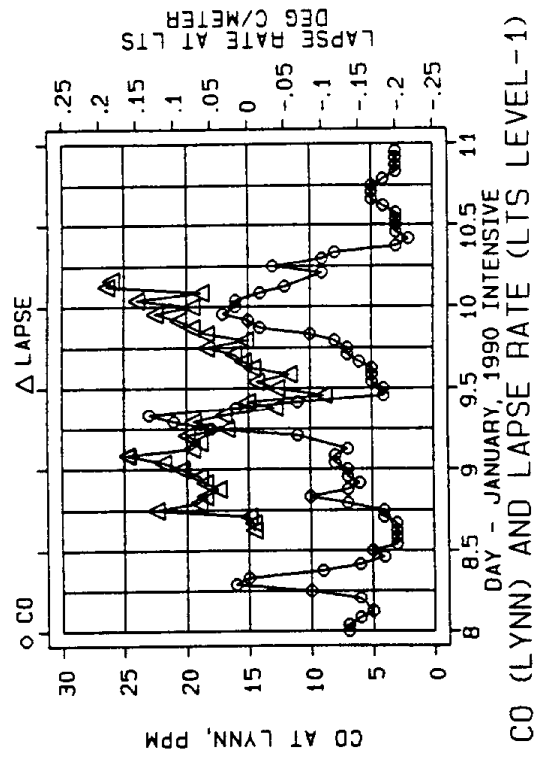
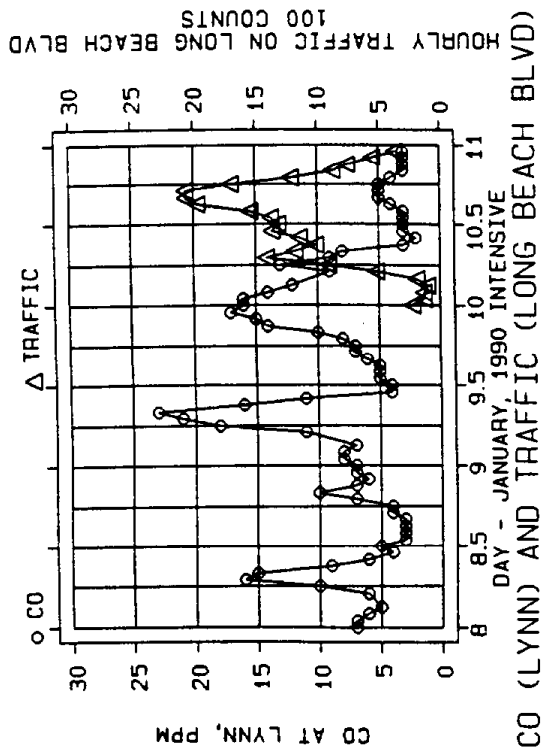


Figure 3-18. CO at LYNN; Traffic at I-5/I-10; Lapse Rate, Wind Speed, and Wind Direction at LTS - December, 1989.



3-34

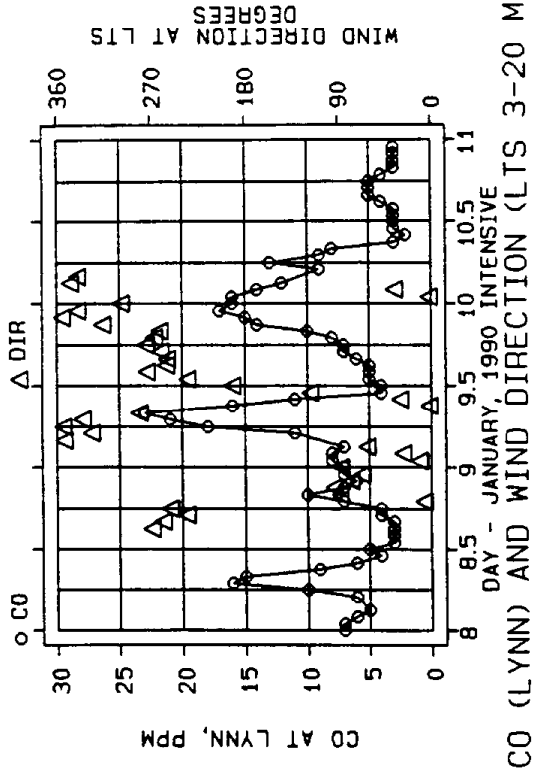
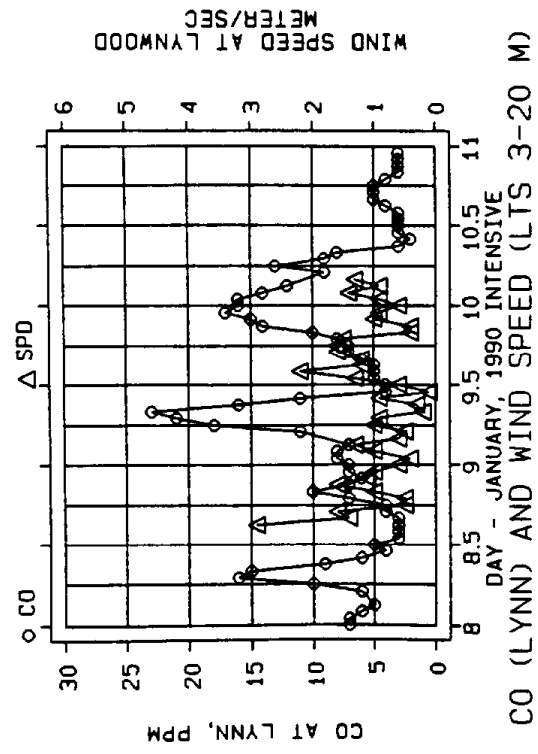
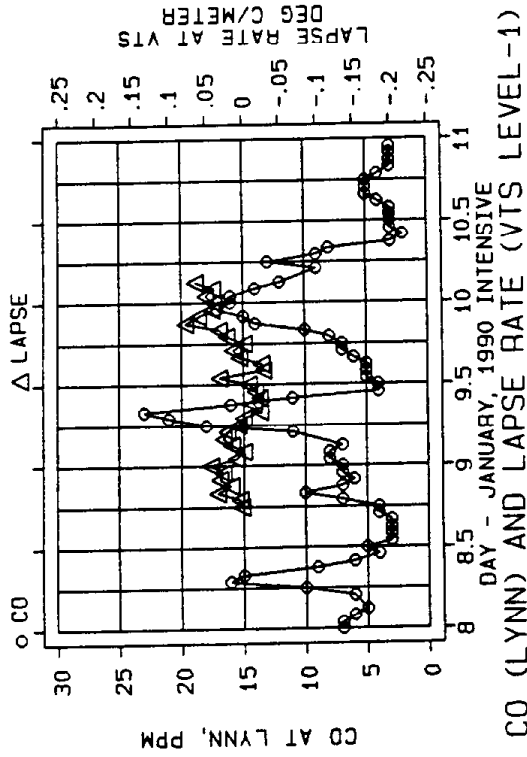
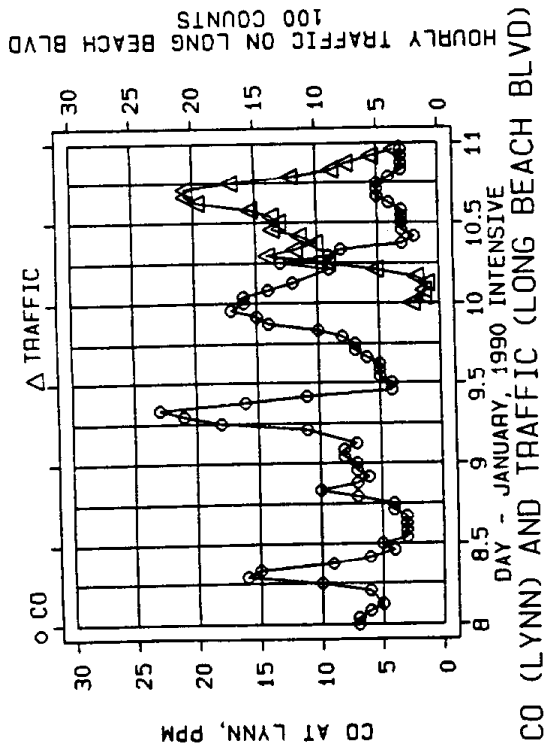


Figure 3-19. CO at LYNN; Traffic on Long Beach Blvd.; Lapse Rate, Wind Speed, and Wind Direction at LTS - January, 1990.



3-35

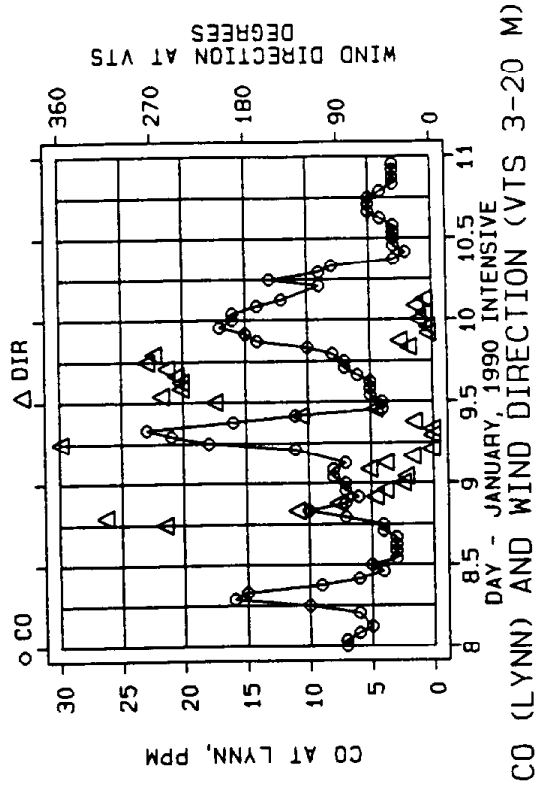
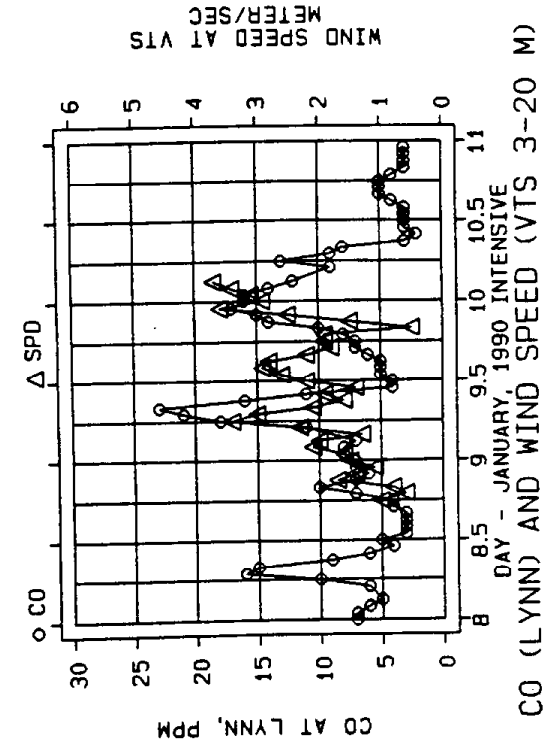


Figure 3-20. CO at LYNN; Traffic on Long Beach Blvd.; Lapse Rate, Wind Speed, and Wind Direction at VTS - January, 1990.

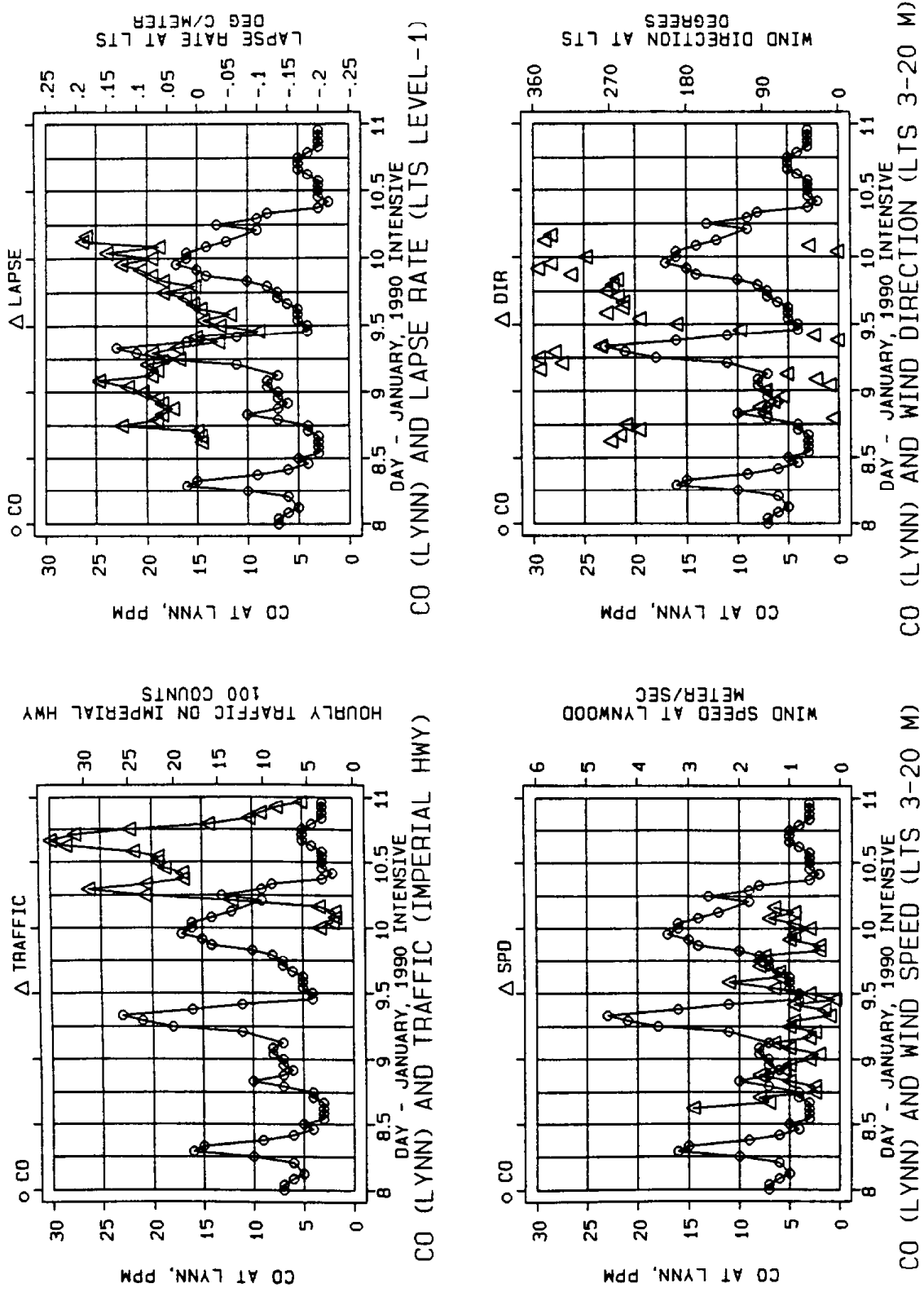
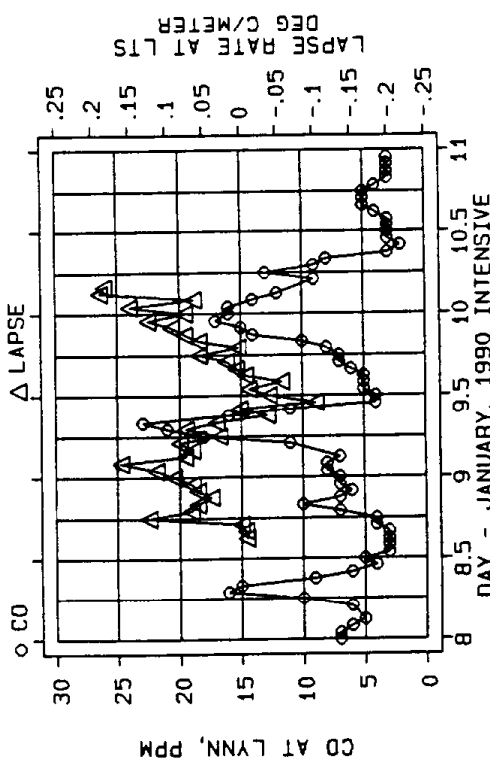
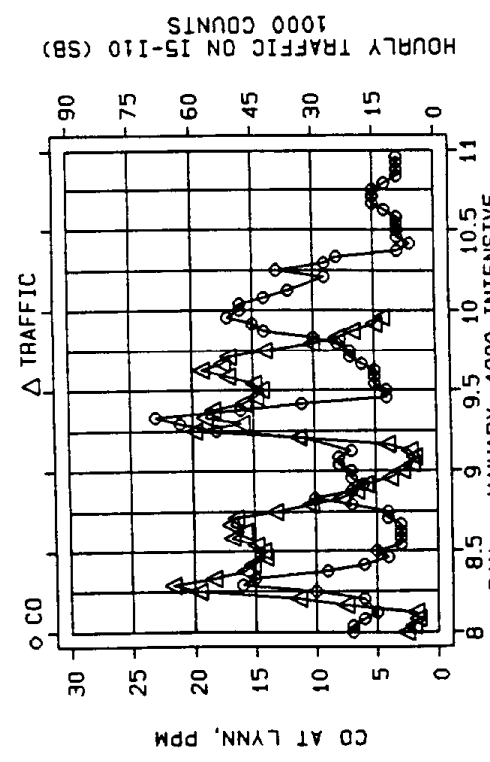


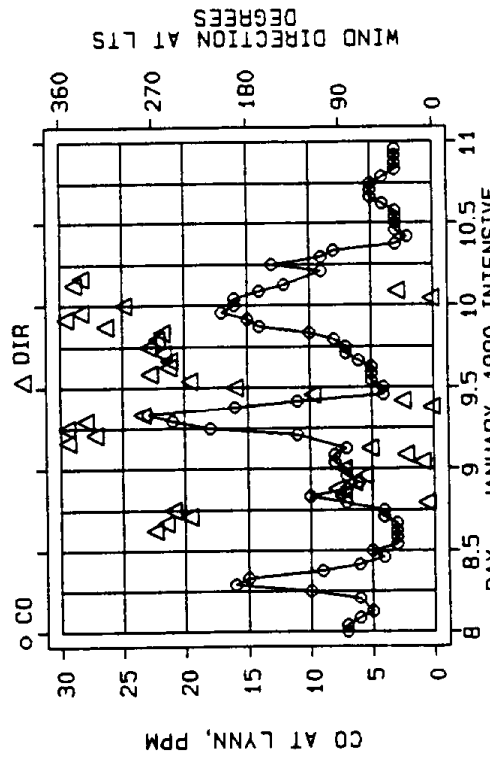
Figure 3-21. CO at LYNN; Traffic on Imperial Highway; Lapse Rate, and Wind Direction at LTS - January, 1990.



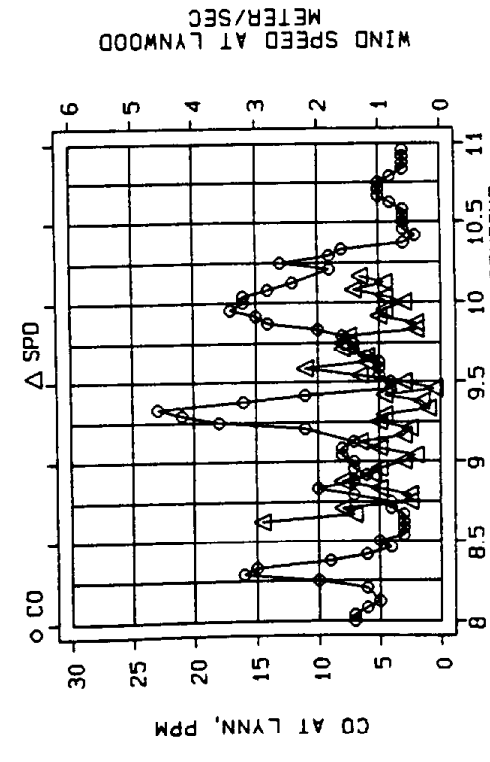
CO (LYNN) AND LAPSE RATE (LTS LEVEL-1)



CO (LYNN) AND TRAFFIC (I5-I10)



CO (LYNN) AND WIND DIRECTION (LTS 3-20 M)



CO (LYNN) AND WIND SPEED (LTS 3-20 M)

Figure 3-22. CO at LYNN; Traffic at I-5/I-10; Lapse Rate, and Wind Direction at LTS - January, 1990.

Blvd. and VTS data. Figure 3-18 has traffic counts on I-5 and LTS data. A similar order is maintained for the January intensive data in Figures 3-19 to 3-22.

For December, the afternoon local and freeway traffic counts reached maximum values at 1500 to 1700, at which time the CO concentration was just starting to increase. Traffic counts decreased as CO levels increased, with both local and freeway traffic falling to about half their maximum by 1700 and the CO level increasing to about half its eventual maximum. The large drop in the count for I-5/I-10 on December 19 is probably due to equipment failure. After 1700, the atmosphere became stable, the wind speed decreased to near zero at LTS at 1800 and to 1 m/s at VTS, and the CO concentration began to increase more rapidly. The wind direction at LTS shifted from westerly at 1700, to northerly at 1800, back to westerly at 1900, and finally to easterly at 2000. The lapse rates at LTS and VTS had similar variation but LTS showed a much more stable layer. The morning traffic, assuming that local traffic on 19 December and 20 December were similar, started to increase an hour before the CO level started to increase. Both reached a maximum during the same hour, coinciding with the last hour of moderately stable air at either tethersonde site. At LTS, the wind speeds were fairly steady at 1 m/sec during the increase of CO levels. The VTS wind speeds were 1 to 2 m/sec higher. CO concentration decreased rapidly after 0700; the lapse rate indicated that the atmosphere became unstable then.

For January, the situation was more complicated. The evening of 8 January started similarly to that of 19 December. At 1700, however, the lapse rate decreased as the wind speed increased. The CO concentration reached a maximum at 1800 and then decreased. There was a slight increase in CO levels at 0100 (Dec. 20) as the air became more stable again. The morning maximum was reached at 0800 as the traffic counts peaked, as the atmosphere became slightly less stable, and as the wind speed decreased. That the morning maximum on 9 January was 7 ppm higher than on 20 December may be attributable to the lower wind speeds on the morning of 9 January. CO concentrations then decreased as the atmosphere became unstable. The evening of 9 January was similar to the evening of 19 December although the atmosphere became stable an hour earlier on 9 January at 1500 and CO started to increase earlier. As in December, wind speed at LTS decreased at 2000 before increasing later in the evening.

The January graphs show an interesting occurrence during the afternoon of 10 January after the intensive was complete. The maximum CO concentration at LYNN occurred between 1400 to 1600, approximately one hour offset from the peak in local traffic counts and appears to be directly attributable to the local traffic. On this particular day, the CO concentration only reached 5 ppm, an increase of 2 ppm from its minimum daytime value. The local wind speeds were moderately high in the evening and prevented the increase of CO. This indirectly shows the effect that a stable atmosphere and low wind speed can have on CO concentrations.

Similarly, CO, meteorological, and traffic data for SCAQMD sites at Hawthorne and Central Los Angeles are shown in Figures 3-23 and 3-24 for December and Figures 3-25 and 3-26 for January. LYNN CO and tethersonde data are also shown. The morning CO maxima at CELA and HAWT occurred at about the same time as at LYNN. The nighttime CO maxima occurred one to two hours earlier at CELA and one to two hours later at HAWT than LYNN.

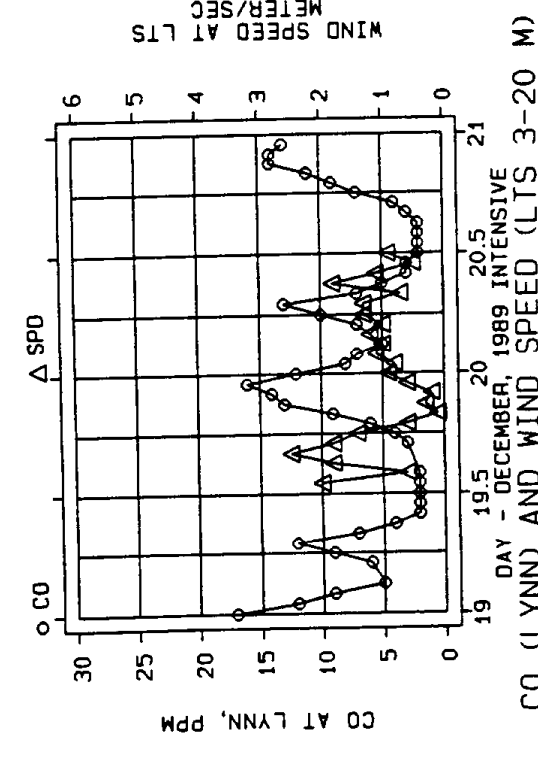
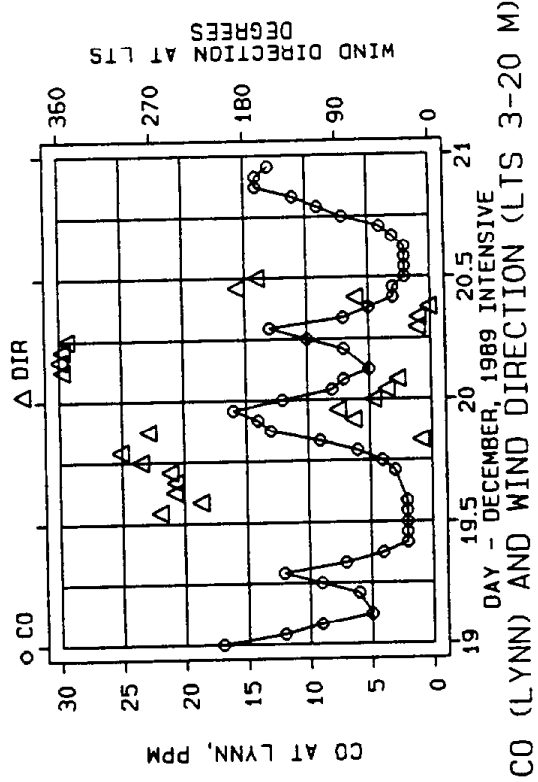
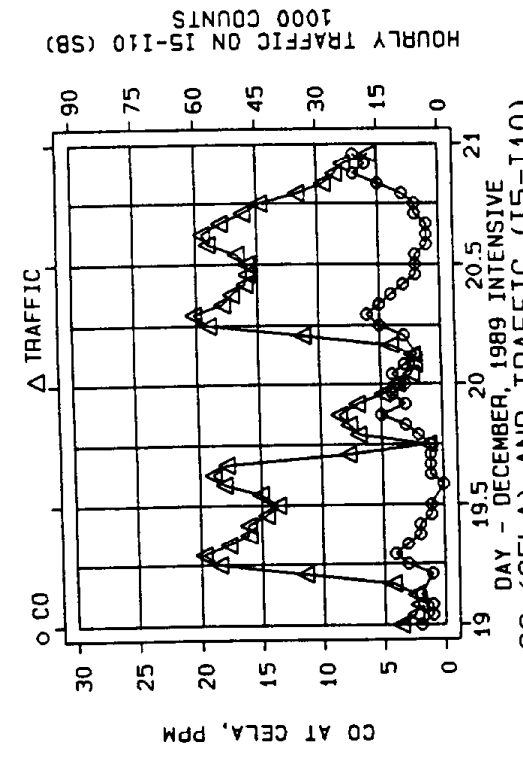
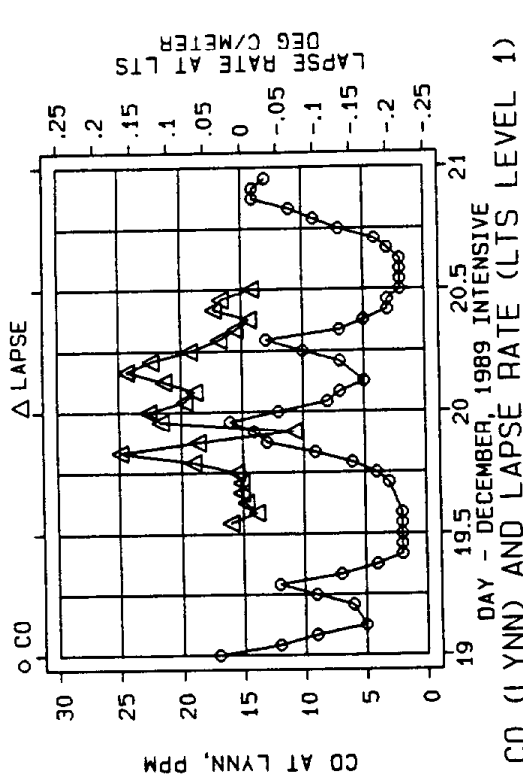


Figure 3-23. CO at CELA; Traffic at I-5/I-10; Lapse Rate, Wind Speed, and Wind Direction at LTS - December, 1989.

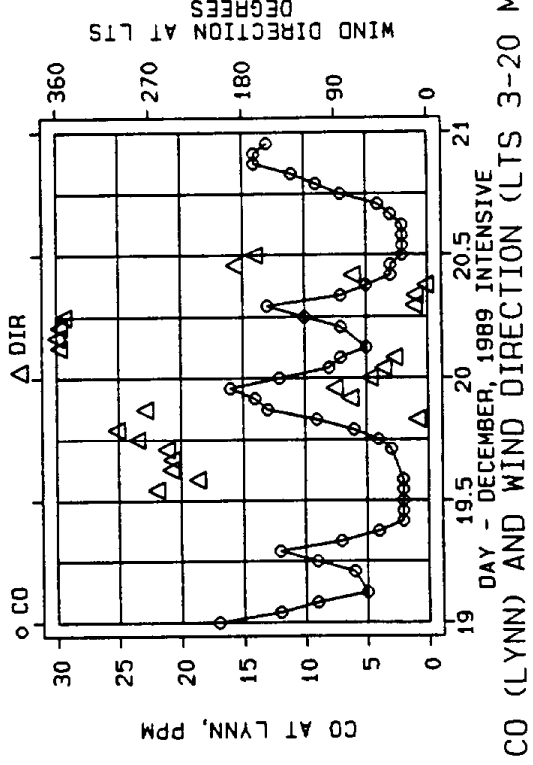
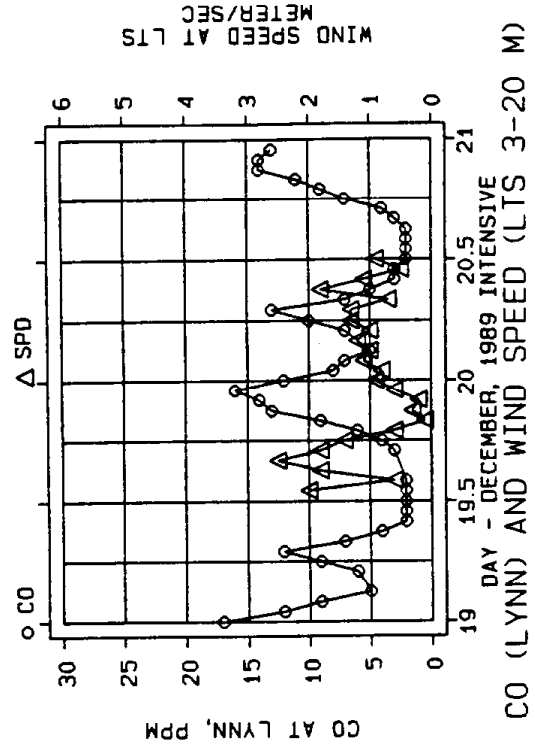
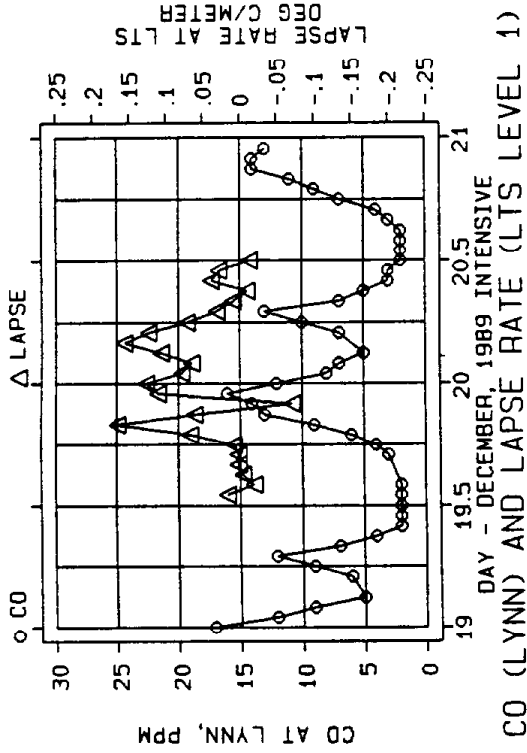
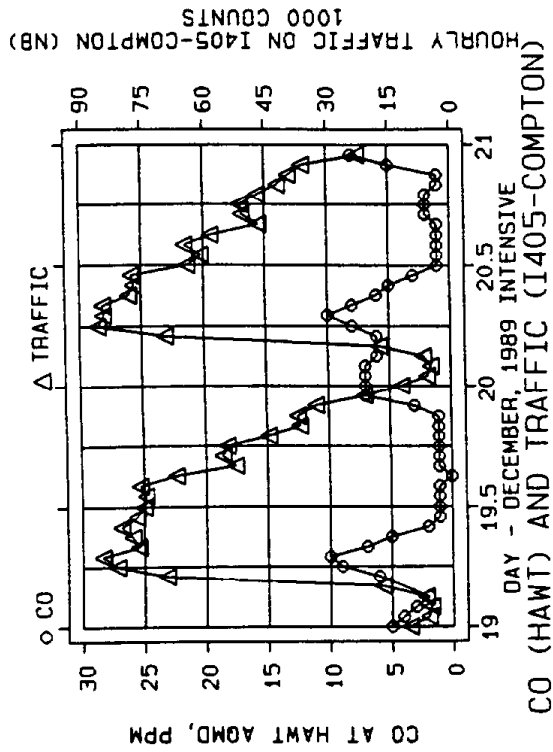


Figure 3-24. CO at HAWT; Traffic at I-405/Compton; Lapse Rate, Wind Speed, and Wind Direction at LTS - December, 1989.

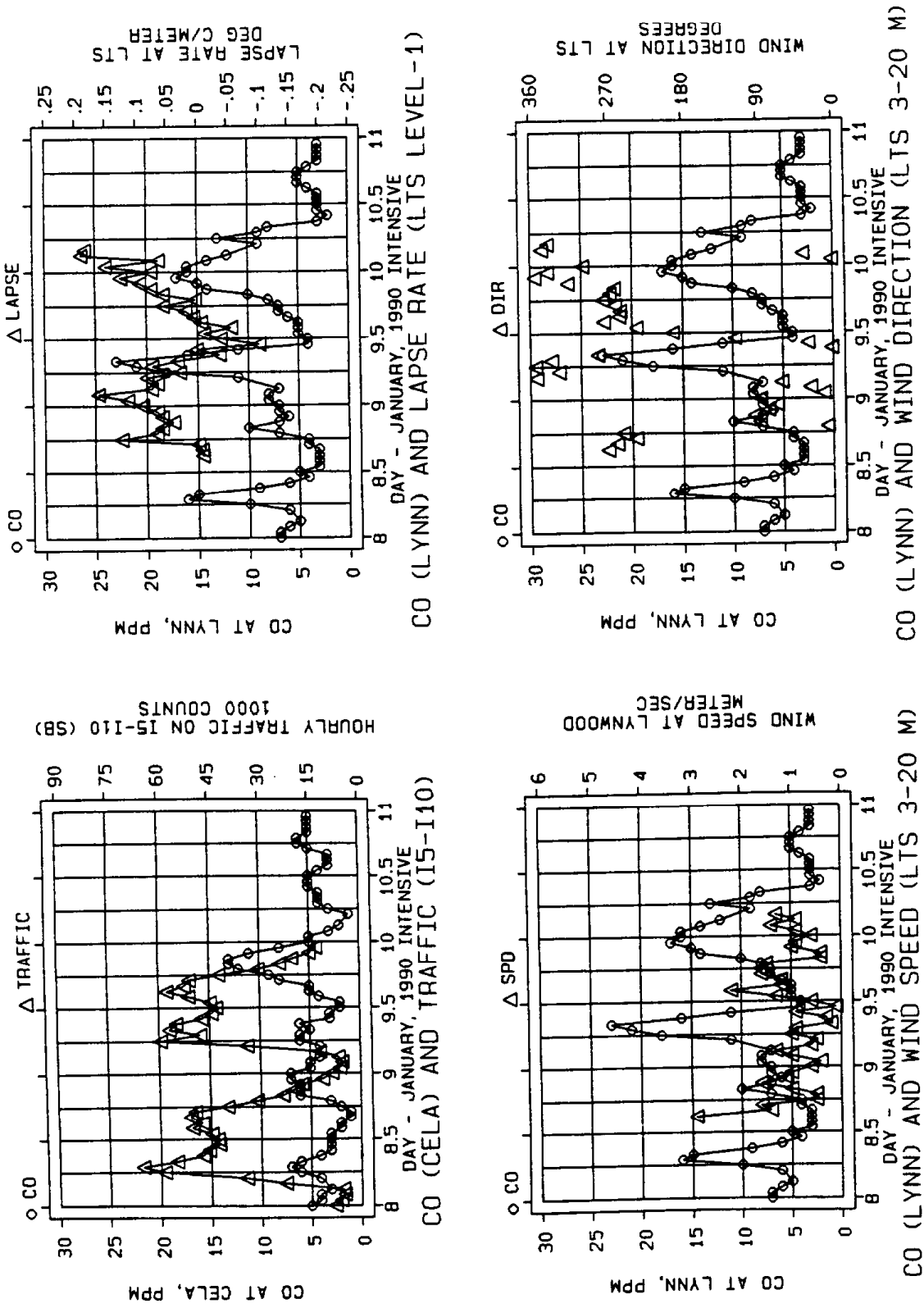


Figure 3-25. CO at CELA; Traffic at I-5/I-10; Lapse Rate, Wind Speed, and Wind Direction at LTS - January, 1990.

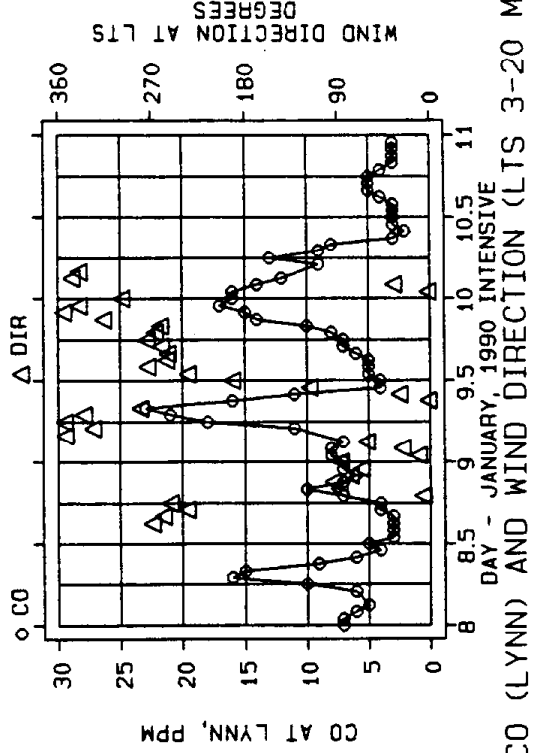
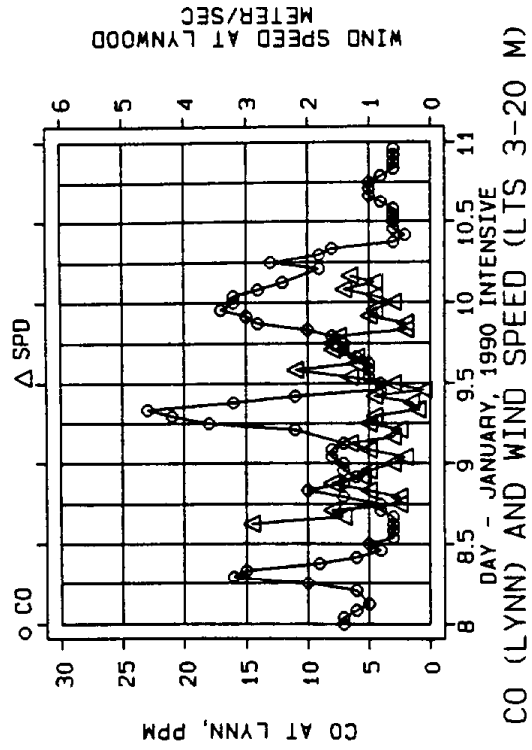
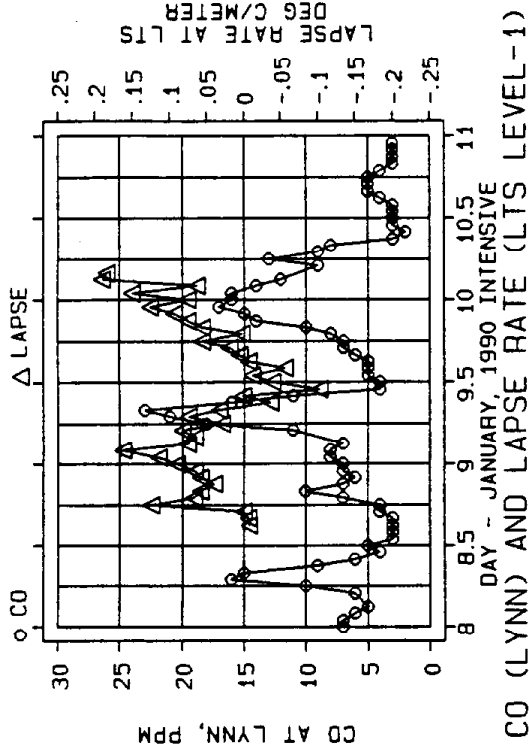
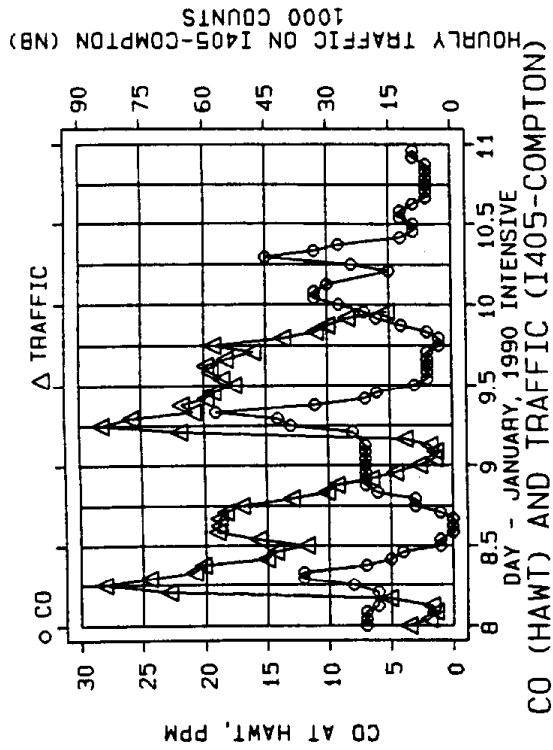


Figure 3-26. CO at HAWT; Traffic at I-405/Compton; Lapse Rate, Wind Speed, and Wind Direction at LTS - January, 1990.

3.9 Empirical Orthogonal Eigenfunction Analysis

Dr. Ronald Henry of the University of Southern California applied a multivariate analysis technique to the CO and wind data from selected sites. The spatial covariances of CO concentrations were analyzed at these sites using a principle component analysis known as Empirical Orthogonal Function (EOF) analysis with an extension to determine possible sources through the Source Identification Through Empirical Orthogonal Functions (SITEOF) model. EOFs provide a means of examining the spatial variation in air quality data that are simultaneously collected at discrete locations distributed over some area of interest. They can, when properly interpreted, indicate the location of sources of air pollution (Henry et al., 1990).

The following sections summarize the method and discuss the application to CO concentrations measure in the Lynwood vicinity. For this work, the analysis consisted of data screening and selection for EOF analysis, initial EOF analysis for general patterns, and application of the SITEOF model.

3.9.1 Background for EOF Analysis

The spatial distribution of an air pollutant depends on several factors, including meteorological conditions such as wind speed and direction, location of sources for the pollutant, and removal mechanisms for the pollutant. Measurements of the pollutant over an particular area will contain information in the relationships among data at different locations regarding the factors governing concentrations of the pollutant. An EOF analysis is one method to identify the information in the data. For this purpose, the EOFs are determined from a principal component analysis of the covariance matrix of the data, which for this work are CO data from the various sites.

Henry et al.(1990) describe the method and derive the equations associated with the EOF analysis and the SITEOF model. A brief summary of the method and its derivation is given here. For simplicity, formulae are given in terms of continuous variables although data are actually available only at discrete sites for discrete time periods. The fundamental basis for the model is the advection equation:

$$\frac{\partial C}{\partial t} = -\vec{V}_H \cdot \nabla C + Q - S \quad (4)$$

where C is CO concentration,
 \vec{V}_h is horizontal wind velocity vector,
Q represents all sources of CO, and
S represents all sinks of CO.

It will be noted that Equation 4 has no diffusion term. Diffusion is included implicitly in Equation 4 because the wind velocity is considered to be a random variable.

By singular value decomposition, the observed concentration data are expressed as

$$C(x, y, t) = C_A(x, y) + \sum_{k=1}^N \alpha_k(t) \Phi_k(x, y) \quad (5)$$

where $C_A(x, y)$ is the average CO at (x, y) ,
 $\Phi_k(x, y)$ is the kth EOF at (x, y) ,
 $\alpha_k(t)$ is the kth time-weighting function at time t , and
 n is the number of EOFs included in the model.

The observed winds are included in the model by calculating the average wind field weighted with the time-weighting functions from the EOF analysis as follows:

$$\bar{W}_k(x, y) = \frac{1}{T} \int_0^T \alpha_k(t) \bar{V}_H(x, y, t) dt \quad (6)$$

where \bar{W}_k is average horizontal wind velocity vector weighted by the kth EOF and
 T is the total time period.

Substitution of Equations 5 and 6 into Equation 4 followed by an average over the time period of interest, gives the average of the CO emission rate minus the CO removal rate as

$$\overline{Q(x, y) - S(x, y)} = \frac{C(x, y, t) - C(x, y, 0)}{T} + \sum_{k=1}^N \bar{W}_k(x, y) \cdot \nabla \Phi_k(x, y) \quad (7)$$

The terms on the right hand side of Equation 7 are quantities that can be derived from the CO data.

3.9.2 Data Screening and Selection

The data considered for EOF analysis included one-hour average CO data from all sites in the SCAQMD's routine monitoring network for the intensive study days of 19 and 20 December, 1989 and 8, 9, and 10 January 1990. Additional spatial resolution was obtained from one- and two-hour average CO data from bag samplers at a number of sites during the intensive study periods in December and January. Not all available data were used. Sites were selected for inclusion in the analysis based on distance from Lynwood and on the amount and reliability of the data.

The first data selection criterion was that the site be within approximately 20 km of LYNN. The routine monitoring sites satisfying this criterion are LGBH, HAWT, CELA, PICO, and WHIT. All bag sample sites also satisfied this criterion although data from a number of sites were discarded from the analysis because there were not enough samples from those sites or the data did not appear valid. From the selected sites, two data sets were constructed, one consisting of all one-hour average data to maximize the time resolution and one containing two-hour average data (including the one-hour data reduced to two-hour averages) to maximize the spatial resolution.

3.9.2.1 One-Hour Average Data

The shortest sample duration or averaging time in the data was one hour, although some sites collected data for two hours. Table 3-7 lists the sites within about 20 km of Lynwood that had one-hour data. Because multivariate analysis requires complete data records with no missing data at any site, only sites with relatively little missing data were included in this analysis. Of the sites in Table 3-7, those with the fewest missing data were the SCAQMD sites and HS02 and HS05, two sites a block north of LYNN. The SCAQMD data are considered to be highly reliable because of the overall quality assurance program in place with its attendant checks on instruments and data validation. The HS10 site had only two more missing hours than HS02 did, but data from the HS10 site were felt to be unreliable for reasons presented in Section 2.1. Data reliability pertaining to the EOF is discussed in more detail in the next section on the two-hour data. Table 3-8 contains the basic statistics of the one-hour data set.

3.9.2.2 Two-Hour Average Data

Table 3-9 lists all sites within about 20 km of Lynwood that have two-hour average data, including sites with one-hour data that were averaged to two hours. Sites with more than seven missing observations were not included in the final data set. Some sites with fewer than seven missing observations were not included either because their data correlated poorly with nearby SCAQMD routine monitoring sites. The HS sites located within 1 and 4 km of LYNN site fell into this category. Table 3-10 correlates all sites with LYNN for all the two-hour average data. CO concentrations at sites HS09 to HS16 had negative or very small correlation with CO concentrations at the LYNN site, while the correlation of the LYNN site with the other SCAQMD sites was always greater than 0.4, even though these sites were much further from LYNN than HS09 to HS16. The sites that did not correlate well with LYNN did not correlate well with each other either. This behavior cannot be explained except as a result of unreliable data from these sites. After careful examination of the correlations of all the data and the time series plots, only sites marked in Table 3-9 had data consistent with the nearby SCAQMD sites. The basic statistics of CO concentrations at these sites are given in Table 3-11.

Figure 3-27 shows the locations of the sites in the final one- and two-hour data sets. The Appendix D contains a listing of the one-hour and two-hour data sets.

3.9.3 Results of EOF Analysis

3.9.3.1 Spatial Correlations of One- and Two-Hour Average Data

Before examining the EOFs of the covariance of the spatial intercorrelations, the intersite correlations of the CO data were computed to gain some insight into the data. The correlations are the same as the covariances except that CO data at each site are divided by their standard deviation to normalize the data to a standard deviation of 1. Table 3-12 gives the intersite correlations of all the sites used in the analysis. In general, sites which were very close to one another, such as LYNN and HS05 or CC10 and CC19, had correlations near 0.9. Conversely,

Table 3-7

Available One-Hour Data

<u>Site</u>	<u>No. of Obs.</u>	<u>Missing Records</u>	<u>Dist. to LYNN (km)</u>
LYNN ^a	63	4	0
LGBH ^a	63	4	11.93
HAWT ^a	63	4	14.76
CELA ^a	63	5	15.31
PICO ^a	63	4	16.93
WHIT ^a	63	4	17.14
HS02 ^a	63	8	0.08
HS03	63	30	0.00
HS05 ^a	63	7	0.11
HS06	63	30	0.05
HS8	63	29	0.20
HS9	63	43	0.97
HS10	63	10	1.02
HS11	63	14	1.15

^a Retained in final data selection.

Table 3-8

Basic Statistics of the One-Hour CO Data Set
(in ppm)

<u>Site</u>	<u>Obs.</u>	<u>Missing Records</u>	<u>CO Concentrations</u>			
			<u>Min.</u>	<u>Max.</u>	<u>Mean</u>	<u>StDev.</u>
LYNN	59	4	2	23	8.4	5.1
HS02	55	8	2.5	20.4	8.2	4.2
HS05	56	7	2.6	16.7	8.3	4.1
LGBH	59	4	2	10	5.7	2.2
HAWT	59	4	0	19	5.1	4.0
CELA	58	5	0	13	4.5	2.9
PICO	59	4	1	13	5.2	2.7
WHIT	59	4	1	12	5.0	2.6

Table 3-9

Available Two-Hour Data for EOF Analysis

<u>Site</u>	<u>No. of Obs.</u>	<u>Missing Records</u>	<u>Dist. to LYNN (km)</u>
LYNN	32	4	0.00
LGBH	32	2	11.94
HAWT	32	2	14.76
CELA	32	3	15.31
PICO	32	2	16.94
WHIT	32	2	17.14
CC05	32	23	17.19
CC06	32	22	21.67
CC08 ^a	32	2	14.06
CC10 ^a	32	2	9.31
CC12	32	20	19.87
CC13	32	2	7.30
CC14	32	14	12.23
CC16 ^a	32	3	9.87
CC17	32	13	6.81
CC18	32	8	10.37
CC19 ^a	32	5	5.80
CC20	32	21	18.19
CC21	32	20	14.38
HS01	32	12	0.15
HS02 ^a	32	7	0.08
HS03	32	17	0.00
HS05 ^a	32	5	0.11
HS06	32	16	0.05
HS07a	32	7	1.09
HS07b	32	5	1.09
HS07c	32	2	1.09
HS08	32	15	0.20
HS09	32	24	0.97
HS10	32	8	1.02
HS12	32	10	1.16
HS13	32	9	1.13
HS14	32	8	3.15
HS15	32	4	2.96
HS16	32	16	3.0

^a Retained in final data selection.

Table 3-10

**Correlations of All Sites with LYNN Site
(Two-Hour Data)**

<u>Site</u>	<u>Correlation</u>
LGBH	0.579
CELA	0.412
HAWT	0.757
WHIT	0.570
PICO	0.621
HS01	0.980
HS02	0.844
HS03	0.852
HS05	0.903
HS06	0.933
HS07a	0.784
HS07b	0.416
HS07c	0.753
HS08	0.917
HS09	-0.551
HS10	-0.625
HS12	-0.395
HS13	-0.208
HS14	-0.037
HS15	0.003
HS16	-0.311
CC05	0.805
CC06	0.540
CC08	0.572
CC10	0.673
CC12	-0.065
CC13	0.644
CC14	0.637
CC16	0.734
CC17	0.025
CC18	0.768
CC19	0.790
CC20	0.695
CC21	0.859

Table 3-11

**Basic Statistics of the Two-Hour CO Data Set
(in ppm)**

<u>Site</u>	<u>Obs.</u>	<u>Missing Records</u>	<u>CO Concentrations</u>			
			<u>Min.</u>	<u>Max.</u>	<u>Mean</u>	<u>StDev.</u>
LYNN	28	4	2	19.5	8.7	5.0
HS02	25	7	2.7	17.3	8.3	4.3
HS05	27	5	2.8	15.5	8.2	4.0
CC08	30	2	1.4	9.9	4.6	2.3
CC10	30	2	1.9	11.6	4.9	2.5
CC16	29	3	1.8	12.9	6.1	3.8
CC19	27	5	1.6	12.8	6.3	3.2
LGBH	30	2	2	10	5.7	2.2
HAWT	30	2	0	15	4.9	4.0
CELA	29	3	0.5	13	4.4	2.9
PICO	30	2	1	12.5	5.1	2.6
WHIT	30	2	1	11.5	4.9	2.5

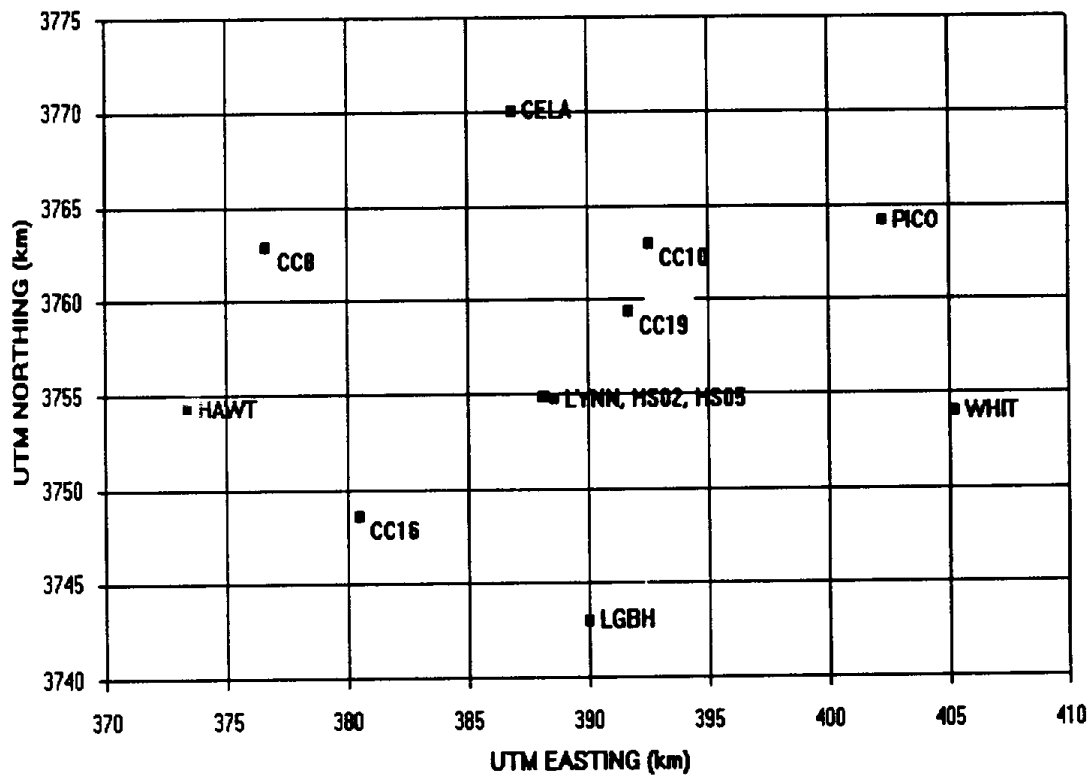


Figure 3-27. Location of Sites Used in EOF Analysis.

Table 3-12

Inter-Site Correlations for All Two-Hour Average CO Data

	LYNN	HS05	HS02	CC19	CC10	CC16	CC08	LGBH	HAWT	CELA	PICO
HS05	0.903										
HS02	0.844	0.931									
CC19	0.790	0.901	0.933								
CC10	0.673	0.835	0.851	0.949							
CC16	0.734	0.551	0.498	0.562	0.388						
CC08	0.572	0.605	0.553	0.608	0.589	0.605					
LGBH	0.579	0.428	0.413	0.349	0.269	0.853	0.691				
HAWT	0.757	0.529	0.478	0.502	0.394	0.946	0.679	0.812			
CELA	0.412	0.717	0.714	0.782	0.877	0.216	0.605	0.181	0.225		
PICO	0.621	0.772	0.771	0.860	0.865	0.504	0.758	0.423	0.497	0.840	
WHIT	0.570	0.693	0.728	0.726	0.756	0.335	0.547	0.329	0.386	0.829	0.731

sites that were most distant from each other had low correlations, e.g., CELA and LGBH had a correlation of 0.18. There was, however, a great deal of variation in the relationship between distance and intersite correlation, as can be seen in Figure 3-28, a plot of correlation versus distance for all sites in the two-hour data set. Simple examination of the intersite correlations did not give any special insights into sources of CO at LYNN or reveal much about the location of sources of CO. An EOF analysis is needed for this.

3.9.3.2 Initial EOF Analysis of One- and Two-Hour CO Data

EOF analysis of the covariance matrix of the one- and two-hour average data sets was carried out. The values of the first three EOFs for both data sets are given in Figures 3-29 to 3-31. These three patterns explain a total of about 93% of the variability in each data set. The EOF analysis of the one-hour data set was based on 47 complete data records at 8 sites, while the results for the two-hour data sets had only 16 periods with all 12 sites reporting. Even though 16 cases was a very small number for a multivariate analysis, examination of the figures shows that the EOFs for the one- and two-hour data sets were almost the same at sites common to both. It can be concluded that EOFs of the two-hour data set are valid although based on a small amount of data.

Winds at Lynwood associated with the first three EOFs were calculated using Equation 6 and the surface winds near LYNN from the wind fields generated by the Diagnostic Wind Model. The direction and magnitude of these winds are given in the figures of the EOFs. Each EOF pattern and the associated surface wind at LYNN is discussed below.

The first EOF (Figure 3-29) explains 69.7% and 66.7% of the variability in the one- and two-hour data, respectively. It expresses the fact that most of the time CO concentrations at all the sites go up and down together. This is the result of the common effects of diurnal variation in CO emissions and meteorological mixing. Remembering that clues to the location of sources are found in the gradients of the EOF, this EOF does not show any strong gradients near LYNN and thus does not indicate the presence of any unusual sources of CO. The surface winds at LYNN associated with this EOF as shown in Figure 3-29 came almost directly from the south (171°).

The second EOF (Figure 3-30) explains 19.8% and 16.7% of the variability in the one- and two-hour data, respectively. It represents a major feature of the variability in the data. The pattern shows high values (positive) at the coastal sites in the south and west and low values (negative) at inland sites to the north and east. The most remarkable feature of this EOF pattern is that the LYNN site is grouped with coastal sites, and the HS02 and HS05 sites, only tenths of a km away, have EOFs less than zero like the inland sites. There was a very large gradient between LYNN and the HS02 and HS05 sites. This indicates the presence of a strong local CO source somewhere between the SCAQMD site and the two nearby HS sites. The wind associated with this EOF was from the northeast (56°), which was consistent with the general direction of transport from the northeast to the southwest indicated by the EOF pattern. The implications of this EOF are discussed in detail in the next section.

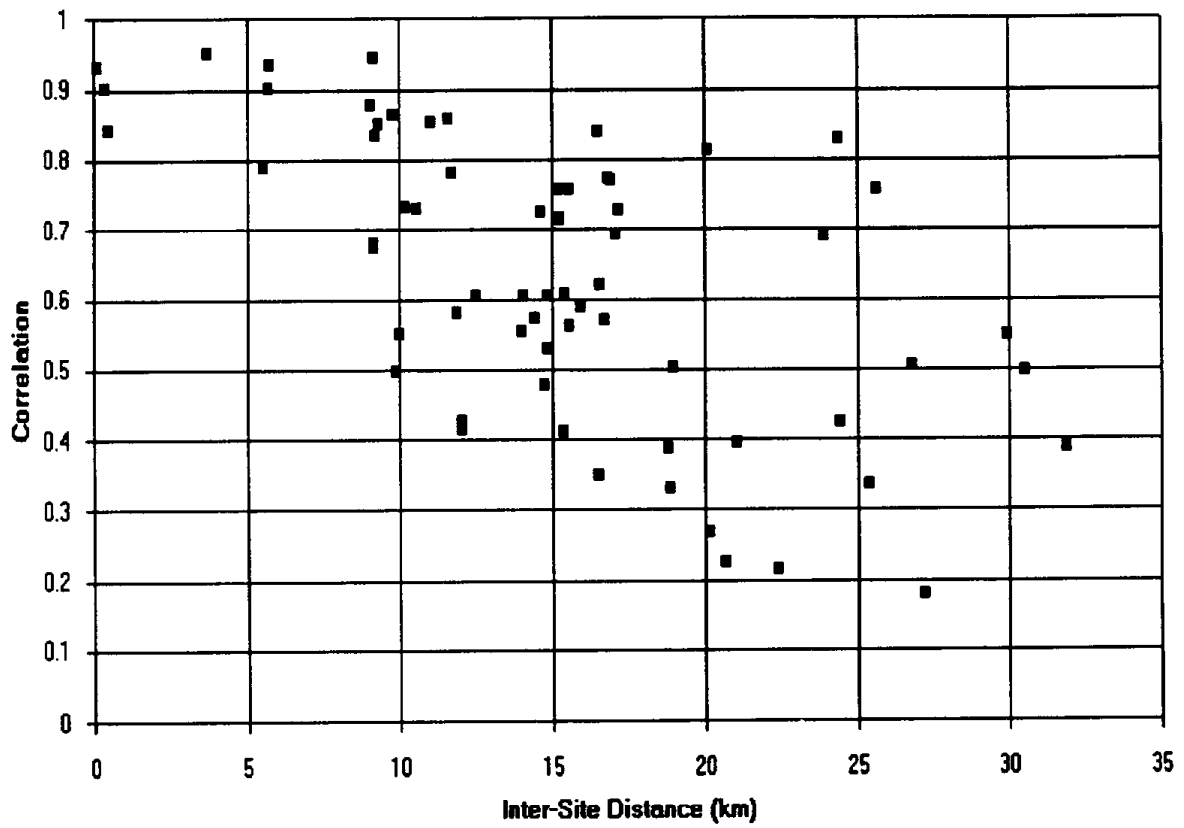


Figure 3-28. Inter-site Correlations versus Distance of All Sites Used in EOF Analysis Based on Two-Hour Average Data.

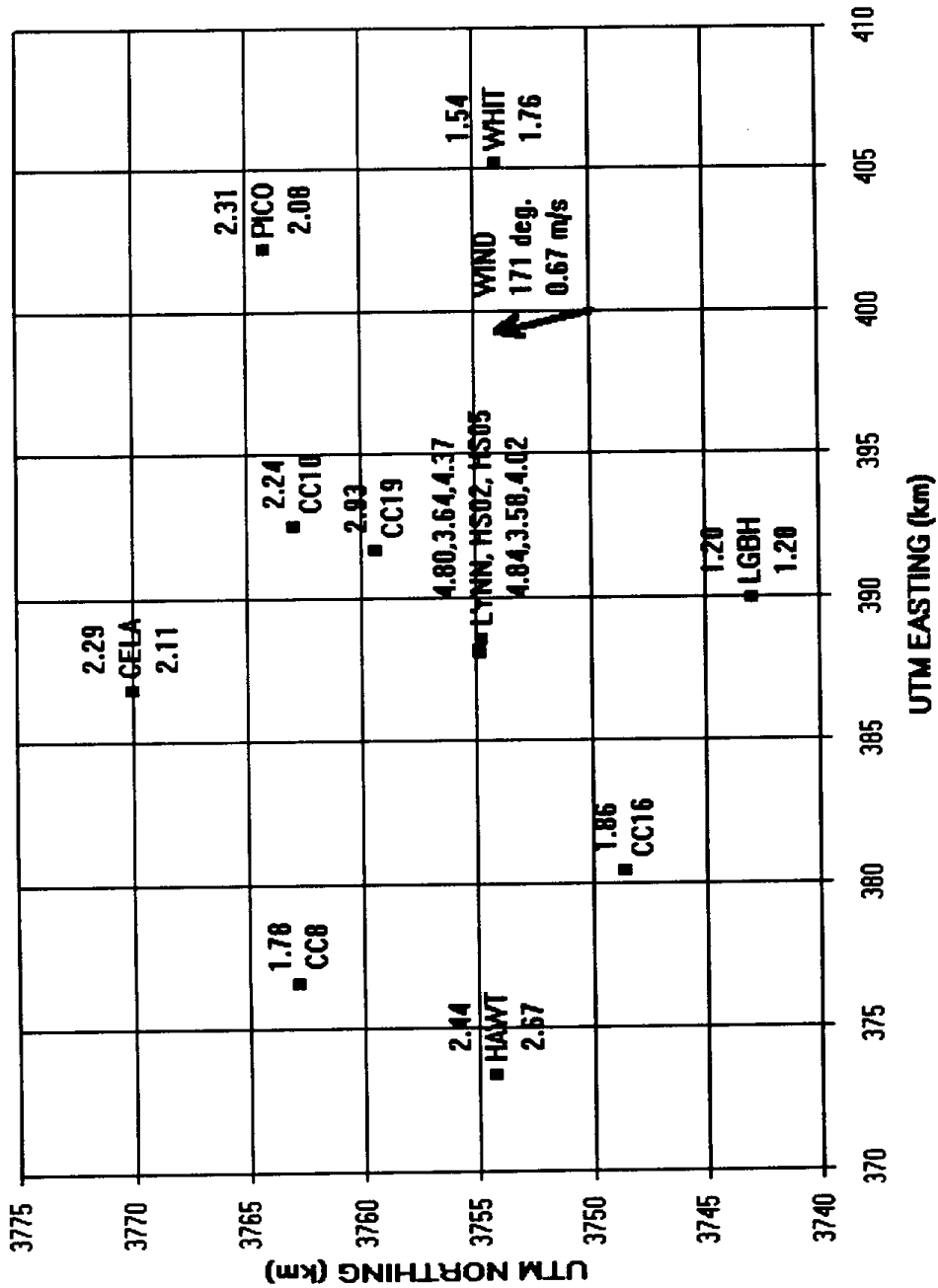


Figure 3-29. First EOF of CO Data. Values are in ppm difference from the mean. The numbers above the site name are for the two-hour average data; the numbers below are for the one-hour average data; explains 68% of two-hour variance.

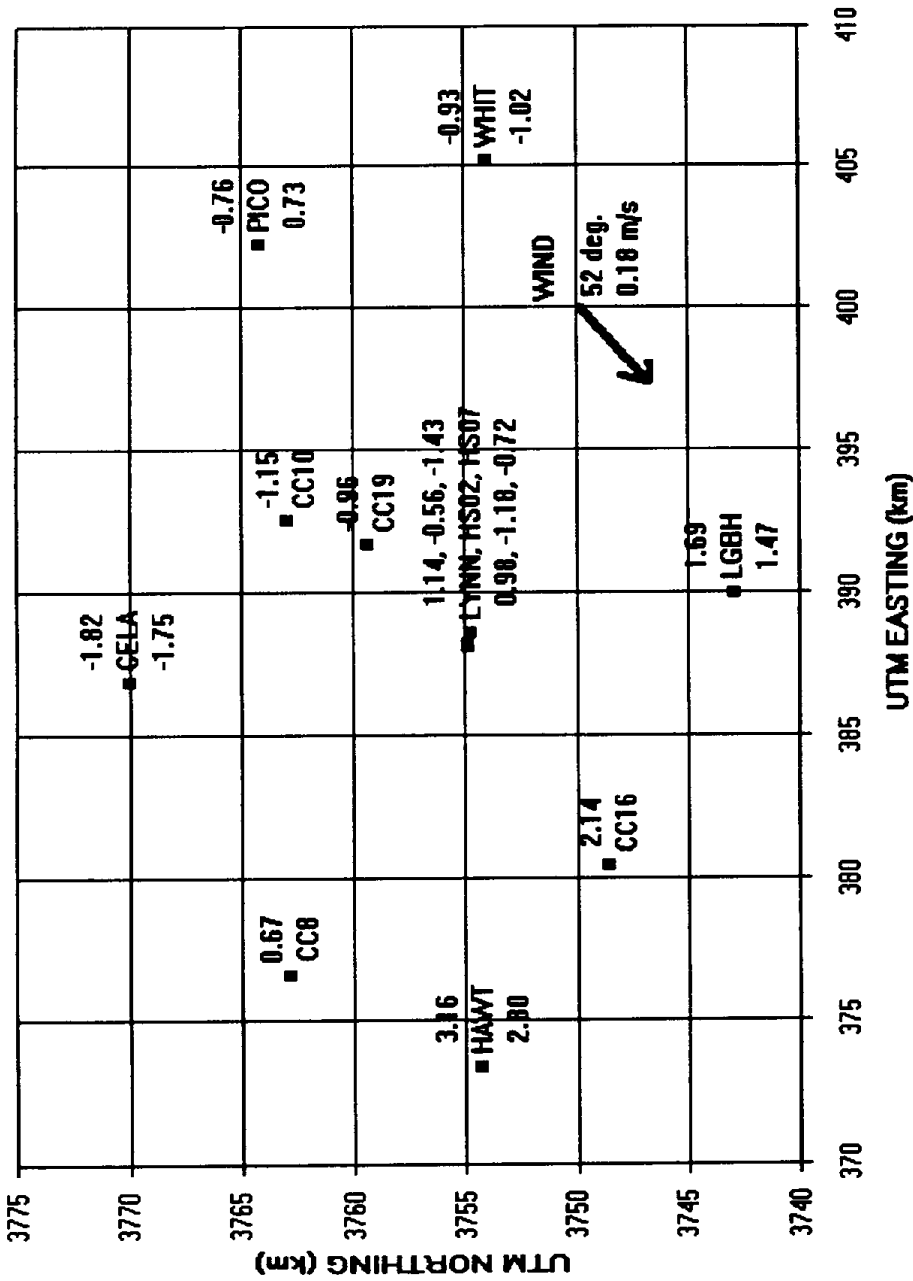


Figure 3-30. Second EOF of CO Data. Values are in ppm difference from the mean. The numbers above the site name are for the two-hour average data; the numbers below are for the one-hour average data; explains 20% of two-hour variance.

Finally, the third EOF (Figure 3-31) explains about 7% of the variability in the CO data for both the one- and two-hour data at all sites. This EOF has relatively high values at LYNN and the two nearby HS sites and low values for all the surrounding sites. In this case, all three Lynwood sites were high (or low) while all the surrounding sites are low (or high). Like the second EOF, this pattern can be explained by a local source (or sources); but, unlike the source in the second EOF, this source caused high values at the LYNN site and the HS sites at the same time. The wind associated with this EOF was from the north-northeast (27°), indicating that the local source could be in the northeast sector somewhere to the north and east of HS sites near LYNN.

3.9.3.3 SITEOF Model Results

A qualitative interpretation of the EOF patterns has been given in the previous section. However, the SITEOF model as described in Henry et al. (1990) can estimate the average of the emission rate of CO minus the removal rate of CO, that is, the average of the net emission rate of CO over the study period. On these temporal and spatial scales, the removal mechanisms for CO are very small compared to the sources so that the SITEOF model essentially gives the emission rates. The spatial region for which this prediction is valid is limited by the spacing between the observation sites. Since the model requires an estimate of the gradient of the EOFs, it is only valid for regions in which a good estimate of the gradient is possible. To estimate the gradient at a point, it must be surrounded by observation sites to the north, south, east, and west. From the site map in Figure 3-27, the only area that satisfies this criterion is the region about 10 to 15 km around the LYNN site. The SITEOF modeling region was chosen to be the 10 km by 15 km rectangle bounded by UTM eastings 380 to 395 and UTM northings 3750 to 3760 to be consistent with the emission inventory, which is based on a 5 km grid set on UTM coordinates that are multiples of 5. The calculations for the model, however, were carried out for the entire region using a 1 km grid spacing. Only the model predictions for the smaller area defined above are given here.

In addition to the one-hour average CO data, the SITEOF model requires hourly wind fields for each grid point and the average mixing height for the entire modeling period. Hourly winds were obtained from the Diagnostic Wind Model. Hourly mixing heights from Section 3.4 were used.

The mixing height was necessary since the model gives an emission rate in units of mass per volume per time. This must be multiplied by the inversion height to obtain an emission rate in the usual units of mass per area per time. The average mixing height for the 64 hours of both intensive periods is 227 m. However, because of missing data, only 45 hours of data were used in the SITEOF model; the average mixing height for these is 182 m. The average emission rate calculated by SITEOF for these 45 hours in the 10 km by 15 km region around Lynwood is 1,896 kg/km²-day. For comparison, the ARB's 1987 Emission Inventory for this region is 1,227 kg/km²-day.

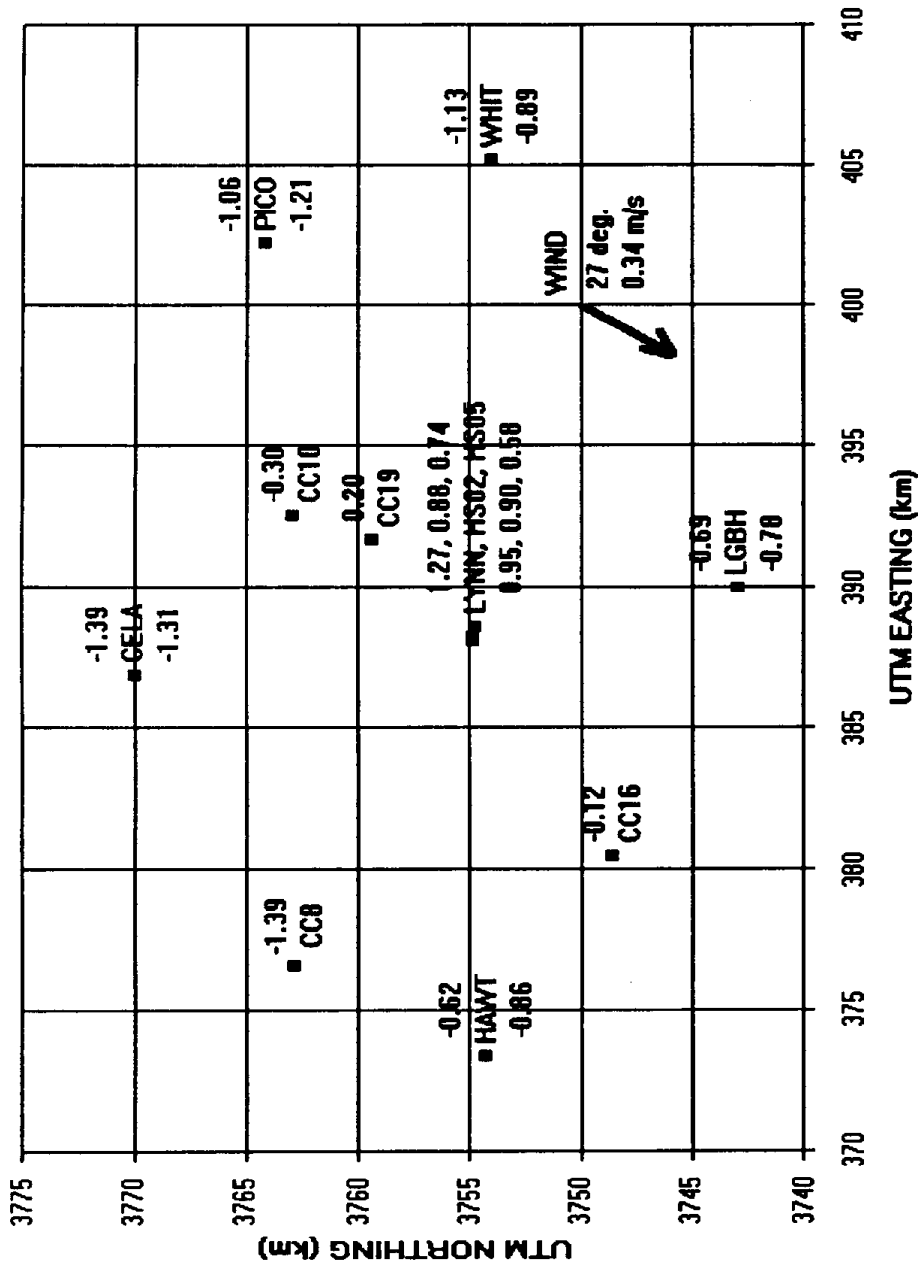


Figure 3-31. Third EOF of CO Data. Values are in ppm difference from the mean. The numbers above the site name are for the two-hour average data; the numbers below are for the one-hour average data; explains 7% of two-hour variance.

3.9.3.4 Discussion of EOF Analysis

The EOF analysis shows the importance of local sources of CO near LYNN, i.e., sources within about 5 km of the site. The first EOF, which accounts for nearly 70% of the variability in the data, is least influenced by local sources. This EOF is the pattern that best explains the variation of CO at all the sites considered and as such is an indicator of the morning and evening peaks in CO concentrations found throughout the SoCAB. Values of this EOF at LYNN and the HS02 and HS05 sites are, however, nearly twice the value at the CC19 site, 5 km away, and more than twice the value at other sites. While the gradient in the EOF is not very large, it does imply that the emission density of CO is higher around LYNN than at other SCAQMD sites.

The second and third EOFs appear to be associated with local sources in the vicinity of Lynwood. The second EOF, which accounts for 16 to 19% of the variability, shows a large gradient between the LYNN site on Long Beach Blvd. and the HS02 and HS05 sites in the 3300 block of Beechwood Ave. The HS sites were located to the east of Long Beach Blvd. and about 100 m to the north and northeast of LYNN. The gradient in this EOF may have resulted from operations associated with the U.S. Post Office located between LYNN and the HS sites. There are likely other sources of CO in the immediate vicinity of LYNN but none that are between it and the HS sites.

The third EOF, which accounts for about 7% of the variability, shows a pattern with high values at LYNN and the two HS sites and low values at all the surrounding sites. This pattern can be explained by local sources of CO that make the LYNN and HS sites high at the same time while not affecting the other sites in the analysis. However, in the absence of reliable data from more sites close to LYNN, the exact location of these local sources cannot be determined.

The gradient in the second EOF may have been a result of higher maximum concentrations at LYNN than at HS02 and HS05 during the intensive periods. Table 3-13 contains the maximum CO concentrations at sites in the vicinity of LYNN for the morning and evening periods during the two intensives. Maximum concentrations at LYNN exceeded those at HS02 and HS05 by 3 to 5 ppm during the morning of 9 January and 2 to 3 ppm during the evening of 19-20 December. However, the average of differences between concentrations at LYNN and at HS sites as shown in Table 3-14 were less than 1 ppm during the intensive periods. An application of the t-Test to the paired differences in CO shows that average concentrations at most HS sites differed little from those at LYNN. Only at HS05 in December and at HS08 in January were the probabilities as low as 5% that the mean differences between concentrations at LYNN and at the sites were zero.

Because of the lack of data covering both space and time, conclusions drawn from individual measurements are somewhat tenuous. As Table 3-13 shows the highest concentration during the January intensive occurred at HS08, which was located on the north side of Imperial Highway and to the east of Long Beach Blvd. This site was not included in the EOF analysis because data were available for only one intensive. The high concentration at HS08 may have been due to a nearby source or just to random differences. Similarly, the peak concentrations

Table 3-13

Maximum CO Concentrations in the Vicinity of LYNN

<u>Site</u>	<u>December Intensive</u>		<u>January Intensive</u>	
	<u>12/19-20</u>	<u>12/20</u>	<u>01/09</u>	<u>01/09-10</u>
	<u>Evening</u>	<u>Morning</u>	<u>Morning</u>	<u>Evening</u>
LYNN	17	13	23	17
HS01	-	-	18	15
HS02	15	12	20	16
HS03	-	-	20	15
HS05	14	13	17	16
HS06	-	-	22	15
HS08	-	-	25	16

Table 3-14

Comparisons of Average CO Concentrations at HS Sites to LYNN

<u>Difference</u>	<u>Intensive</u>	<u>Number</u>	<u>Difference</u>		<u>Probability of Zero Difference</u>	
			<u>Mean PPM</u>	<u>Std. Dev. PPM</u>	<u>t-STAT</u>	<u>%</u>
LYNN - HS02	BOTH	51	0.32	2.83	0.80	42.53
LYNN - HSO2	DEC	20	-0.36	1.16	-1.38	18.40
LYNN - HS02	JAN	31	0.76	3.46	1.22	23.38
LYNN - HS03	JAN	33	0.30	3.34	0.52	60.60
LYNN - HS05	BOTH	53	0.08	2.28	0.26	79.69
LYNN - HS05	DEC	20	-0.58	1.20	-2.16	4.34
LYNN - HS05	JAN	33	0.48	2.68	1.04	30.72
LYNN - HS06	JAN	33	0.34	2.32	0.96	34.36
LYNN - HS08	JAN	34	-0.82	2.41	-1.99	5.54

at HS03, located at LYNN, were several ppm less than those at LYNN. This could point to a systematic problem in the bag sample measurements. The difference between concentrations at LYNN and HS03 were small for the January intensive, the only available data at HS03.

The SITEOF model estimate of CO emission rates is almost 55% higher than the emission inventory estimate. While errors in the SITEOF model under all conditions have not yet been characterized, studies with artificial data sets have indicated an error of no more than 10%. If the error in the mixing height is also about 10%, then the error in the SITEOF model result is about 20%. Thus, it is unlikely that all the difference between the model and inventory emission rates is due to model errors. Another possible explanation is that the results of the SITEOF model are for a particular 45 hours, while the emission inventory is for average conditions. CO emissions may have been unusually high during these 45 hours, although neither the measured concentrations nor the vehicle counts indicate this to be an unusual period. Finally, it is possible the emission inventory was incorrect in its estimates of known sources in the area or there may be sources that were not included in the inventory.

3.9.3.5 Conclusions from EOF Analysis

The primary conclusions to be drawn from the data selection and EOF analysis are as follows:

- Much of the CO data from the special study appears to be unreliable for use in temporal analysis.
- The unusually high CO concentration at LYNN is probably caused by sources about 5 km or less from the site.
- A strong local source of CO lies between LYNN and the HS02 and HS05 sites. This source may be associated with operations of the U.S. Post Office between LYNN and the HS sites.
- Other local sources of CO exist but their location cannot be determined because of the lack of reliable data.
- The SITEOF model estimates CO emission rates in the 10 km x 15 km region around LYNN that are 55% higher than shown in the emission inventory.

Based on the above conclusions, any future study of CO at LYNN should concentrate on the region within 5 or 10 km of the site. Also, short-term intensive studies do not produce the quantity of data needed for an EOF analysis. If EOFs are to be used in a future study, hourly data should be taken for at least two weeks at as many locations as possible in a uniform grid within 5 to 10 km of LYNN.